

UNCLASSIFIED

AD NUMBER
ADB014691
NEW LIMITATION CHANGE
TO Approved for public release, distribution unlimited
FROM Distribution authorized to U.S. Gov't. agencies only; Test and Evaluation; JAN 1975. Other requests shall be referred to Air Force Materials Lab., Composite and Fibrous Materials Branch, Wright-Patterson AFB, OH 45433.
AUTHORITY
AFWAL ltr, 19 Nov 1982

THIS PAGE IS UNCLASSIFIED

✓
AFML-TR-76-47

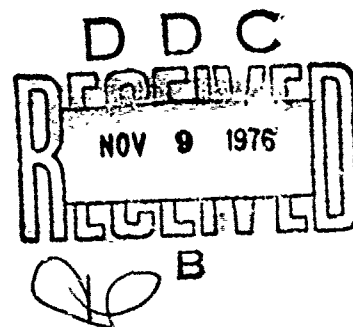
ADB014691

HEAT RESISTANT AND NONFLAMMABLE MATERIALS

FABRIC RESEARCH LABORATORIES

APRIL 1976

TECHNICAL REPORT AFML-TR-76-47
REPORT FOR PERIOD JANUARY 1975 - DECEMBER 1975



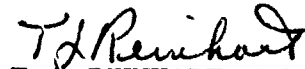
Distribution limited to U.S. Government agencies only; test and evaluation; January 1975. Other requests for this document must be referred to the Air Force Materials Laboratory, Nonmetallic Material Division, Composite and Fibrous Materials Branch, AFML/MBC, Wright-Patterson Air Force Base, Ohio 45433.

AIR FORCE MATERIALS LABORATORY
AIR FORCE WRIGHT AERONAUTICAL LABORATORIES
AIR FORCE SYSTEMS COMMAND
WRIGHT-PATTERSON AIR FORCE BASE, OHIO 45433

NOTICE

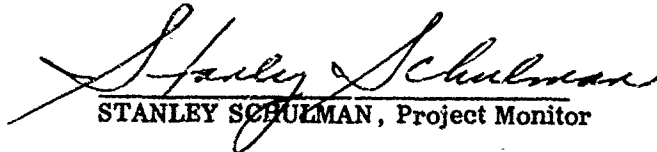
When Government drawings, specifications, or other data are used for any purpose other than in connection with a definitely related Government procurement operation, the United States Government thereby incurs no responsibility nor any obligations whatsoever; and the fact that the government may have formulated, furnished, or in any way supplied the said drawings, specifications, or other data, is not to be regarded by implication or otherwise as in any manner licensing the holder or any other person or corporation, or conveying any rights or permission to manufacture, use or sell any patented invention that may in any way be related thereto.

FOR THE DIRECTOR



T. J. REINHART, Chief

Composite and Fibrous Materials Branch
Nonmetallic Materials Division


STANLEY SCHULMAN, Project Monitor

Copies of this report should not be returned unless return is required by security considerations, contractual obligations, or notice on a specific document.

(9) Annual rept. 1 Jan - 31 Dec 75

SECURITY CLASSIFICATION OF THIS PAGE (When Data Entered)

REPORT DOCUMENTATION PAGE		READ INSTRUCTIONS BEFORE COMPLETING FORM
1. REPORT NUMBER AFML-TR-76-47 (19)	2. GOVT ACCESSION NO.	3. RECIPIENT'S CATALOG NUMBER
4. TITLE (and Subtitle) HEAT RESISTANT AND NONFLAMMABLE MATERIALS		5. TYPE OF REPORT & PERIOD COVERED Annual Report 1 January 1975 - 31 December 1975
6. PERFORMING ORG. REPORT NUMBER		7. CONTRACT OR GRANT NUMBER(s) (15) F33615-75-C-5168
8. AUTHOR(s) N. J. Abbott, M. M. Schoppee, J. Skelton		9. PERFORMING ORGANIZATION NAME AND ADDRESS Fabric Research Laboratories, Inc 1000 Providence Highway, Dedham, Mass. 02026
10. PROGRAM ELEMENT, PROJECT, TASK AREA & WORK UNIT NUMBERS (11) Apr 76		11. CONTROLLING OFFICE NAME AND ADDRESS (16) 7320
12. REPORT DATE APRIL 1976		13. NUMBER OF PAGES 127 (12) 139p
14. MONITORING AGENCY NAME & ADDRESS (if different from Controlling Office)		15. SECURITY CLASS. (of this report) Unclassified
16. DISTRIBUTION STATEMENT (of this Report) Distribution limited to U. S. Government agencies only; test and evaluation; January 1975. Other requests for this document must be referred to the Air Force Materials Laboratory, Nonmetallic Materials Division, Composite and Fibrous Materials Branch, AFML/MB, Wright-Patterson Air Force Base, Ohio 45433		17. DISTRIBUTION STATEMENT (of the abstract entered in Block 20, if different from Report) Same
18. SUPPLEMENTARY NOTES None		19. KEY WORDS (Continue on reverse side if necessary and identify by block number) Nonflammable fibers, radiant heat, tensile properties, degradation, HT-4, Durette, Nomex, Kynol, cotton, nylon, polyester, fire protection
20. ABSTRACT (Continue on reverse side if necessary and identify by block number) The tensile properties of spun-yarn, flight-suit weight HT-4, Durette, Nomex I, Kynol, cotton, nylon and polyester fabrics have been measured during exposure to bilateral radiant heat fluxes in the range 0.2 to 0.9 cal/cm ² /sec. Specially designed test equipment allows testing at times as short as a few seconds after initiation of exposure. All of the fabrics tested lost at least 50% of their strength in the first 6 seconds of exposure at flux levels of 0.4 cal/cm ² /sec and at least 75% of their strength 54 cm		

DD FORM 1473 EDITION OF 1 NOV 65 IS OBSOLETE

SECURITY CLASSIFICATION OF THIS PAGE (When Data Entered)

133275

20. Abstract (Cont.)

after 5 seconds at 0.7 cal/cm²/sec and above. Of those fabrics tested, HT-4 provides the greatest degree of protection and polyester provides the least protection against a high heat flux.

Studies were also made of launderability of HT-4 fabric, abrasion of Kevlar webbing, weaving of BBB fabric, and other analyses requested by AFML.

ACCESSION for	
NTIS	White Section <input type="checkbox"/>
DDC	Buff Section <input checked="" type="checkbox"/>
UNANNOUNCED	<input type="checkbox"/>
JUSTIFICATION	
BY	
DISTRIBUTION/AVAILABILITY CODES	
Dist.	AVAIL. and/or SPECIAL
B	

FOREWORD

This report was prepared by Fabric Research Laboratories, Dedham, Mass., under U. S. Government Contract No. F33615-75-C-5168. The work was initiated under Project 7320, "Fibrous Structural Materials," and was conducted from January 2, 1975 through December 31, 1975. It was administered under the direction of the Air Force Materials Laboratory, Air Force Systems Command, with Mr. Stanley Schulman acting as project engineer.

Mr. Norman J. Abbott was the FRL director responsible for the overall program. The laboratory studies were carried out by Mrs. Meredith M. Schoppee and Mr. John Skelton. The photomicrographs were taken by Mr. Leo Barish. The authors wish to express their appreciation to Dr. Milton M. Platt, vice-president of FRL, for handling contractual matters and for many helpful discussions throughout the course of the work.

This report was submitted by the authors in April 1976.

This technical report has been reviewed and is approved for publication.

TABLE OF CONTENTS

<u>Section</u>	<u>Page</u>
I INTRODUCTION	1
II MECHANICAL PROPERTIES OF FABRICS IN RADIANT HEAT ENVIRONMENT	2
1. Thermal Environment	2
2. Fabric Tensile Properties	7
3. Conclusions	13
4. Future Work	13
III REACTION OF HT-4 FABRIC TO LAUNDERING	15
IV ABRASION OF KEVLAR WEBBINGS	15
V CROSS-SECTIONS OF NOMEX, HT-4 AND E-11 FABRICS	17
VI CROSS-SECTIONS OF DYED KYNOL/NOMEX BLEND	17
VII BBB FABRIC	17
VIII DEFECTS IN POLYCARBON FABRIC	18
IX EXAMINATION OF FAILED DRONE RETRIEVAL PARACHUTE WEBBING	20
APPENDIX	89
REFERENCES	127

LIST OF ILLUSTRATIONS

<u>Figure</u>		<u>Page</u>
1	Quartz Faced Radiant Heaters and Test Chamber	21
2	Unilateral Heat Flux Measured with Calorimeter at Various Distances from Surface of a Single Quartz Heater	22
3	Temperature of Quartz Heaters in Unilateral and Bilateral Configurations as a Function of the Electrical Energy Supplied to Each Surface	23
4	Emissivity of Quartz Radiant Heat Source	24
5	Initial Radiant Heat Flux on Fabric Surface in the Bilateral Configuration	25
6	Estimated Temperature Rise of Specimen Located Between Quartz Heaters in Bilateral Configuration	26
7	Strength Retention of HT-4 Fabric in the Filling Direction at Various Bilateral Radiant Heat Flux Levels	27
8	Strength Retention of Durette Fabric in the Warp Direction at Various Bilateral Radiant Heat Flux Levels	28
9	Strength Retention of Nomex I Fabric in the Warp Direction at Various Bilateral Radiant Heat Flux Levels	29
10	Strength Retention of Kynol Fabric in the Warp Direction at Various Bilateral Radiant Heat Flux Levels	30
11	Strength Retention of Cotton Fabric in the Filling Direction at Various Bilateral Radiant Heat Flux Levels	31
12	Strength Retention of Nylon Fabric in the Warp Direction at Various Bilateral Radiant Heat Flux Levels	32
13	Strength Retention of Polyester Fabric in the Warp Direction at Various Bilateral Radiant Heat Flux Levels	33
14	Rupture Elongation of HT-4 Fabric in the Filling Direction at Various Bilateral Radiant Heat Flux Levels	34
15	Rupture Elongation of Durette Fabric in the Warp Direction at Various Bilateral Radiant Heat Flux Levels	35
16	Rupture Elongation of Nomex I Fabric in the Warp Direction at Various Bilateral Radiant Heat Flux Levels	36

LIST OF ILLUSTRATIONS (Cont.)

<u>Figure</u>		<u>Page</u>
17	Rupture Elongation of Kynol Fabric in the Warp Direction at Various Bilateral Radiant Heat Flux Levels	37
18	Rupture Elongation of Cotton Fabric in the Filling Direction at Various Bilateral Radiant Heat Flux Levels	38
19	Rupture Elongation of Nylon Fabric in the Warp Direction at Various Bilateral Radiant Heat Flux Levels	39
20	Rupture Elongation of Polyester Fabric in the Warp Direction at Various Bilateral Radiant Heat Flux Levels	40
21	Initial Modulus of HT-4 Fabric in the Filling Direction at Various Bilateral Radiant Heat Flux Levels	41
22	Initial Modulus of Durette Fabric in the Warp Direction at Various Bilateral Radiant Heat Flux Levels	42
23	Initial Modulus of Nomex I Fabric in the Warp Direction at Various Bilateral Radiant Heat Flux Levels	43
24	Initial Modulus of Kynol Fabric in the Warp Direction at Various Bilateral Radiant Heat Flux Levels	44
25	Initial Modulus of Cotton Fabric in the Filling Direction at Various Bilateral Radiant Heat Flux Levels	45
26	Initial Modulus of Nylon Fabric in the Warp Direction at Various Bilateral Radiant Heat Flux Levels	46
27	Initial Modulus of Polyester Fabric in the Warp Direction at Various Bilateral Radiant Heat Flux Levels	47
28	Duration of Exposure at Various Heat Flux Levels for which HT-4 Fabric Retains 25% and 50% of Its Original Strength	48
29	Duration of Exposure at Various Heat Flux Levels for which Durette Fabric Retains 25% and 50% of Its Original Strength	49
30	Duration of Exposure at Various Heat Flux Levels for which Nomex I Fabric Retains 25% and 50% of Its Original Strength	50
31	Duration of Exposure at Various Heat Flux Levels for which Kynol Fabric Retains 25% and 50% of Its Original Strength	51

LIST OF ILLUSTRATIONS (Cont.)

<u>Figure</u>		<u>Page</u>
32	Duration of Exposure at Various Heat Flux Levels for which Cotton Fabric Retains 25% and 50% of Its Original Strength	52
33	Duration of Exposure at Various Heat Flux Levels for which Nylon Fabric Retains 25% and 50% of Its Original Strength	53
34	Duration of Exposure at Various Heat Flux Levels for which Polyester Fabric Retains 25% and 50% of Its Original Strength	54
35	Fabric Ignition Times at Various Bilateral Radiant Heat Flux Levels	55
36	Comparison of the Strength Retention of HT-4 Fabric in the Filling Direction at Similar Unilateral and Bilateral Heat Flux Levels	56
37	Comparison of the Rupture Elongation of HT-4 Fabric in the Filling Direction at Similar Unilateral and Bilateral Radiant Heat Flux Levels	57
38	Comparison of the Initial Modulus of HT-4 Fabric in the Filling Direction at Similar Unilateral and Bilateral Radiant Heat Flux Levels	58
39	Strength Retention of HT-4 Fabric in the Filling Direction at Various Temperatures	59
40	Strength Retention of Durette Fabric in the Warp Direction at Various Temperatures	60
41	Strength Retention of Nomex I Fabric in the Warp Direction at Various Temperatures	61
42	Strength Retention of Kynol Fabric in the Warp Direction at Various Temperatures	62
43	Strength Retention of Cotton Fabric in the Filling Direction at Various Temperatures	63
44	Rupture Elongation of HT-4 Fabric in the Filling Direction at Various Temperatures	64
45	Rupture Elongation of Durette Fabric in the Warp Direction at Various Temperatures	65
46	Rupture Elongation of Nomex I Fabric in the Warp Direction at Various Temperatures	66

LIST OF ILLUSTRATIONS (Cont.)

<u>Figure</u>		<u>Page</u>
47	Rupture Elongation of Kynol Fabric in the Warp Direction at Various Temperatures	67
48	Rupture Elongation of Cotton Fabric in the Filling Direction at Various Temperatures	68
49	Initial Modulus of HT-4 Fabric in the Filling Direction at Various Temperatures	69
50	Initial Modulus of Durette Fabric in the Warp Direction at Various Temperatures	70
51	Initial Modulus of Nomex I Fabric in the Warp Direction at Various Temperatures	71
52	Initial Modulus of Kynol Fabric in the Warp Direction at Various Temperatures	72
53	Initial Modulus of Cotton Fabric in the Filling Direction at Various Temperatures	73
54	Appearance of Abraded Kevlar Webbing: Face in Contact with Hexagonal Bar	74
55	Appearance of Abraded Kevlar Webbing: Unabraded Surface	75
56	Original Appearance of Kevlar Webbing	76
57	Section Parallel to the Warp Yarns of Kevlar Webbing in Bending Test Configuration Before Cycling	77
58	Section Parallel to the Warp Yarns of Kevlar Webbing in Bending Test Configuration After 3200 Cycles	78
59	Cross-Section of Nomex Fibers	79
60	Cross-Section of HT-4 Fibers	80
61	Cross-Section of E-11 Blend	81
62	Cross-Section of Dyed Kynol/Nomex Blend	82
63	Failed Drone Retrieval Parachute Webbing: Back Side	83
64	Failed Drone Retrieval Parachute Webbing: Face Side	86

LIST OF TABLES

<u>Table</u>		<u>Page</u>
1	Fabric Description and Properties at 70°F	3
2	Greatest Radiant Heat Flux at Which Various Fabrics Retain 25% and 50% of Their Original Strength for 3 and 6 Second Exposures	9
3	Fabric Ignition Times at Various Bilateral Radiant Heat Flux Levels	10
4	Fabrics Which Retain 25% and 50% of Their Original Strength Over Short Exposures at Various Radiant Heat Flux Levels	14
5	Laundering Shrinkage of Calendered and Uncalendered HT-4 Fabric	16
6	Strength of Carbon Yarns	19
7	Tensile Properties of HT-4 Fabric in the Filling Direction at Various Bilateral Radiant Heat Flux Levels	89
8	Tensile Properties of Durette Fabric in the Warp Direction at Various Bilateral Radiant Heat Flux Levels	95
9	Tensile Properties of Nomex I Fabric in the Warp Direction at Various Bilateral Radiant Heat Flux Levels	102
10	Tensile Properties of Kynol Fabric in the Warp Direction at Various Bilateral Radiant Heat Flux Levels	106
11	Tensile Properties of Cotton Fabric in the Filling Direction at Various Bilateral Radiant Heat Flux Levels	111
12	Tensile Properties of Nylon Fabric in the Warp Direction at Various Bilateral Radiant Heat Flux Levels	114
13	Tensile Properties of Polyester Fabric in the Warp Direction at Various Bilateral Radiant Heat Flux Levels	117
14	Tensile Properties of HT-4 Fabric in the Filling Direction at Various Unilateral Radiant Heat Flux Levels	120
15	Tensile Properties of HT-4 Fabric in the Filling Direction at Various Temperatures in Circulating Hot Air	122

LIST OF TABLES (Cont.)

<u>Table</u>		<u>Page</u>
16	Tensile Properties of Durette Fabric in the Warp Direction at Various Temperatures in Circulating Hot Air	123
17	Tensile Properties of Nomex I Fabric in the Warp Direction at Various Temperatures in Circulating Hot Air	124
18	Tensile Properties of Kynol Fabric in the Warp Direction at Various Temperatures in Circulating Hot Air	125
19	Tensile Properties of Cotton Fabric in the Filling Direction at Various Temperatures in Circulating Hot Air	126

I. INTRODUCTION

During the first year of this contract attention has been centered on measuring the tensile properties of a number of fabrics made from nonflammable fibers while they were exposed to a high radiant heat flux for various times. This measurement provides information which relates the ability of the fabric to retain useful mechanical properties, and therefore, to continue to provide protection to a person wearing a flight suit or other garment when close to or surrounded by flame. Such data has never before been obtained and the results reveal for the first time characteristics of these fabrics which are of prime importance to determining their usefulness in many potential Air Force applications.

In addition, during the year we have carried out a number of other small investigations of materials of specific interest to the Air Force including: laundering of HT-4 fabric, abrasion of Kevlar webbing, fabric cross-sections, weaving of BBB fabric, examination of defects in a polycarbon-fabric, and examination of the failed drone retrieval parachute webbing.

II. MECHANICAL PROPERTIES OF FABRICS IN A RADIANT HEAT ENVIRONMENT

Introduction

Adequate real-life testing of fabrics designed to protect the wearer against a high heat flux fire environment is precluded by the very nature of the problem. The effect of large fires on instrumented clothed manikins can be investigated with reasonable accuracy yielding valuable information on fabric heat transfer and thermal shrinkage behavior. Fabric flammability can be assessed by such laboratory tests as Limiting Oxygen Index or by measurements of ignition times and burning rates in a flammability chamber. However, an active wearer makes implicit demands on protective garments which cannot easily be simulated by a manikin or by passive laboratory tests. Of course, the fabric of his suit must not ignite or melt, but it must retain its integrity during the time the wearer is actively escaping from a large fire; it must bend, stretch and conform and must generally continue to exhibit the flexibility which makes a textile fabric the obvious choice of material for clothing. If the fabric becomes so weakened or embrittled during exposure that it tears or disintegrates during slight stressing, it can no longer provide adequate protection from the heat of a flame. Knowledge of the mechanical properties of fabrics during the first few seconds of exposure to a high heat flux is presently lacking; this work is aimed toward the objective of providing this information. Once the basic mechanical properties of a number of fabrics have been determined over a range of relevant environmental conditions, then it will be possible to predict the practical limits of fabric protective capability with some justified confidence.

Under an earlier AFML contract [1] a test method was developed at FRL which makes it possible to follow dynamically changes in the tensile properties of a fabric during the course of short-term exposure to a high radiant heat flux, and, thereby, to determine the rate at which deterioration proceeds. During this current year the rupture strength, rupture elongation and initial modulus of several fabrics subjected to radiant heat fluxes from 0.2 to 0.9 cal/cm²/sec have been measured for exposure times of a few seconds to one minute. The fabrics tested were: HT-4, Durette, Nomex I, Kynol, the best available heat-resistant polymeric fabrics; and cotton, nylon and polyester, commonly used fibers in current Air Force clothing. All of the fabrics were woven from spun yarns and are in the weight range of 4-6 oz/yd², the usual range for flight suit fabrics; a description of the fabrics tested and their tensile properties under ambient conditions are given in Table 1.

1. Thermal Environment

The high levels of radiant heat required for this testing were supplied by two facing quartz infrared heating panels* mounted in a chamber which is itself mounted in an Instron tensile test machine. The faces of the quartz panels measure 12 inches in the vertical direction, 6 inches in the horizontal direction and are spaced 0.5 inch apart. A specially-designed rod and plunger

*Hugo N. Cahnman Assoc., Kew Gardens, New York

TABLE 1

FABRIC DESCRIPTION AND PROPERTIES AT 70°F

Fabric	Weight (oz/yd)	Thickness (a) (inch)	Air Permeability (cu ft/min/sq ft)	Initial Modulus (lbs/inch) Warp Fill	Rupture Elongation (%)		Rupture Load (lbs/inch) Warp Fill	
					Warp	Fill	Warp	Fill
HT-4 sage green plain weave 54 x 47	4.6	0.012	84	1320 1550	10.2	12.4	122	118
Nomex I sage green 2/2 twill 122 x 81	4.0	0.009	139	860 880	33.2	23.7	116	76
Durette golden brown plain weave 51 x 42	4.3	0.018	215	790 390	18.1	24.1	68	49
Kynol brownish orange 2/1 twill 50 x 35	4.7	0.017	192	710 360	7.4	8.9	31	18
Nylon, Type 66 white plain weave 38 x 39	6.5	0.020	37	540 520	38.0	40.9	132	126
Kodel polyester white plain weave 37 x 38	6.5	0.017	43	660 750	27.9	27.4	94	102
Cotton untreated, white plain weave 41 x 41	6.5	0.022	23	960 1160	28.5	22.2	83	91

(a) at 3.3" psi

(b) at a differential pressure of 0.5 inch of water.

system attached to the door of the chamber in which the heaters are housed in conjunction with a special jaw and jaw holder arrangement, shown in Figure 1, allows insertion of fabric test specimens in less than one second midway between the facing heater surfaces which have previously been brought to thermal equilibrium. This rapid insertion makes possible carefully controlled exposure times prior to testing.

The test chamber is vented to the outside atmosphere to rid the test area of noxious gases produced by the test fabrics during heating and possible subsequent combustion. The rate of replacement of the air in the chamber during testing is 1.7 cu ft/sec or one complete chamber volume change in ~5 seconds.

The thermal output of the individual heater panels was characterized using a water-cooled calorimeter to measure the net heat flux (radiant flux less convective losses) at various distances from the surface of a single heater and various positions over the surface. The surface temperature of the heaters at various levels of electrical energy input was monitored simultaneously by Chromel-Alumel thermocouples located behind the centers of the quartz panels. The uniformity of the flux was found to be within $\pm 4\%$ of the average value over the central 8 inch by 2 inch area at a distance of 0.25 inch from the surface. The variation of net heat flux with the surface temperature of the heater at various distances from the surface is shown in Figure 2; also included in this figure is the amount of electrical energy which must be supplied to the heaters to maintain the temperatures indicated. Electrical energy E is computed from the applied voltage V and resistance R of the heater as follows:

$$E = \frac{0.0371 V^2}{AR} \text{ (cal/cm}^2\text{/sec)} \quad (1)$$

where 0.0371 is the conversion factor to $\text{cal/cm}^2\text{/sec}$ from watts/inch^2 , $R = 5.3$ ohms for a single heater and A , the area of the heater surface, is 72 square inches. Comparison of the amount of electrical energy supplied with the radiant energy measured at a distance of 0.05 inch from the heater surface shows, in Figure 2, an approximately uniform 7% loss in energy which is assumed to be the result of radiation and convection losses from the sides and back of the heater. The difference between the flux measured at 0.05 inch and that measured at 0.25 or 0.50 inch is taken to be an estimate of the convective losses from the quartz surface over this distance.

When the heaters are in the bilateral configuration, direct measurement of the net heat flux on a surface midway between them is precluded by the unavailability of a suitably thin, double-sided, water-cooled calorimeter; therefore, in this configuration the thermal environment between the two quartz surfaces must be inferred from temperature measurements and estimates of the surface emissivity. Throughout the following discussion the following assumptions concerning the radiative properties of the quartz surfaces will be made in order to simplify the theoretical considerations:

1. The surfaces are gray: the emissivity ϵ is not equal to unity; the emissivity ϵ is equal to absorptivity α and both ϵ and α are independent of the wavelength of the incident and emitted

radiation [2]. The gray body assumption does not exclude variations in ϵ and α with temperature, and since the wavelength of the radiation emitted from the heaters is known to vary uniformly with surface temperature, the effect of wavelength on emissivity is indirectly included when the emissivity as a function of temperature is known. In the bilateral configuration both heaters are at the same temperature and, therefore, the radiation each surface receives from the other is of the same wavelength as that emitted, a further justification for the gray body assumption.

2. The surfaces are diffuse: the intensity of both emitted and reflected radiation is spatially uniform [2]. As mentioned previously, the net heat flux was found to be uniform within $\pm 4\%$ over the central 8 inch by 2 inch area of a single heater; therefore, this assumption is reasonable within this area and greatly simplifies the description of thermal radiation exchange between heaters.

The emissivity of the quartz surfaces may be calculated from the Stefan-Boltzmann equation for gray bodies [2]:

$$Q = \epsilon(T)\sigma T^4 \quad (2)$$

where Q is the radiant heat energy ($\text{cal/cm}^2/\text{sec}$) emitted from a surface at a temperature T ($^\circ\text{K}$) which has an emissivity $\epsilon(T)$ at that temperature, and σ is the Stefan-Boltzmann constant, $1.354 \times 10^{-12} \text{ cal/cm}^2/\text{sec}/^\circ\text{K}^4$. The temperature of the heaters in the unilateral configuration as a function of the net electrical energy supplied (less the 7% convective losses from the back and sides of the heater) is plotted in Figure 3; corresponding pairs of values of energy and temperature inserted in Equation 2 yield the emissivity values plotted in Figure 4 at various temperatures. Also included in Figure 4 are literature values of emissivity for various quartz surfaces which serve to lend further credence to the calculated values.

The surface temperature of the heaters in the bilateral configuration is also shown in Figure 3. The temperatures reached in the bilateral configuration are higher than in the unilateral configuration for the same amount of electrical energy supplied to each surface because of the additional amount of radiant energy impinging on each heater in the form of both emitted and reflected radiation from the opposing heater. The net radiant heat exchange q between the two quartz surfaces at a temperature T_1 and an opaque surface at a temperature T_2 inserted between them is given by the following expression for a double parallel-plate geometry [5]:

$$q = \frac{2\sigma(T_1^4 - T_2^4)}{\frac{1}{\epsilon_1(T_1)} + \frac{1}{\epsilon_2(T_2)} - 1} \quad (3)$$

Derivation of this expression assumes that all of the radiation leaving one surface arrives at the other (a form factor of unity). The form of Equation 3 reduces to that of Equation 2 when $T_2 = 0$, $\epsilon_2(T_2) = 1$, the situation which exists when a single source radiates into empty space. A one-inch wide specimen inserted between the closely spaced heater surfaces can be assumed to receive all of the radiation leaving that portion of those surfaces directly opposed by the fabric structure and therefore Equation 3 can be used to determine the initial incident radiant heat flux on the specimen; values of initial heat flux so calculated are plotted in Figure 5 as a function of heater temperature. The initial temperature of the specimen is $T_2 = 21^\circ\text{C} = 294^\circ\text{K}$; the fabric emissivity $\epsilon_2(T_2)$ is assumed to be 0.9 at all temperatures [6]; the emissivity $\epsilon_1(T_1)$ of the heater surface is taken from Figure 4. Although the values determined from Equation 3 can be approximated quite closely using Equation 2, it is clear from Equation 3 that as the temperature of the fabric specimen rises, the net radiant flux on it decreases, eventually reaching zero as T_2 approaches T_1 . Furthermore, as the temperature of the specimen rises, the convective losses from its surfaces will also rise. Thus, the net heat flux at the fabric surface including both radiative and convective components is not precisely known after the first instant of exposure. The fabric temperature, however, should eventually approach the equilibrium temperature of the heaters since neither the area nor the mass of the one-inch wide fabric specimens is sufficiently large in comparison to the area and mass of the heaters to alter the equilibrium temperature of the quartz surfaces during the course of fabric exposure.

An estimate of the time necessary for a fabric specimen to reach the equilibrium temperature of the heaters can be made by iterating between Equation 3 and the following expression relating temperature rise ΔT_2 in a specific time interval Δt to the net radiant flux q_k on the fabric in the k th time interval and the specific heat C_p of the fabric material:

$$\Delta T_2 = \frac{q_k A \Delta t}{C_p W} \quad (4)$$

where A is the effective area of the specimen and W , its weight. Values for the quantities in Equation 4 appropriate for the estimate being sought are: specific heat $C_p = 0.3$ [7]; an effective specimen area equivalent to 80% of the 1 inch by 12 inch strip area to account for the openness of the fabric structure, $A = 60 \text{ cm}^2$; a specimen weight, $W \approx 1 \text{ gm}$, determined from the fabric weights given in Table 1; and a time interval, $\Delta t \approx 1 \text{ second}$. For the first iteration, $q_{k=1}$ is taken from Figure 5 at the appropriate value of T_1 ; this value is inserted in Equation 4 to give the temperature rise ΔT_2 in the first time interval. This value of ΔT_2 is then added to the initial value of $T_2 = 21^\circ\text{C} = 294^\circ\text{K}$ and the new value of T_2 used in Equation 3 to find $q_{k=2}$ for the next iteration. The results of this iterative process for driving temperatures of 300, 400, and 600°C are plotted in Figure 6; as shown, the equilibrium temperature of the heaters is closely approached by the fabric specimen within ~10 seconds after the initiation of exposure.

2. Fabric Tensile Properties

The tensile properties of the various fabrics at several bilateral radiant heat flux levels ranging from $0.2 \text{ cal/cm}^2/\text{sec}$ to $0.9 \text{ cal/cm}^2/\text{sec}$ are given in Figures 7-27 for exposure times ranging up to one minute. The strength retention of the fabrics is shown in Figures 7-13; the rupture elongation in Figures 14-20; and the modulus in Figures 21-27. The heat flux levels noted on each of these figures represent the approximate radiant heat flux on the fabric specimen during the first instant of exposure. The temperature of the infrared source, also noted in the figures, is an indication of the equilibrium temperature which the specimen temperature is approaching. Each data point in Figures 7-27 generally represents the average of three tests at the conditions indicated; individual items of data are tabulated in the Appendix, Tables 7-13. The HT-4 and cotton fabrics were tested in the filling direction since this is the direction of lower yarn crimp for these fabrics; the other fabrics were tested in the warp direction. All of the fabrics were scoured prior to testing.

A fabric gauge length of 13.5 inches was necessary to allow placement of the jaw attachments outside the region of high heat flux between the heaters. The rupture elongation and modulus values determined directly from the Instron load-time curves may be somewhat in error because of the ~1.5 inch portion of the fabric gauge length which is not located in the high flux region between the heaters. When the fabric modulus in the heated region is less than that in the unheated region, the approximate value of the rupture elongation taken directly from the Instron chart can be shown to be somewhat low and that for the modulus, somewhat high. The error is largest when the modulus of that portion of the fabric specimen between the heaters falls to zero; in this case the error may be as large as 12.5% of the stated value.

The fastest available crosshead speed, 20 inches per minute (~150% per minute strain rate), was employed to minimize the duration of the actual tensile test. The duration of exposure indicated for each of the data points in Figures 7-13 showing strength retention and in Figures 14-21 showing rupture elongation represents the time from initiation of exposure to rupture of the specimen. The data points in Figures 21-27 showing fabric modulus are plotted for exposure times measured to the start of rapid load buildup of the specimens.

The character of the strength retention curves in Figures 7-13 is similar for all the fabrics tested with the exception of nylon and polyester. The HT-4, Durette, Nomex I, Kynol and cotton fabrics show a sharp initial drop in strength retention followed at the lower values of incident flux by stabilization at a relatively constant value. At incident flux levels of 0.6, 0.8 and $0.9 \text{ cal/cm}^2/\text{sec}$ all of the fabrics tested lost 90% of their strength in the first 10 seconds of exposure. At $0.4 \text{ cal/cm}^2/\text{sec}$ the HT-4 retained 40% of its strength at 10 seconds; the cotton retained 25%; and the remaining fabrics retained less than 10%. The strength of the nylon and polyester fabrics decreased steadily to the zero strength level, which coincided in each case with melting of the specimen, at all levels of flux investigated.

The rupture elongation and modulus curves of Figures 14-21 show some interesting trends and trend reversals as exposure time is increased. The rupture elongation values which increase and then decrease for the Durette and Kynol suggest material flow followed by resolidification. The modulus of the HT-4 fabric drops at short exposures followed by an increase at longer exposure times although not to the original level. Only the modulus of the Durette fabric rises above its initial value; this rise occurs at short exposure times for the lower heat fluxes; the modulus then drops sharply as the exposure time is increased. Thus only for the Durette is there any evidence of stiffening during exposure.

It is estimated that an airman has between 3 and 6 seconds to escape from a jet fuel fire. If during this period of intense physical activity, his suit should lose its integrity and, hence, its protective capability, his chances of escaping without severe burns would be severely lessened. The length of time during which the fabric of his suit retains a significant portion of its original strength will strongly affect the degree of protection afforded by his clothing while it is under thermal and mechanical stress. The length of time over which the various test fabrics retain 50% and 25% of their original strength at various heat flux levels is plotted in Figures 28-34; the data points contained in these figures were obtained by interpolation from the strength retention-exposure time curves of Figures 7-13. Using the 3 and 6 second exposure times as the criteria, the greatest heat flux which each fabric can withstand and still retain either 25% or 50% of its strength can be easily determined from Figures 28-34; these flux values are summarized in Table 2.

If fabric performance is compared within groups according to fabric weight and color on the basis of the data in Table 2, the various fabrics rank best to worst in their ability to withstand short exposures to high heat flux as follows: darker colored fabrics in the weight range 4.0-4.7 oz/yd² - HT-4, Kynol, and Durette and Nomex I at the same level; white fabrics with a weight of 5 oz/yd²; cotton, nylon, and polyester. The properties of a darker colored, lighter weight cotton fabric should be determined and compared with those of HT-4, Durette, Nomex I and Kynol to establish the ranking of cotton within the group of commonly used protective fabrics.

The similarities in behavior of the several fabrics in a high radiant heat flux environment are, however, more striking than the differences. For a group of fabrics which includes the most heat-resistant polymeric fabrics available, a cellulosic fabric and two thermoplastic fabrics, the limits of usefulness for short-term exposure in a high radiant heat flux environment are not widely divergent.

Another aspect of the behavior of the various fabrics in high heat fluxes should be considered in ranking their performance, namely whether the fabrics readily ignite or melt. Times to ignition at various levels of bilateral heat flux are shown in Figure 35 and Table 3 for HT-4, Durette, Nomex I, Kynol and

TABLE 2

GREATEST RADIANT HEAT FLUX AT WHICH VARIOUS FABRICS
RETAIN 25% AND 50% OF THEIR ORIGINAL STRENGTH
FOR 3 AND 6 SECOND EXPOSURES

	Fabric Heat Flux (cal/cm ² /sec)			
	25% Strength Retention		50% Strength Rete.	
	3 sec	6 sec	3 sec	6 sec
HT-4	>0.9	0.7	0.7	0.4
Durette	0.6	0.4	0.5	0.3
Nomex I	0.6	0.4	0.5	0.3
Kynol	>0.8	0.5	0.5	0.3
Cotton	>0.8	0.6	0.7	0.4
Nylon	0.6	0.4	0.5	0.3
Polyester	0.6	0.3	0.4	0.2

TABLE 3
FABRIC IGNITION TIMES
AT VARIOUS BILATERAL RADIANT HEAT FLUX LEVELS

Incident Radiant Heat Flux (cal/cm ² /sec)	Time to Ignition (seconds)				
	<u>HT-4</u>	<u>Durette</u>	<u>Nomex I</u>	<u>Kynol</u>	<u>Cotton</u>
0.2	-----none*-----				
0.3	-----none-----				~3.5 min
0.4	-----none-----				40
0.6	-----none			2 min	11
0.8	none	~1.5 min	none	23	5
0.9	30	22	4	8	3
1.0	13	10	4	2	2
1.1	9	6	2	2	2
1.2	4	4	2	1	2

*within 5 minutes

cotton. These data are specific to the high rate of air replacement in the test chamber; ignition times for fabrics exposed to high radiant heat flux in an atmosphere containing a less abundant supply of oxygen would very likely be longer than those given in Table 3 and Figure 35. HT-4 and Nomex I are superior in this context since they do not ignite at bilateral heat flux levels below $0.9 \text{ cal/cm}^2/\text{sec}$. Cotton, on the other hand, ignites at flux levels as low as $0.2 \text{ cal/cm}^2/\text{sec}$ although the exposure time required to produce ignition is 3 minutes at this flux level. For each of the fabrics the strength falls to zero either at or before ignition. The nylon and polyester fabrics melt at those times indicated in Figures 12 and 13 at which the strength falls to zero. The Nomex fabric also shows evidence of some melting at flux levels as low as $0.6 \text{ cal/cm}^2/\text{sec}$ although Nomex does not ignite until a flux level of $0.9 \text{ cal/cm}^2/\text{sec}$ has been reached. The fabrics rank best to worst according to their ignition behavior in this particular test configuration as follows: HT-4, Nomex I, Durette, Kynol and cotton.

Some preliminary measurements of the tensile properties of the HT-4 fabric irradiated unilaterally were also made in order to determine if this different heating pattern causes changes in the fabric tensile properties different from those observed for bilateral heating for the same total radiant heat flux on the specimen. Specimens were tested in the unilateral configuration at heat fluxes of $0.2\text{-}0.3 \text{ cal/cm}^2/\text{sec}$ and $0.3\text{-}0.5 \text{ cal/cm}^2/\text{sec}$. The average value of strength retention, rupture elongation and initial modulus are plotted in Figures 36-38 respectively; data for bilaterally heated specimens is included for comparison. Individual test results are given in the Appendix, Table 14.

Determination of the radiant heat flux on a specimen is somewhat more uncertain in the unilateral than in the bilateral case. In the unilateral configuration where a single heater radiates to cool surroundings, there is a large difference between the internal temperature and the surface temperature of the heat source; in the bilateral configuration where each heater radiates toward an equally hot surface, this differential between internal and surface temperature is minimal. Both the internal and surface temperatures and their corresponding unilateral heat flux values are noted in the legends of Figures 36-38. The heat flux corresponding to the lower surface temperature of the heat source probably more accurately describes the actual flux in the unilateral case. Also included in the legend is the range in equilibrium temperature between the side of the fabric facing away from the heater and that facing towards it; these temperatures were measured by means of a thermocouple against the respective surfaces.

The tensile properties of the HT-4 fabric specimens heated unilaterally at a flux of $0.2\text{-}0.3 \text{ cal/cm}^2/\text{sec}$ are in excellent agreement with those determined for specimens heated bilaterally at a flux of $0.2 \text{ cal/cm}^2/\text{sec}$. The tensile properties determined unilaterally at $0.3\text{-}0.5 \text{ cal/cm}^2/\text{sec}$ lie generally between those determined bilaterally at 0.3 and $0.4 \text{ cal/cm}^2/\text{sec}$. Therefore, within the framework of the uncertainties involved, it seems reasonable to conclude that the tensile properties of the HT-4 fabric heated unilaterally are the same as those for the fabric heated bilaterally at the same total heat flux on the specimen. Further testing of more of the fabrics in the series should be carried out in order to confirm the generality of this observation.

Throughout the foregoing discussion initial incident heat flux was considered the primary variable affecting fabric performance. Imposed heat flux does indeed govern the rate of heating of the fabric specimens and is therefore the determining factor in fabric performance during that short time interval before the fabrics have attained their equilibrium temperature. Thermal equilibrium has probably been reached in those instances where the strength retention-exposure time curves undergo a drastic change in slope followed by a relatively constant level of strength retention with further increasing exposure time. The strength retention curves for the HT-4, Durette, Nomex I, Kynol and cotton fabrics in Figures 7-11 respectively show such changes in slope generally between 8-15 seconds after the onset of exposure - a time interval in good agreement with that estimated by Equations 3 and 4 and shown in Figure 6. After thermal equilibrium has been reached and the fabric temperature remains at a value close to that of the heater surface, it is reasonable to expect that the fabric tensile properties will be largely a function of fabric temperature.

In order to compare the equilibrium tensile properties of fabrics subjected to a large radiative heat impulse with similar properties of fabrics heated to various temperatures in hot air, tensile tests were performed on the HT-4, Durette, Nomex I, Kynol and cotton fabrics in a circulating hot-air oven at temperatures ranging from 200°C to 500°C. The fabrics were exposed at temperature for 10 minutes prior to testing. A gauge length of 5.0 inches and a crosshead speed of 10 inches per minute were employed. Values of the tensile properties obtained are listed individually in Tables 15-19 in the Appendix; average values of strength retention, rupture elongation and initial modulus at various air temperatures are presented graphically in Figures 39-43, 44-48 and 49-53 respectively. The tensile properties measured after a one-minute exposure to various bilateral radiant heat flux levels are included and are plotted at the appropriate equilibrium temperature of the quartz heaters. In Figures 39, 44 and 49 data for the HT-4 fabrics obtained during unilateral testing are also included.

For all fabrics with the exception of Kynol the observed variation of rupture strength retention with specimen temperature in hot air is well matched by that obtained for bilaterally irradiated specimens. The rupture elongation values agree well for the HT-4 and cotton fabrics, but for the Durette, Nomex I and Kynol fabrics the level of rupture elongation in the irradiated specimens is much lower than that for those specimens heated more slowly although the shape of the curves is similar in each case. The lack of agreement in this property may relate in part to the shape of the stress-strain curve which for these three materials shows a definite yield and subsequent flow region; the stress-strain curves for the HT-4 and cotton, on the other hand, exhibit an increasing slope to failure. The modulus values, like the strength retention values, show generally good agreement between those specimens heated slowly in air and those heated quickly by radiation. The tensile properties of the unilaterally heated HT-4 fabric, plotted as a function of the average specimen equilibrium temperature in Figures 39, 44, and 49, are in generally good agreement with the those properties measured during bilateral radiant and convective heating even though the specimen equilibrium temperature in the unilateral case is not uniform and its measurement is subject to the errors inherent in thermocouple measurement in a radiant heat environment.

The equilibrium tensile strength retention, initial modulus, and, in some cases, the rupture elongation of fabrics irradiated at high heat flux levels, may be closely approximated by those tensile properties determined in air at the same specimen temperature. However, the transient tensile properties of the irradiated fabrics, particularly rupture elongation and modulus cannot be predicted for times prior to the achievement of thermal equilibrium without knowledge of the exact rate of temperature rise for a particular fabric in a particular heat flux.

3. Conclusions

Using specially designed test equipment the tensile strength, rupture elongation and modulus of fabric specimens can be reliably measured at high radiant heat flux levels after exposure times of a few seconds. The capacity of the various fabrics tested to protect an active wearer against thermal damage is limited by their ability to retain a significant portion of their original strength for times long enough to permit escape from a hot environment. None of those fabrics tested, which included HT-4, Durette, Nomex I, Kynol, cotton, nylon and polyester, could withstand with any appreciable degree of strength retention radiant heat fluxes higher than $0.9 \text{ cal/cm}^2/\text{sec}$ for times longer than 3 seconds. Of the fabrics tested, HT-4 fabric retains the greatest amount of strength and, hence, offers the greatest degree of protective capability, during exposures to heat fluxes as high as $0.9 \text{ cal/cm}^2/\text{sec}$ for exposure times of a few seconds to one minute; polyester fabric offers the poorest protective capability under these conditions.

Table 4 summarizes those fabrics in the lighter weight group which includes HT-4, Durette, Nomex I and Kynol, which can withstand 3 and 6 second exposures to various radiant heat fluxes in the range 0.2 and $0.9 \text{ cal/cm}^2/\text{sec}$ while retaining either 25% or 50% of their original strength. As shown, HT-4 and Kynol fabric each retain 25% of their strength for 3 seconds at flux levels as high as $0.8 \text{ cal/cm}^2/\text{sec}$; Durette and Nomex I retain 25% strength for 3 seconds at flux levels of $0.6 \text{ cal/cm}^2/\text{sec}$. The general range of radiant heat flux values over which most of the fabrics offer some degree of protection to an active wearer during short exposures is startlingly low.

4. Future Work

The strength retained by a fabric during thermal exposure is most important in determining its ability to remain intact under physical stress. However, the ability of the fabric to resist tearing and survive flexing without cracking during exposure are also important aspects of its protective capacity and should be investigated. Tearing strength determinations can be made using the experimental arrangement described herein for bilateral tensile testing by modifying the standard tongue-tear test specimen so that it is symmetrical with respect to the direction of applied force and applied heat. The changes during exposure in all of the fabric tensile properties, including rupture elongation and modulus, will undoubtedly influence the fabric tearing behavior.

The changes in bending stiffness of the fabric subjected to bilateral radiant heat while it is being flexed could also be determined using the present test equipment in conjunction with a test method which involves rolling loops of fabric between parallel plates, in this case, the heater surfaces themselves. This bending test would also yield information about interfiber frictional forces and adhesions.

TABLE 4

FABRICS WHICH RETAIN 25% AND 50% OF THEIR ORIGINAL STRENGTH
OVER SHORT EXPOSURES AT VARIOUS RADIANT HEAT FLUX LEVELS

Incident Radiant Heat Flux (cal/cm ² /sec)	25% Strength Retention		50% Strength Retention	
	<u>3 sec</u>	<u>6 sec</u>	<u>3 sec</u>	<u>6 sec</u>
0.2	all	all	all	all
0.4	all	HT-4 Durette Nomex I	HT-4 Durette Nomex I	HT-4
0.6	all	HT-4	HT-4	none
0.8	HT-4 Kynol	none	none	none
0.9	HT-4	none	none	none

As mentioned earlier in the text, the tensile properties of additional fabrics should be determined with heaters in the unilateral configuration in order to validate the conclusion that only total heat flux and not heating pattern is relevant to the rate of fabric degradation in a radiant heat environment. The properties of cotton fabrics of lower weight and darker color should be determined and compared with those of the HT-4, Durette, Nomex I and Kynol.

In addition, the mechanical properties of new protective fabrics in a radiant heat environment may be determined using the test methods developed as the need arises.

III. REACTION OF HT-4 FABRIC TO LAUNDERING

Sixteen green HT-4 fabric samples were repeatedly laundered to determine the amount of shrinkage and change in surface appearance which would result. The fabrics were identified according to their constructions as 101, 102, 103 or 104. Those marked with a suffix A had been calendered, those marked with B had not. Duplicate specimens of each of the eight fabric types were sent to FRL, one to be removed after 5 laundering cycles, and the other after 15 cycles.

Laundering was done in a Kenmore Model 600 automatic washer and a Kenmore electric tumble dryer. Each cycle consisted of the standard wash in water containing 50 grams of AATCC standard detergent (without optical brightener) at a temperature of 140°F, and a setting corresponding to a 12-minute wash. The fabrics were removed from the washer immediately following the final spin cycle, and tumble-dried for 60 minutes at 140°-160°F.

Shrinkage was measured after 5 and 15 launderings, and the results are given in Table 5. Changes in surface appearance were determined visually by viewing the fabrics on a flat horizontal surface under diffuse illumination. These changes consisted of the development of frosting and pilling, and are recorded in Table 5 in qualitative terms as noticeable, appreciable or severe. These ratings are based on comparisons within each group, but may not represent comparisons between groups.

IV. ABRASION OF KEVLAR WEBBINGS

Preliminary measurements carried out using the AFML Webbing Abrader have shown that Kevlar webbing has very poor resistance to abrasive damage. For example, a 1-inch wide 2/2 herringbone twill (center reversal) webbing woven from 1500 denier Kevlar 29 yarn showed a strength reduction of 80% after 2500 cycles of rubbing on the hexagonal bar of the abrader, which compares very unfavorably with a loss of less than 10% which is characteristic of nylon webbings of a similar construction. The abraded webbing shows some unusual features which are worthy of more detailed study. The webbing face which is in contact with the hexagonal bar during the abrasion shows very serious deterioration of the surface warp yarns, as might be anticipated (Figure 54). However, a large amount of structural reorganization on the other face of the webbing is also apparent where the magnitude of the crimp in the warp yarn is greatly increased, causing the webbing to take on the appearance of a looped pile fabric (Figure 55), which differs considerably from the original appearance (Figure 56). There is a concomitant increase in the

TABLE 5

LAUNDERING SHRINKAGE OF CALENDERED
AND UNCALENDERED HT-4 FABRIC

Fabric Identification Number	No. of Launderings	% Shrinkage		Frosting and Pilling
		Warp	Filling	
101A*	5	0.1	0.7	Noticeable
101B*	5	0.5	2.9	Appreciable
101A	15	0.1	1.4	Appreciable
101B	15	0.6	2.8	Severe
102A	5	0	0.3	Noticeable
102B	5	(0.3)**	2.4	Appreciable
102A	15	(0.3)	1.6	Appreciable
102B	15	(0.5)	0.7	Severe
103A	5	0.3	0.3	Noticeable
103B	5	0.7	1.6	Appreciable
103A	15	0.3	0.6	Appreciable
103B	15	0.4	1.6	Severe
104A	5	0.5	0.5	Noticeable
104B	5	1.7	0.7	Appreciable
104A	15	1.0	0.5	Appreciable
104B	15	1.8	0.3	Severe

A* = Calendered

B* = Uncalendered

**() Increase

thickness of the fabric, and a decrease in length of the abraded region. The webbing geometry is quite stable in its deformed state, and the excess crimp cannot be pulled out by simple hand elongation. The stability of the configuration is emphasized when it is realized that the foreshortening of the webbing takes place against an imposed tension of five pounds.

In an attempt to understand the underlying mechanics of this phenomenon, samples of webbing were subjected to controlled cycles of bending deformation in the FRL bending tester. In this test technique loops of webbing are constrained between two parallel plates which are moved relative to each other so as to roll the loop of fabric back and forth. This subjects each element of the webbing to a repetitive cycle of bending between zero strain and a maximum curvature set by the geometry of the plate separation and the thickness of the fabric. Figure 57 shows a section along the warp yarns of a Kevlar webbing bent in the same configuration as in the FRL bending tester. Figure 58 shows the same fabric in the identical configuration after 3200 cycles of bending. The flexed webbing shows the same characteristics as were found for the webbing tested on the hexagonal bar abrader: greatly increased crimp height, leading to an increase in the fabric thickness, together with a foreshortening of the flexed region. There is no surface abrasion of the webbings in the FRL tester, but it is clear that the high loops of unconsolidated yarns would be very prone to abrasive damage. It appears that there is some feature of the Kevlar webbings which is conducive to this very unusual, and hitherto unreported, type of deformation on repeated bending. These observations have obvious implications in view of the potential utilization of Kevlar in applications where there will be a flexing component of loading.

V. CROSS-SECTIONS OF NOMEX, HT-4 AND E-11 FABRICS

Figures 59, 60 and 61 show cross-sections made of yarns taken from dyed fabrics made from Nomex and HT-4, as well as a new fiber type referred to by E. I. DuPont de Nemours & Company, Inc. as E-11. The Nomex fiber has an elongated, dogbone shaped cross section. The cross-section of HT-4 fiber is round. E-11 is seen to be made up primarily of Nomex fibers, with evidence of a few HT-4 fibers which were blended in.

VI. CROSS-SECTION OF DYED KYNOL/NOMEX BLEND

Figure 62 shows a cross-section which was made of yarn taken from a dyed Kynol/Nomex blended fabric. The section shows the Nomex fibers to be undyed, and the Kynol fibers dyed throughout the whole of the cross-section, except for a few Kynol fibers (identified by their round cross-section) which appear to be completely undyed.

VII. BBB FABRIC

We received from AFML 1.8 lb of 185 denier, 50 filament BBB yarn, and 0.036 lb of 37 denier, 10 filament BBB yarn, with a request to weave some lightweight fabric. There was insufficient 37 denier yarn for weaving, so nothing was done with it. The 185 denier yarn was woven into a fabric similar in construction to MIL-C-8021 Type I.

Six yards of 3-1/4 inch wide tape was woven first to develop a suitable construction, and then 7 yards of 18-1/2 inch wide fabric was woven in the same construction. This was a 2 x 2 twill, 70 ends and picks per inch, using singles yarn in warp and filling, 5Ztpi twist in the warp, zero twist in the filling.

Both of these items were delivered to AFML.

VIII. DEFECTS IN POLYCARBON FABRIC

We were asked to examine a defective piece of polycarbon fabric which has been obtained by the Air Force from an unnamed source. Certain defects were obvious even on casual examination. The fabric was lined with warp streaks caused by a few warp yarns which were blacker and shinier than the rest. The surface was covered with protruding broken yarn ends. There were many knots and yarn splices. There were many long warp floats over several filling yarns in a basic double-face, 8-harness satin woven structure. There were clear signs that the fabric had been creased and, indeed, the piece was folded when we saw it, though good practice in handling such fabric would require a fairly large diameter roll to minimize damage while stored.

More detailed examination of faults revealed the following:

1. Several locations of obvious damage to warp and filling yarns, particularly at clearly identifiable old fabric creases.
2. Some locations where broken filling yarns caused long warp floats.
3. Some long warp floats which do not seem to be associated with broken filling yarns.
4. Some warp floats which appear to be long are, in fact, due to excess length of yarn in the loop.
5. Many splices in warp yarns.
6. Several instances of bunched and knotted warp yarns on the surface of the fabric, associated with a warp yarn break a few inches away.

Faults 1 and 2 are most likely the result of rough handling after weaving. Faults 3 and 4 probably are weaving faults. Faults 5 and 6 are the results of warp yarn breaks, probably due to problems during weaving.

Some warp and filling yarns were carefully unravelled from the fabric and their strength measured in an Instron tester after embedding the ends of the yarns of epoxy resin. The gauge length was ten inches, jaw speed one inch per minute. The results are given in Table 6.

TABLE 6
STRENGTH OF CARBON YARNS

Individual Warp Yarn Strength (lb)			From Warp Streaks	Individual Filling Yarn Strength (lb)	
8.6	8.4	8.6	6.0	10.7	10.8
9.5	8.6	12.0	10.4	10.0	11.1
7.7	13.1	8.4	9.1	10.9	8.6***
5.5	9.6	13.6	8.6	9.0	10.0
7.9*	6.8	15.9	9.4	9.2	8.6
12.5	9.7	12.3	10.1	7.3	7.0***
10.4	15.1	10.7	10.4	9.3	9.5
8.4	7.6	7.4	7.9	11.2	10.3
11.0	9.5	11.6		10.0	9.7
11.9	7.5	10.8		11.2	10.4
10.9	8.6**	11.1		10.9	5.6***
11.1	10.3	12.5		10.4	10.4
6.7	9.3	5.1		10.9	9.5
				10.0	10.2
Avg. 9.9 lb			Avg. 9.0 lb	Avg. 10.1 lb	
CV(%) 24.7			CV(%) 16.6	CV(%) 9.1	
Range 5.1-15.9 lb			Range 6.0-10.4 lb	Range 7.3-11.2 lb	

*Warp streak

**Long float

***Obvious damage - broken filaments - not included in average

Although the variability of the strength values is high, there is no indications that the yarn contains weak spots. The minimum strength quoted in the specification is six pounds. Only three out of a total of 75 specimens tested had strengths lower than this. There is no evidence that the blacker, shinier yarn causing the warp streaks differs significantly in strength from the remaining warp yarns. However, the yarn twist was somewhat higher than the 1.5 tpi in the specification given to us.

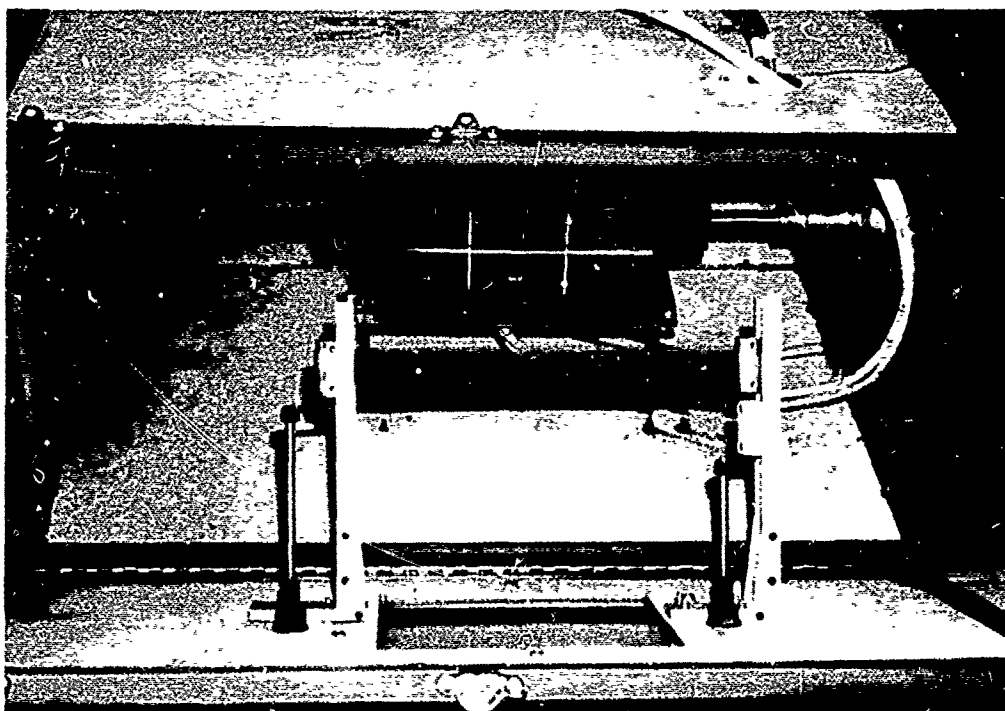
In summary, it appears that the yarn used came from two lots differing in appearance, but all the yarn would seem to be of reasonable strength. There is some evidence of weaving faults, and considerable evidence of unduly rough handling of the fabric. In particular, creasing of the fabric has damaged both warp and filling yarns.

IX. EXAMINATION OF FAILED DRONE RETRIEVAL PARACHUTE WEBBING

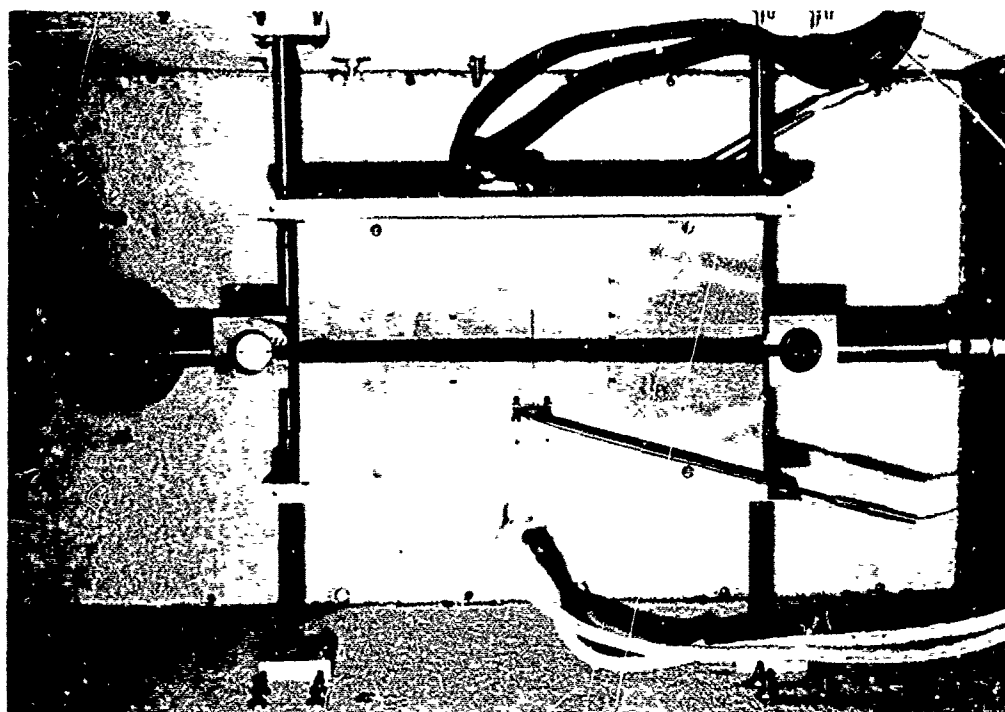
A sample of a parachute skirt engagement webbing which had failed during a retrieval maneuver was examined, and photomicrographs of the ruptured ends taken. We understand that the retrieval hook penetrated the canopy material and slid along the skirt webbing, nipping the canopy as it travelled, and creating sufficient frictional heat that the inner surface of the webbing suffered thermal damage. The hook was stopped by impacting a vertical member, causing the skirt engagement webbing to break some 15 inches away in the damaged section. It was stated that at the instant of failure the instrumented retrieval winch recorded a tension of ~4100 pounds. It was also observed that the break showed fibers of uniform length about halfway through the webbing, typical of a cutting action, and of non-uniform length through the rest of the cross-section, typical of a normal tensile failure.

This characteristic of the break is clearly shown in the photomicrographs, Figures 63a,b,c and 64a,b,c. Figure 63a shows the appearance of the two ends from the back side of the webbing, to which some canopy fabric is still sewn. The uneven nature of the break is clearly seen in this figure as well as in Figures 63b and c which are enlarged views of the broken ends. Figure 64a,b,c shows the same broken ends as viewed from the face side of the webbing, from which the apparent cutting is not visible.

Our examination confirms the previous observation that the webbing seems to be partially cut from the inside, but gives no clue as to the cause of the cutting.



(a)



(b)

Figure 1. Quartz Faced Radiant Heaters and Test Chamber:
(a) Specimen on Track Ready for Insertion;
(b) Specimen in Place Between Heaters.

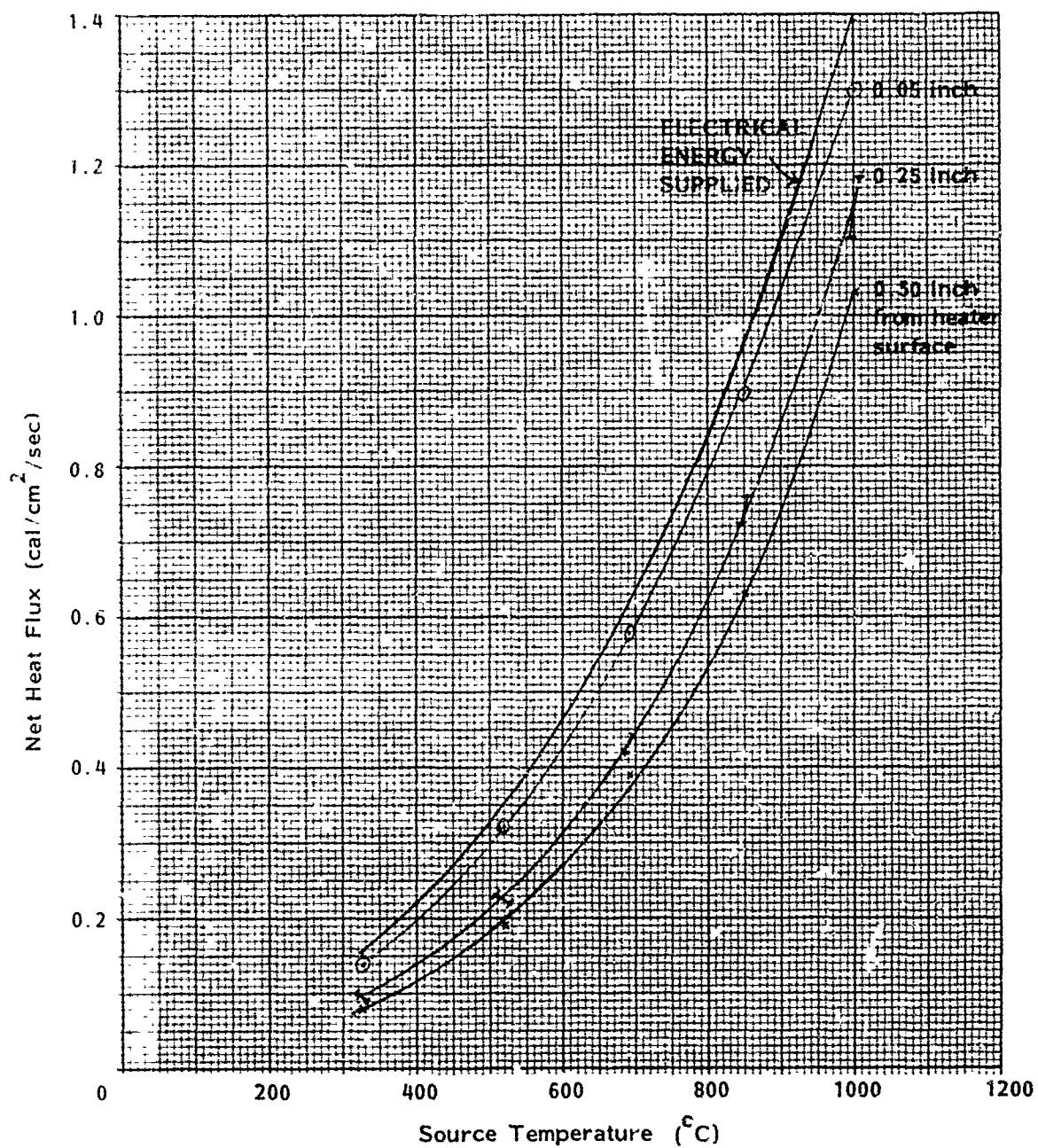


Figure 2. Unilateral Heat Flux Measured with Calorimeter at Various Distances from Surface of a Single Quartz Heater

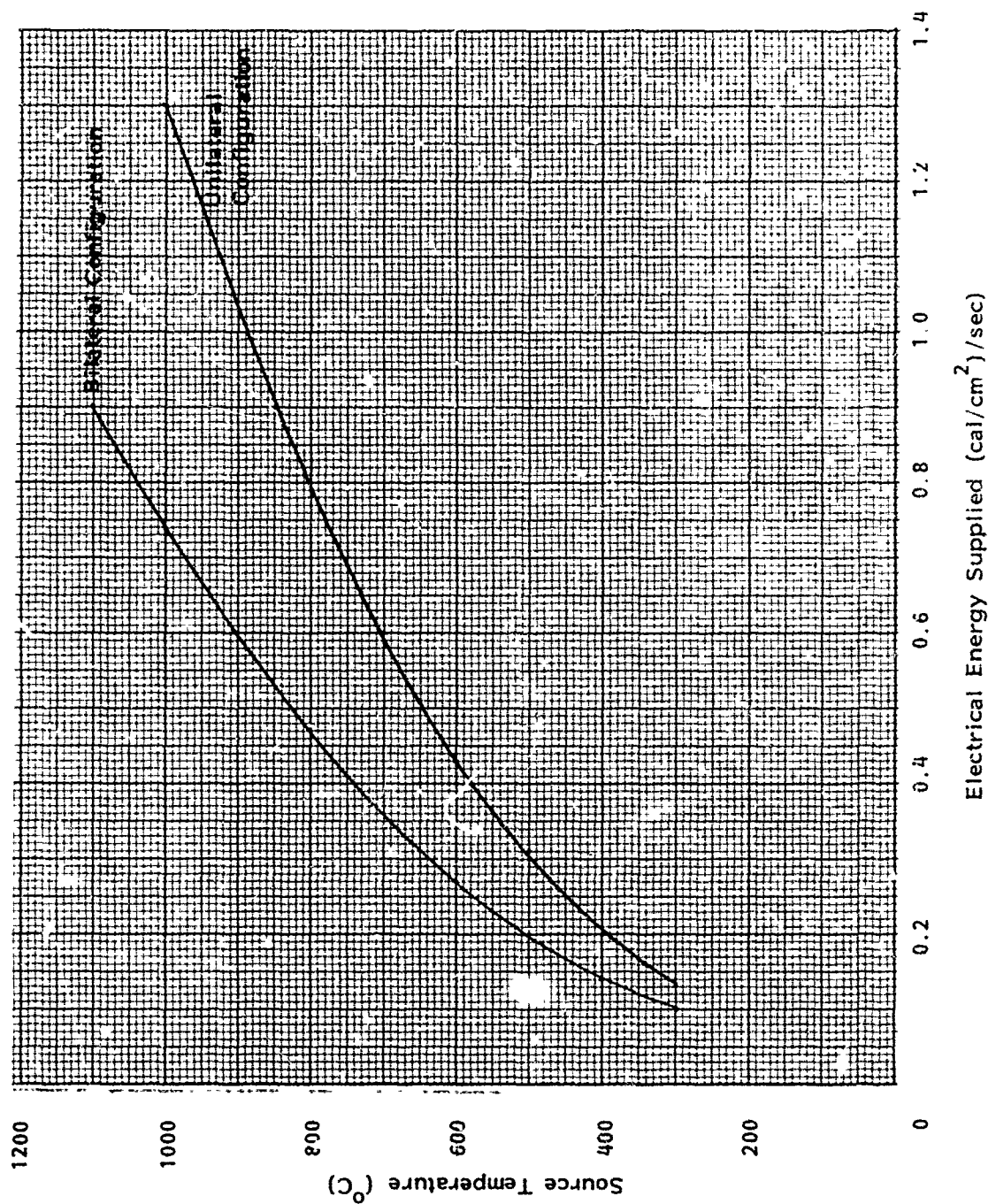


Figure 3. Temperature of Quartz Heaters in Unilateral and Bilateral Configurations as a Function of the Electrical Energy Supplied to Each Surface

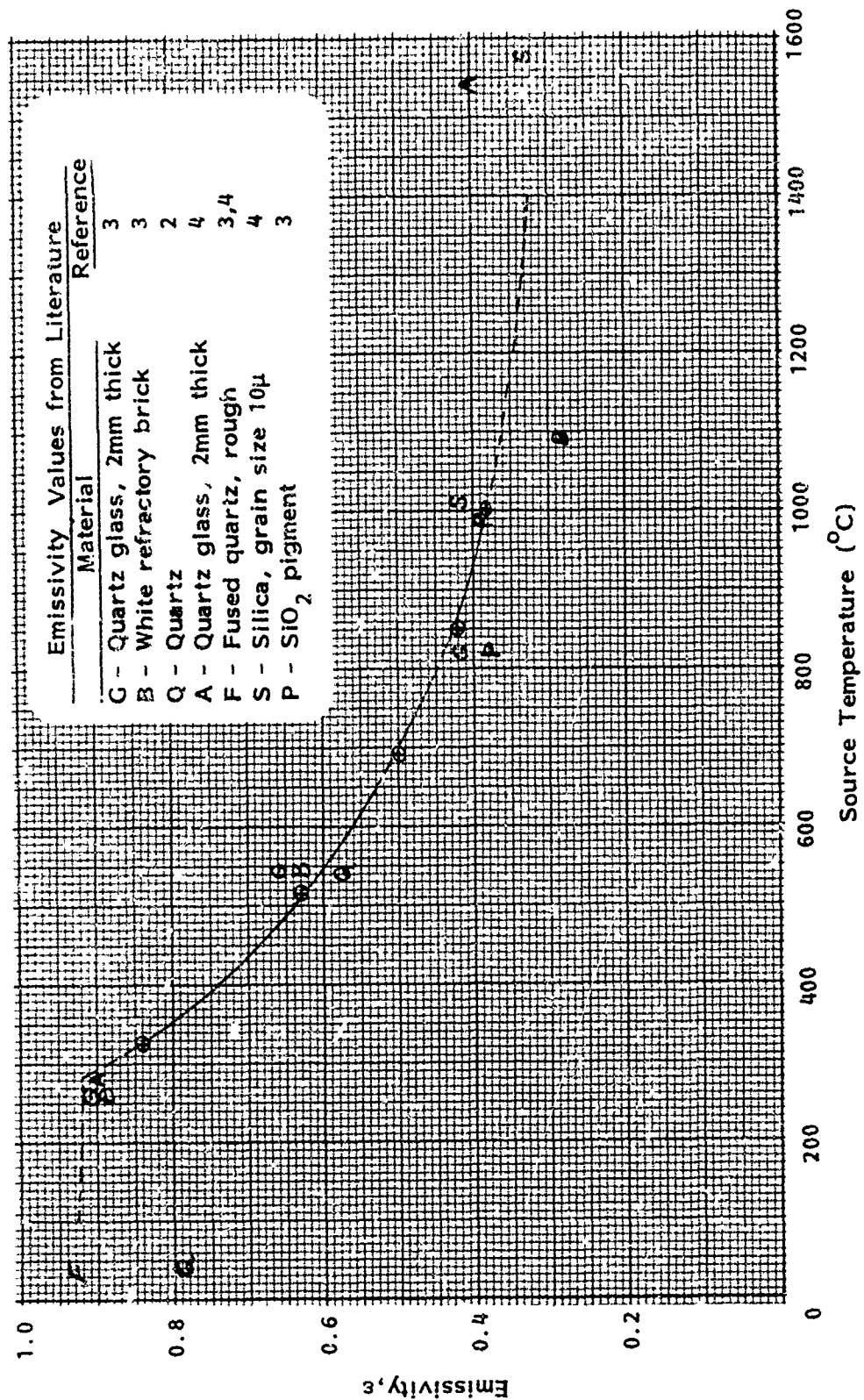


Figure 4. Emissivity of Quartz Radiant Heat Source

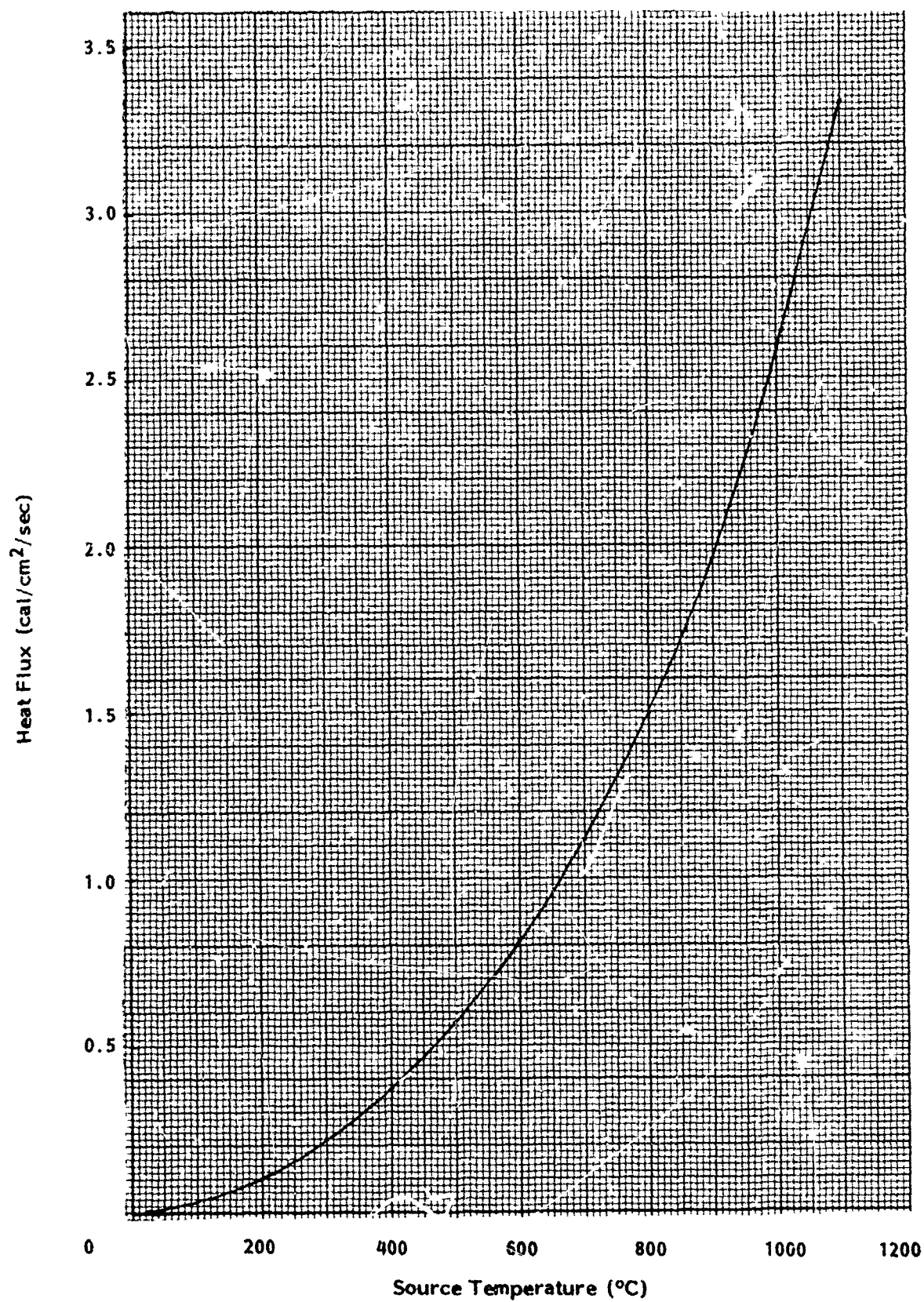


Figure 5. Initial Radiant Heat Flux on Fabric Surface in the Bilateral Configuration

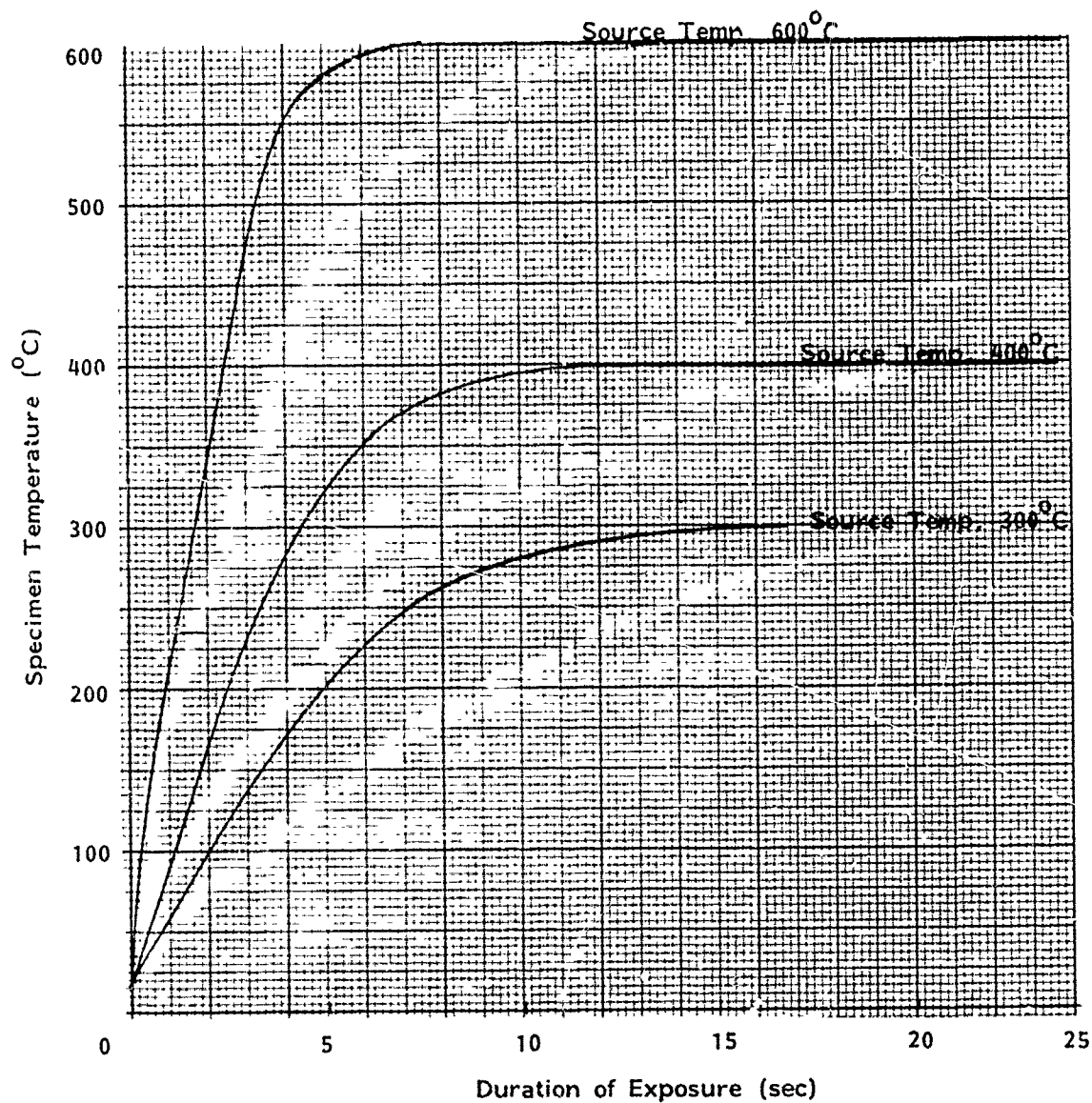


Figure 6. Estimated Temperature Rise of Specimen Located Between Quartz Heaters in Bilateral Configuration

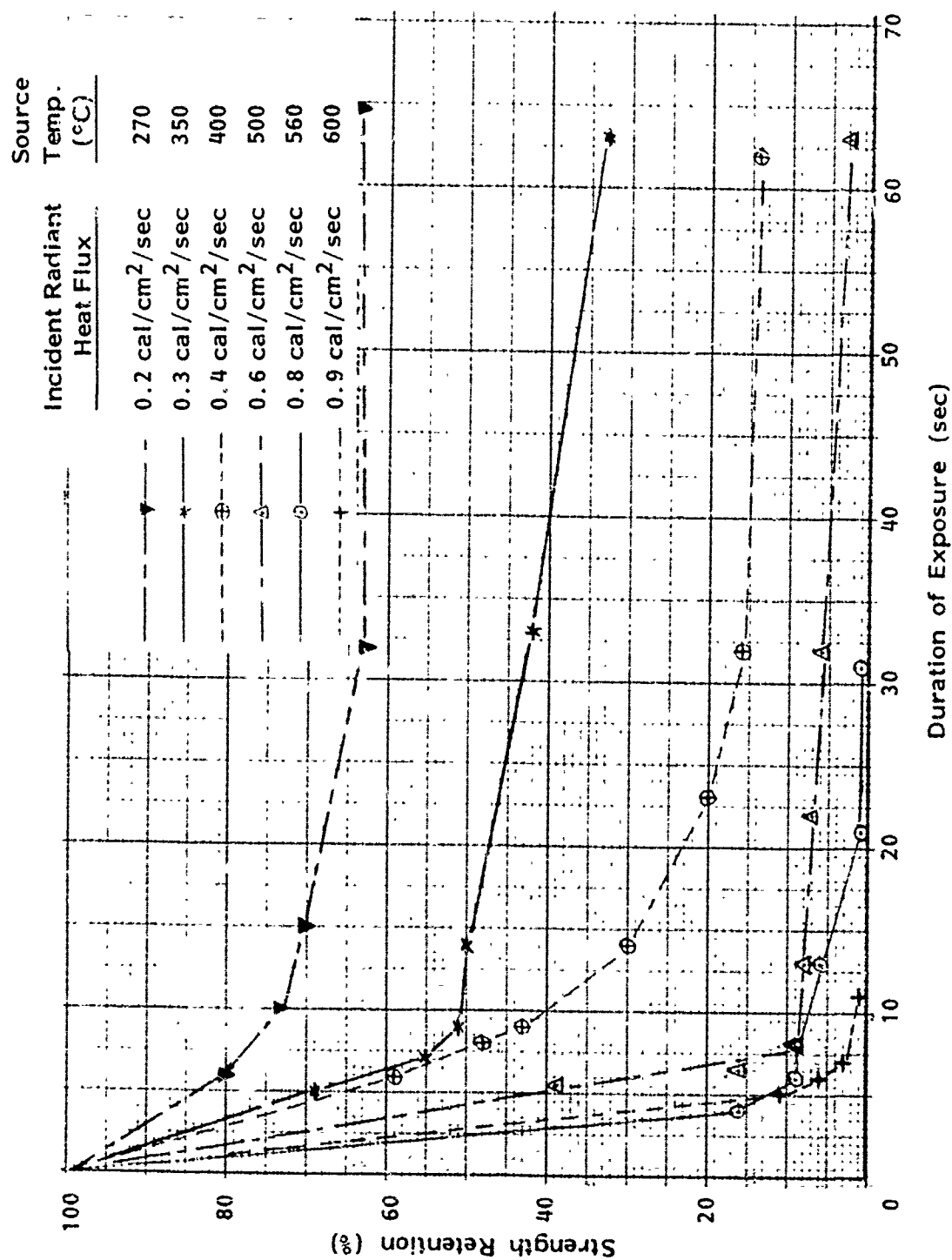


Figure 7. Strength Retention of HT-4 Fabric in the Filling Direction at Various Bilateral Radiant Heat Flux Levels

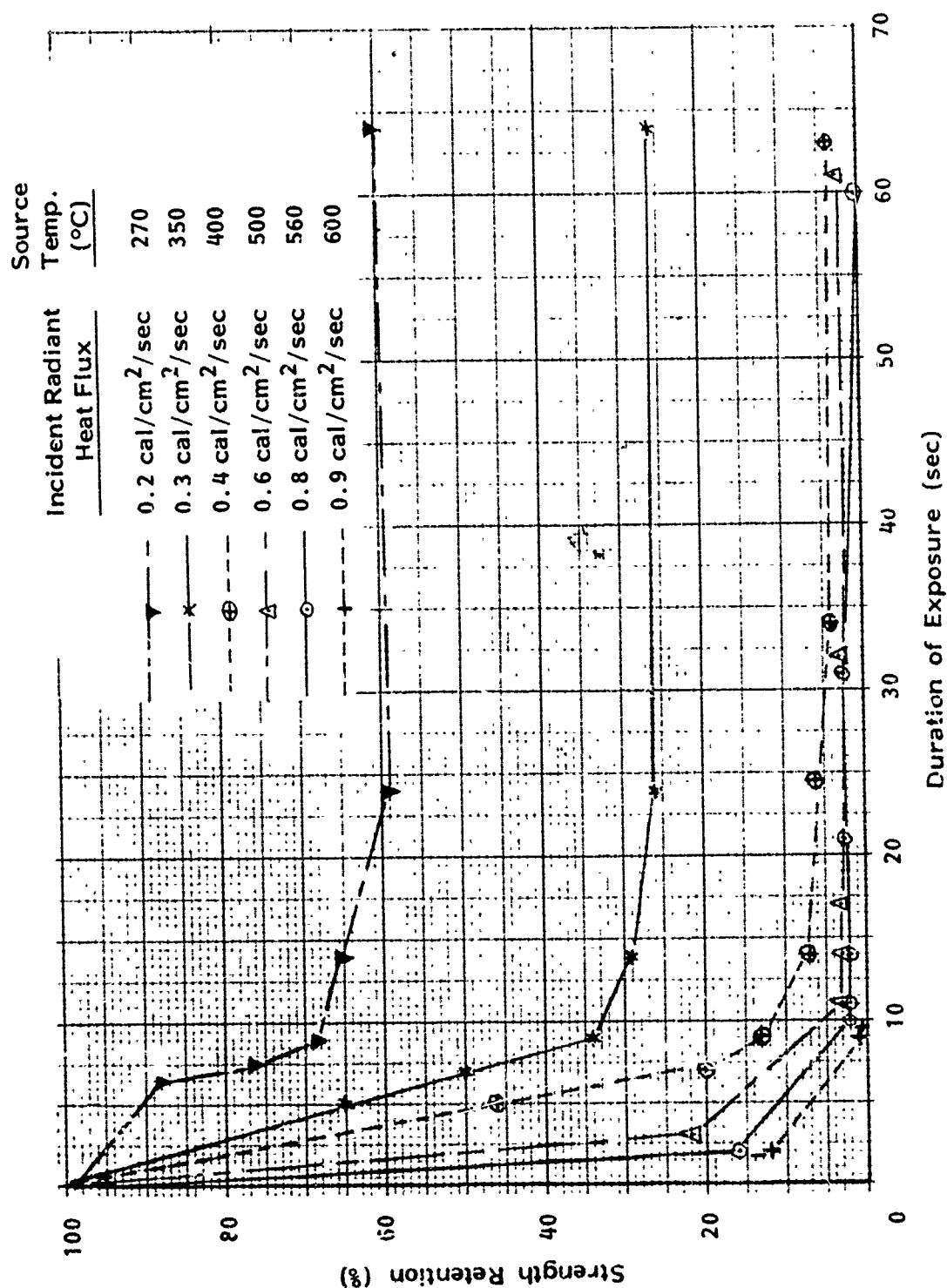


Figure 8. Strength Retention of Durette Fabric in the Warp Direction at Various Bilateral Radiant Heat Flux Levels

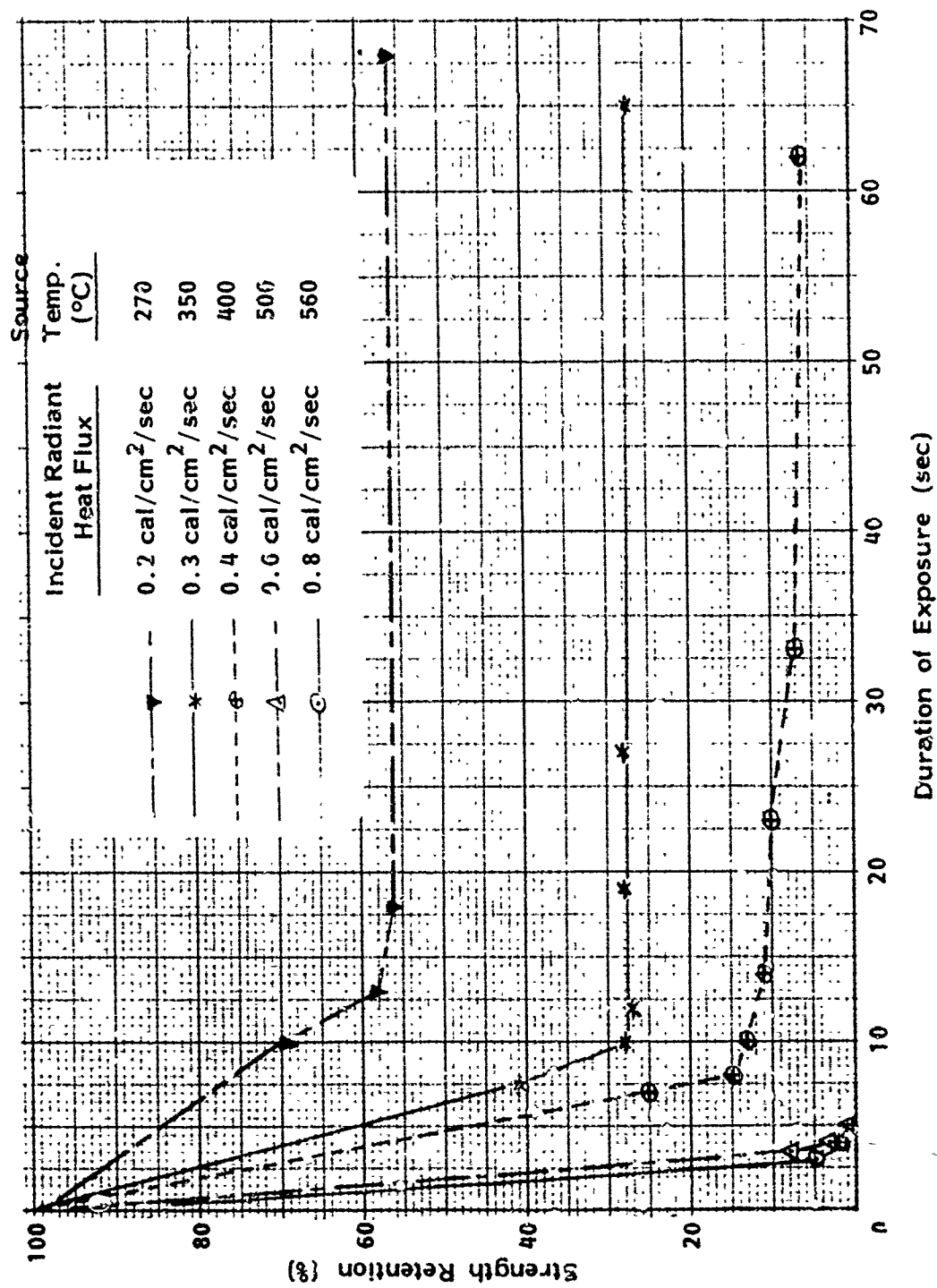


Figure 9. Strength Retention of Nomex I Fabric in the Warp Direction at Various Bilateral Radiant Heat Flux Levels

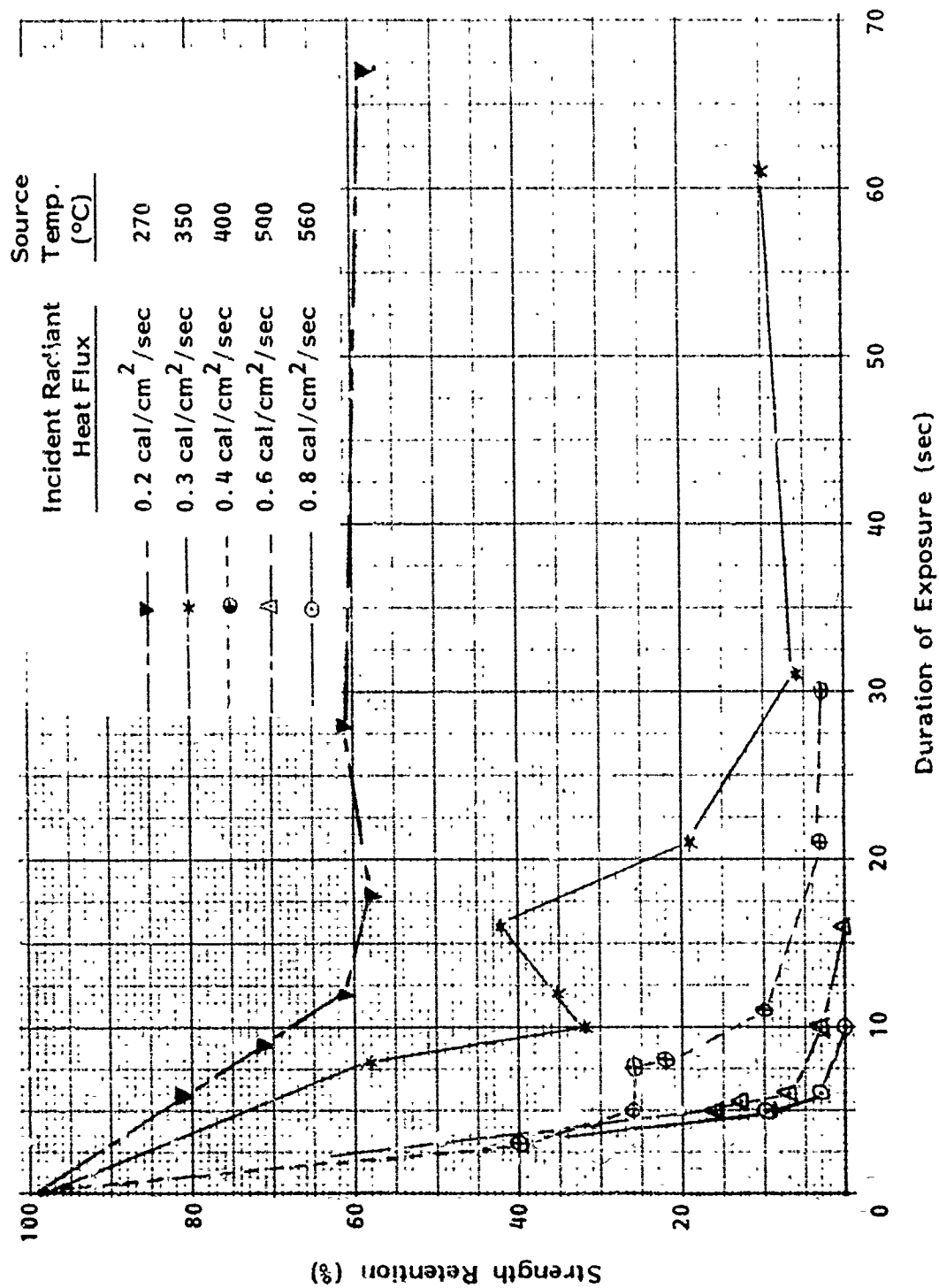


Figure 10. Strength Retention of Kynol Fabric in the Warp Direction at Various Bilateral Radiant Heat Flux Levels

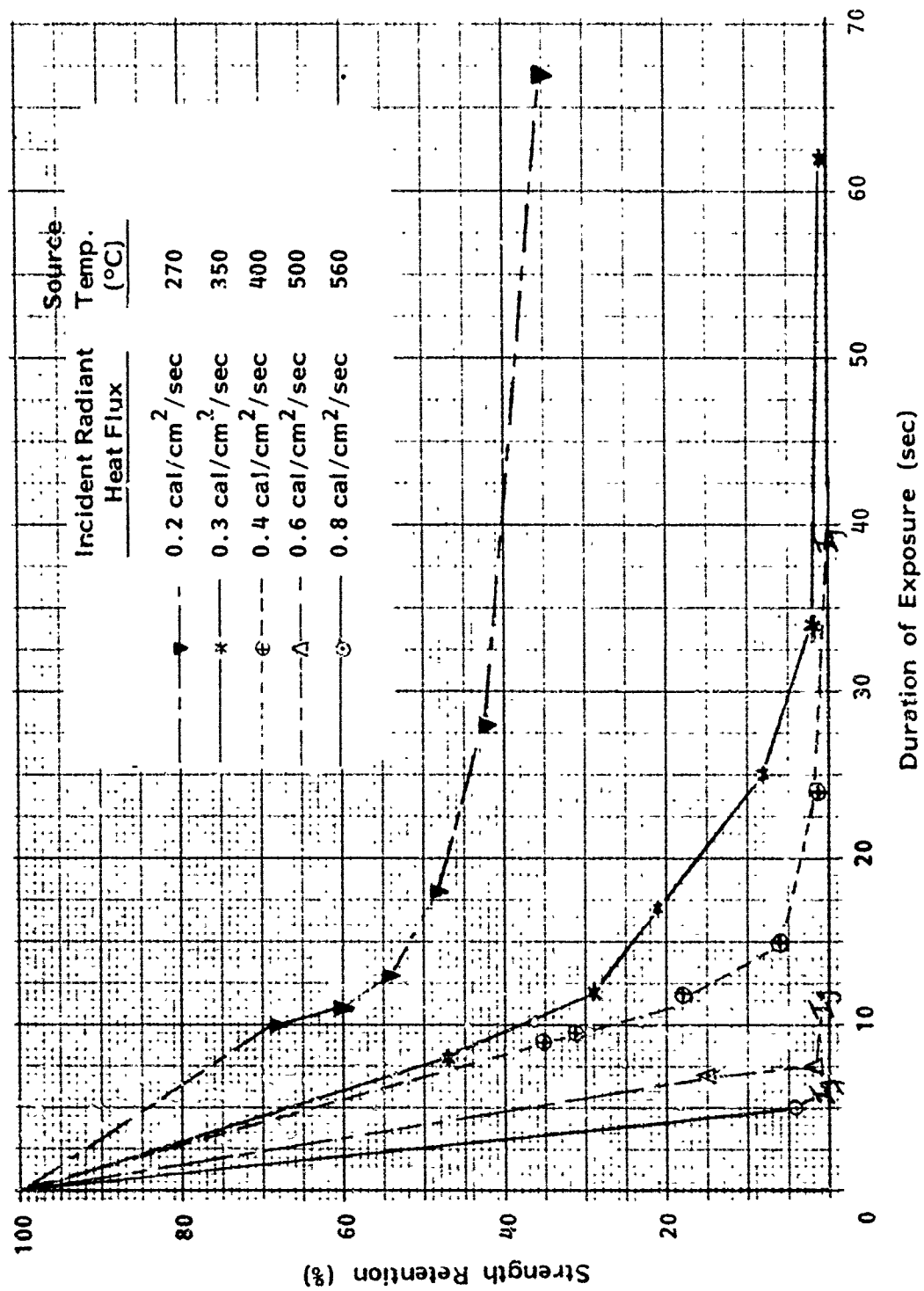


Figure 11. Strength Retention of Cotton Fabric in the Filling Direction at Various Bilateral Radiant Heat Flux Levels

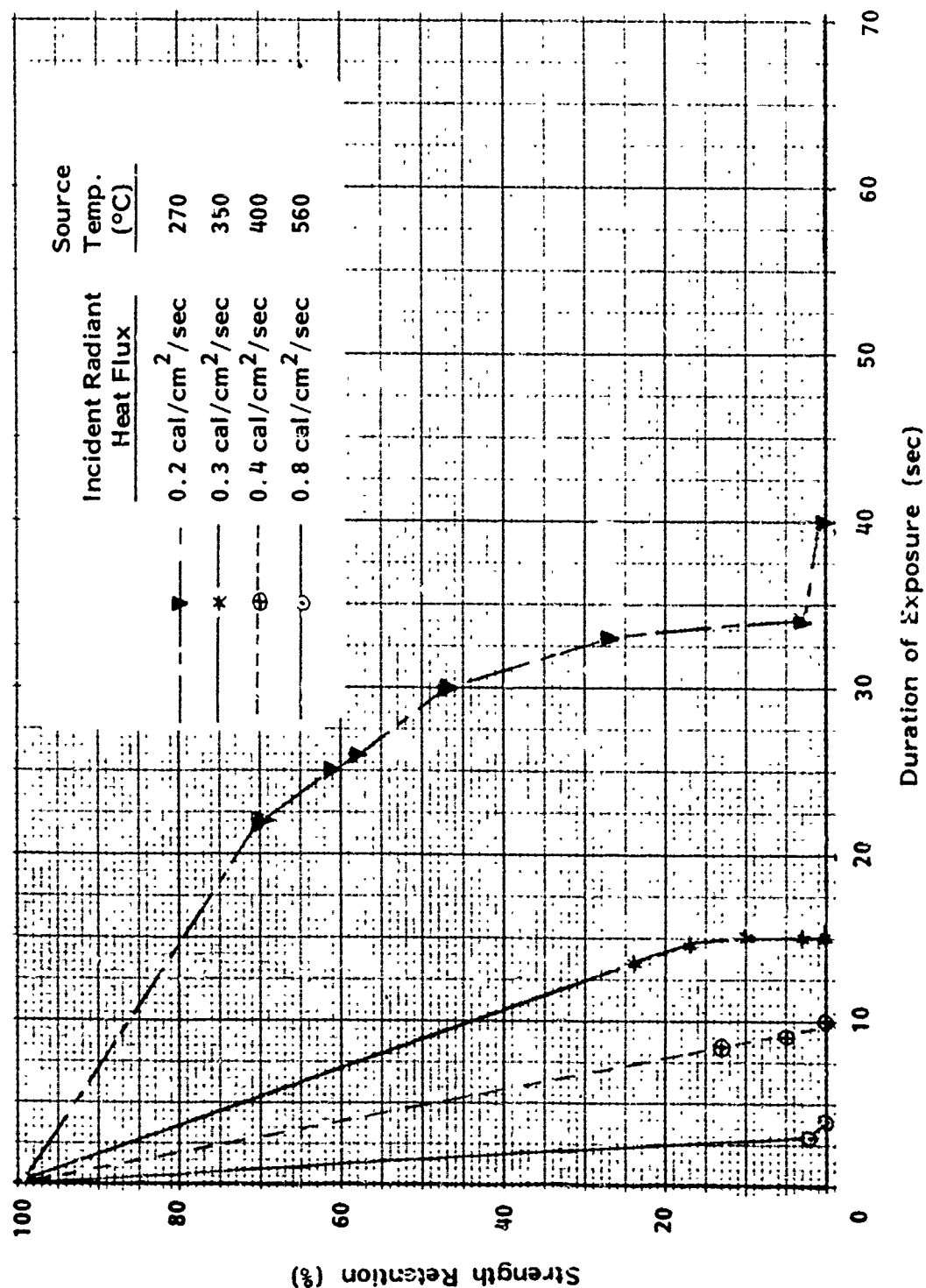


Figure 12. Strength Retention of Nylon Fabric in the Warp Direction at Various Bilateral Radiant Heat Flux Levels

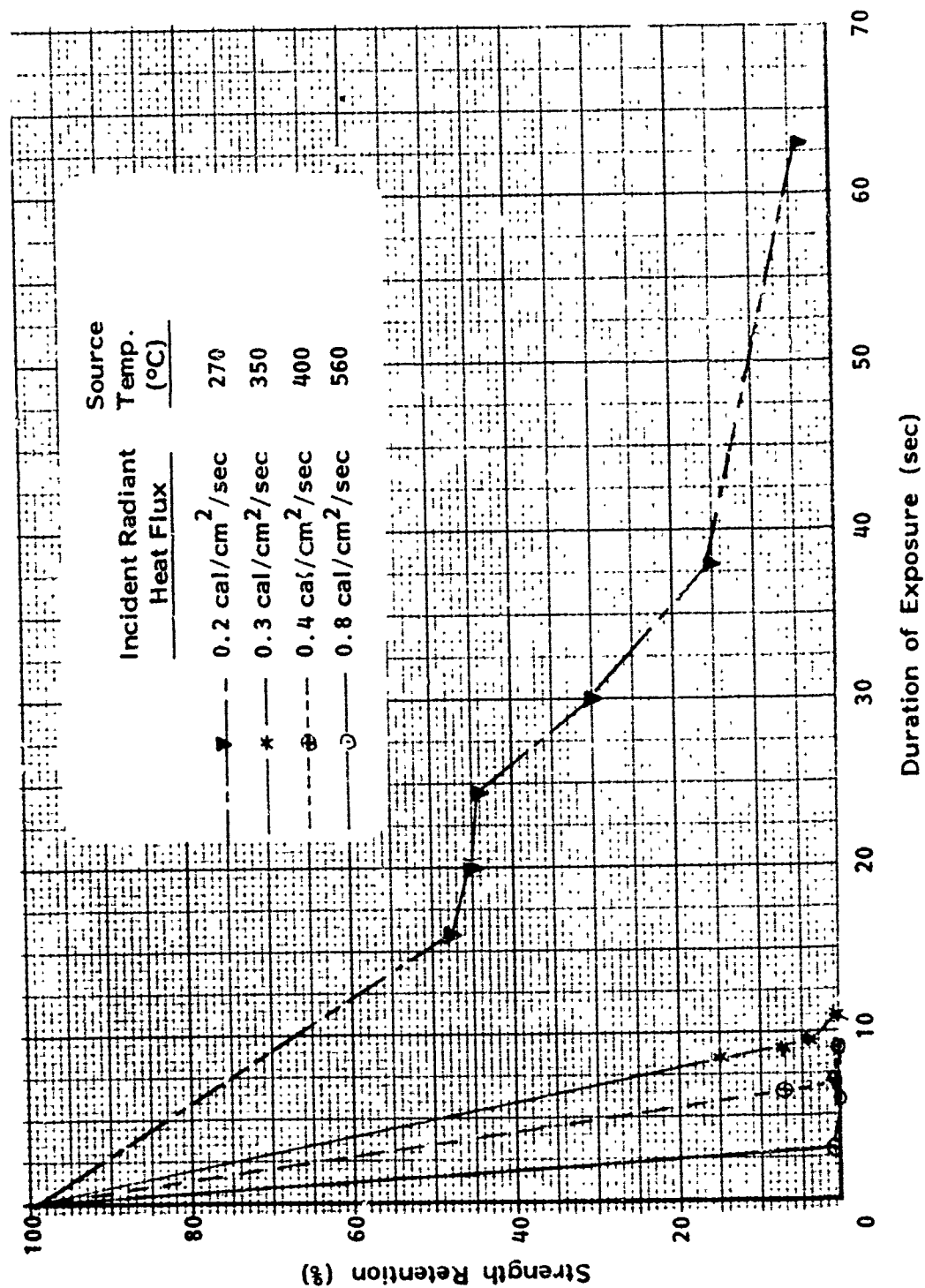


Figure 13. Strength Retention of Polyester Fabric in the Warp Direction at Various Bilateral Radiant Heat Flux Levels

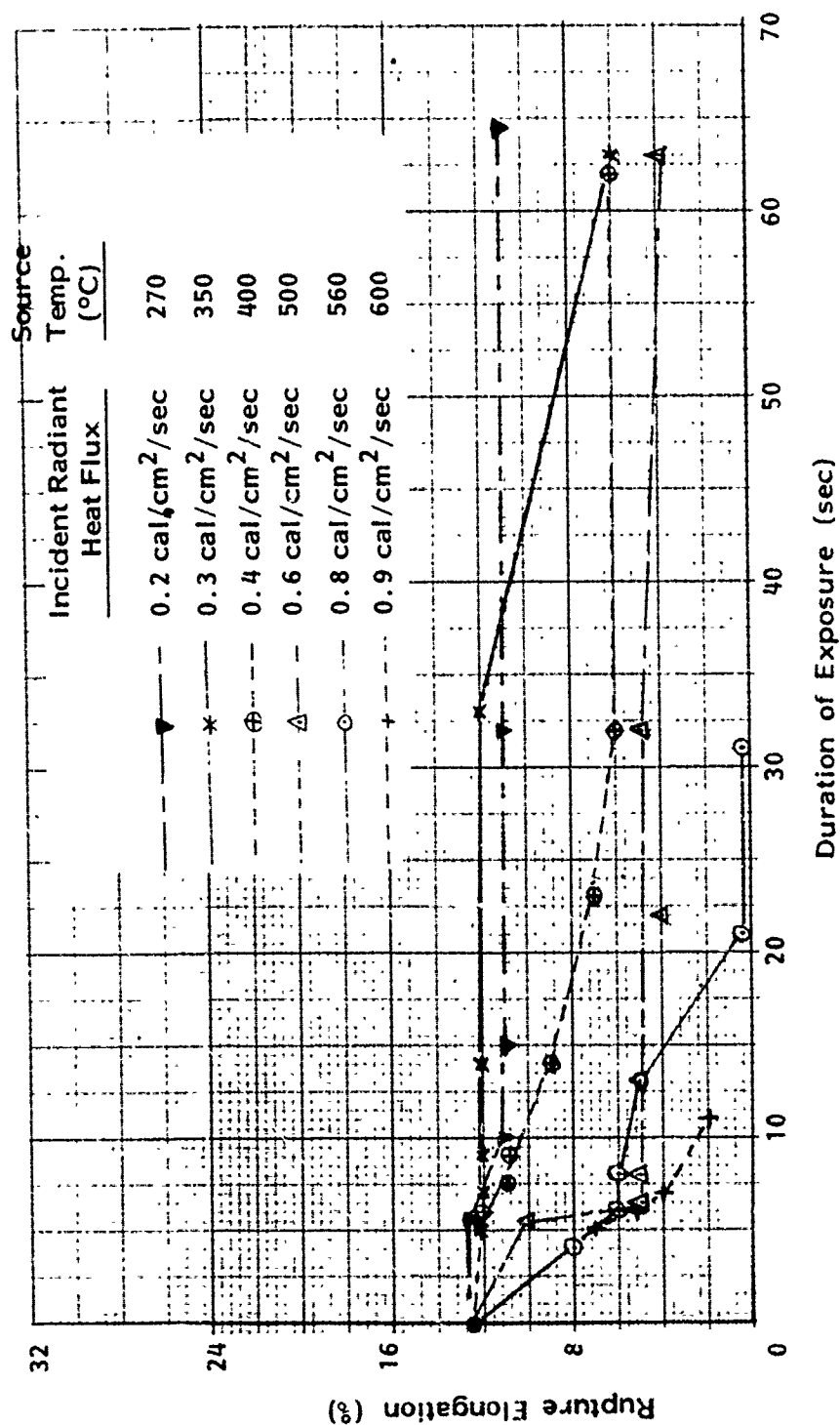


Figure 14. Rupture Elongation of HT-4 Fabric in the Filling Direction at Various Bilateral Radiant Heat Flux Levels

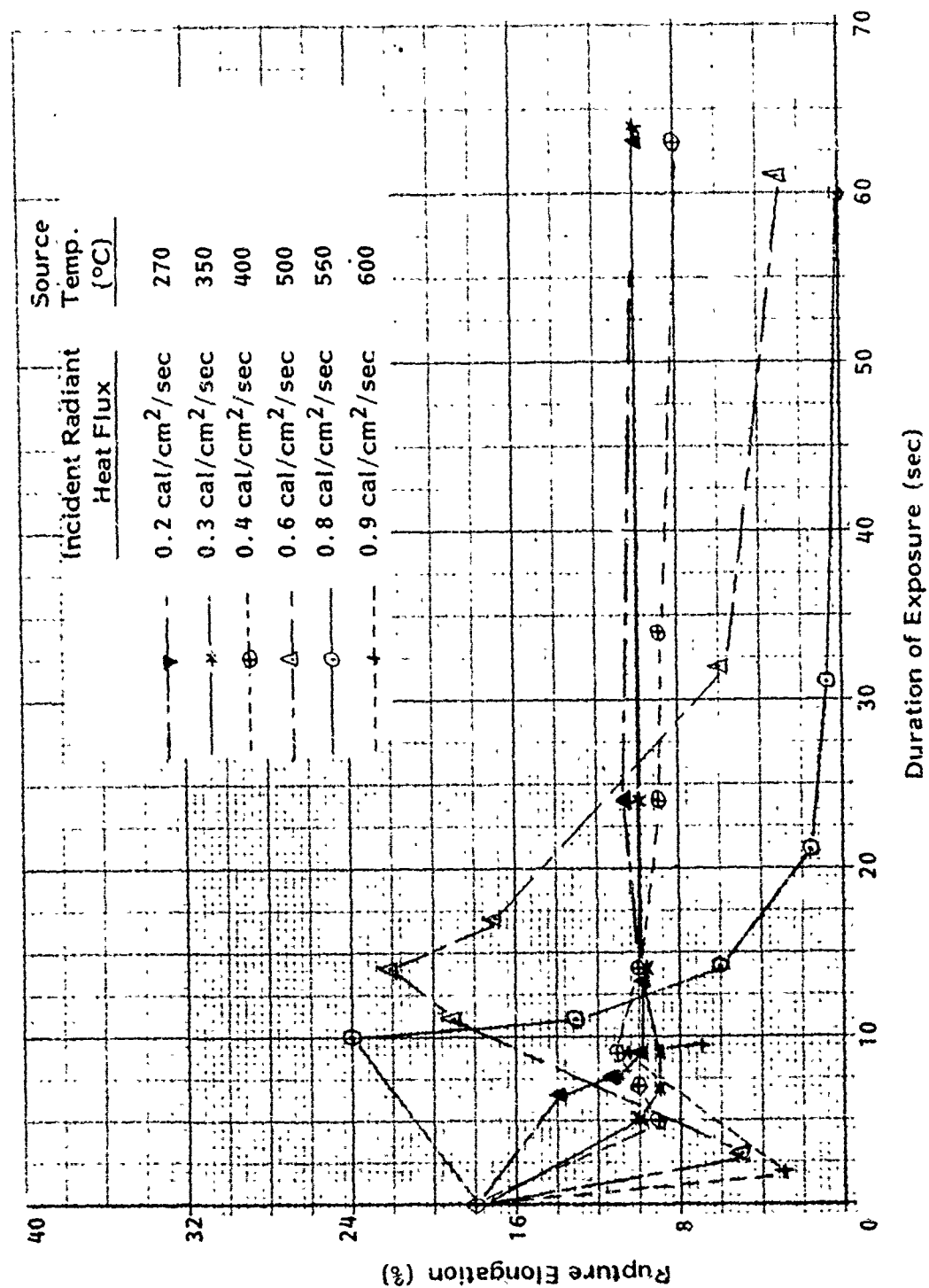


Figure 15. Rupture Elongation of Durette Fabric in the Warp Direction at Various Bilateral Radiant Heat Flux Levels

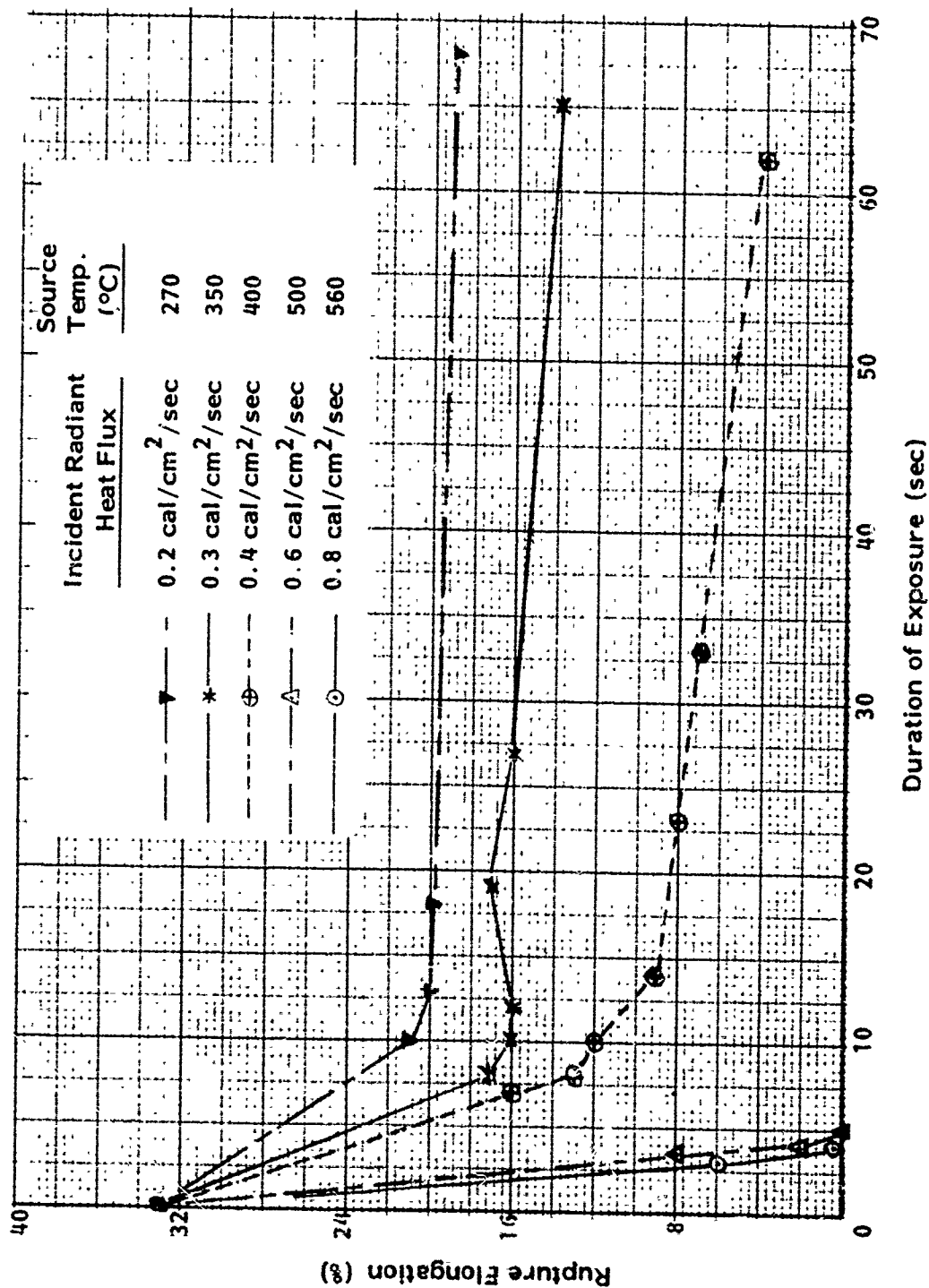


Figure 16. Rupture Elongation of Nomex I Fabric in the Warp Direction at Various Bilateral Radiant Heat Flux Levels

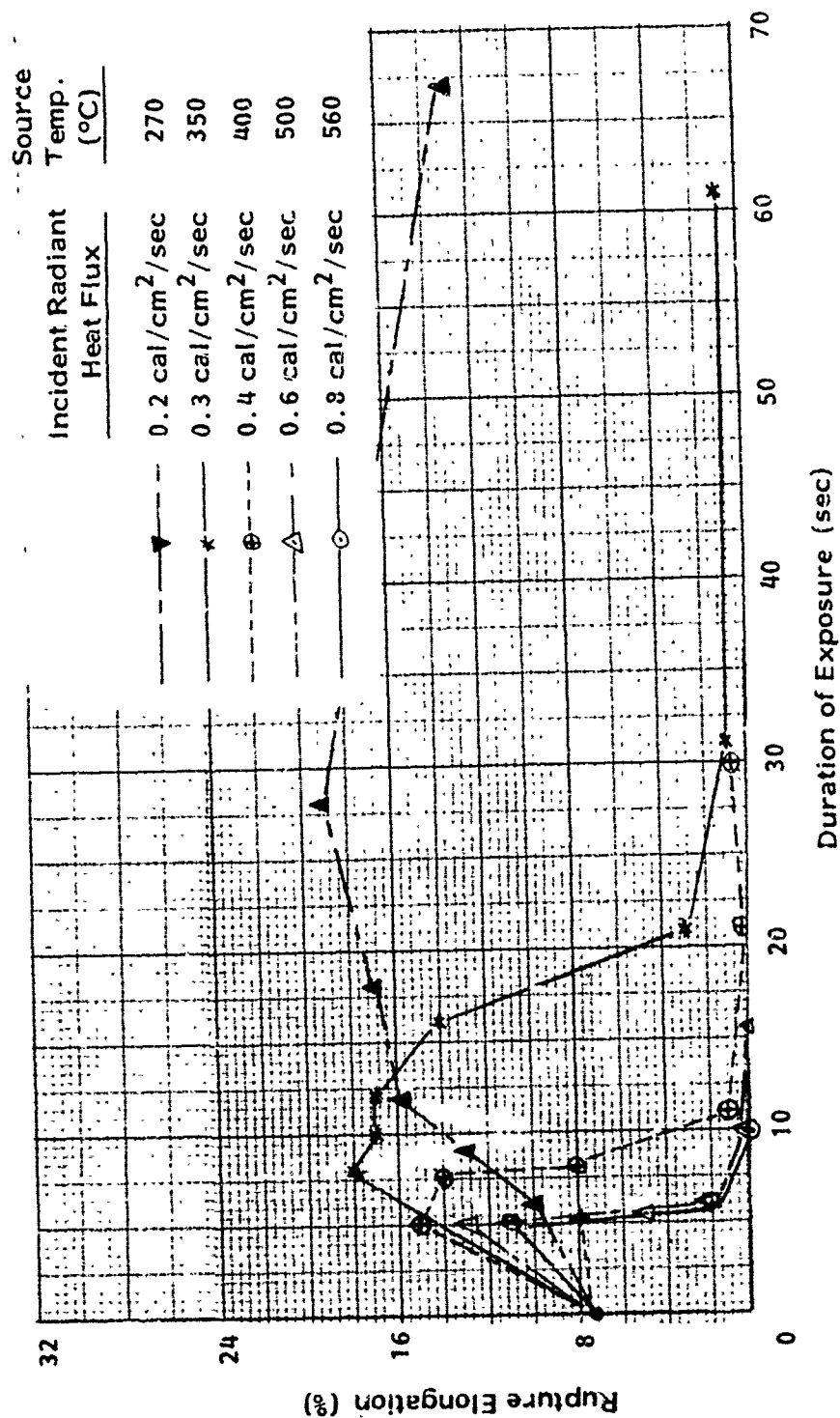


Figure 17. Rupture Elongation of Kynol Fabric in the Warp Direction at Various Bilateral Radiant Heat Flux Levels

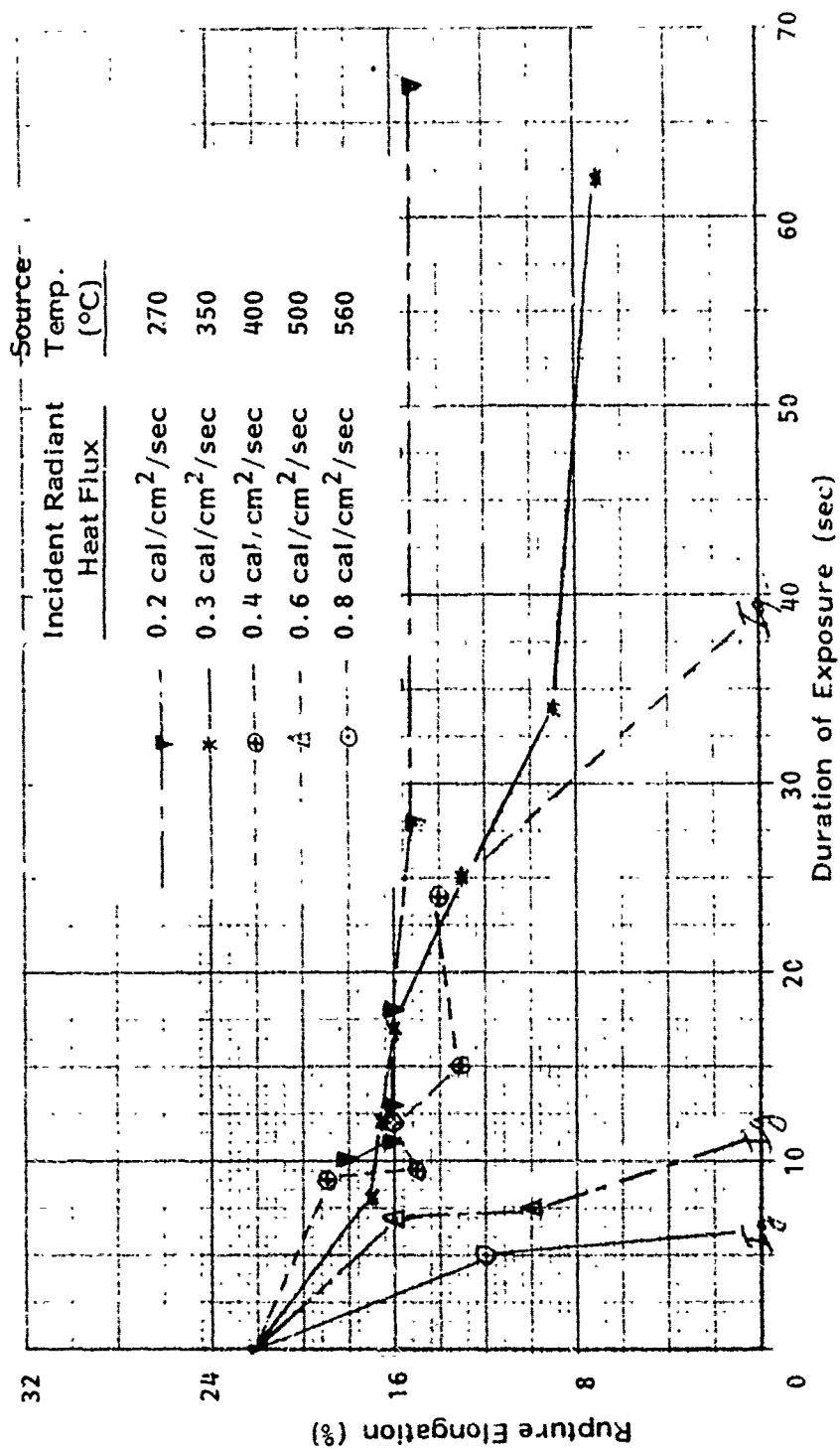


Figure 18 . Rupture Elongation of Cotton Fabric in the Filling Direction at Various Bilateral Radiant Heat Flux Levels

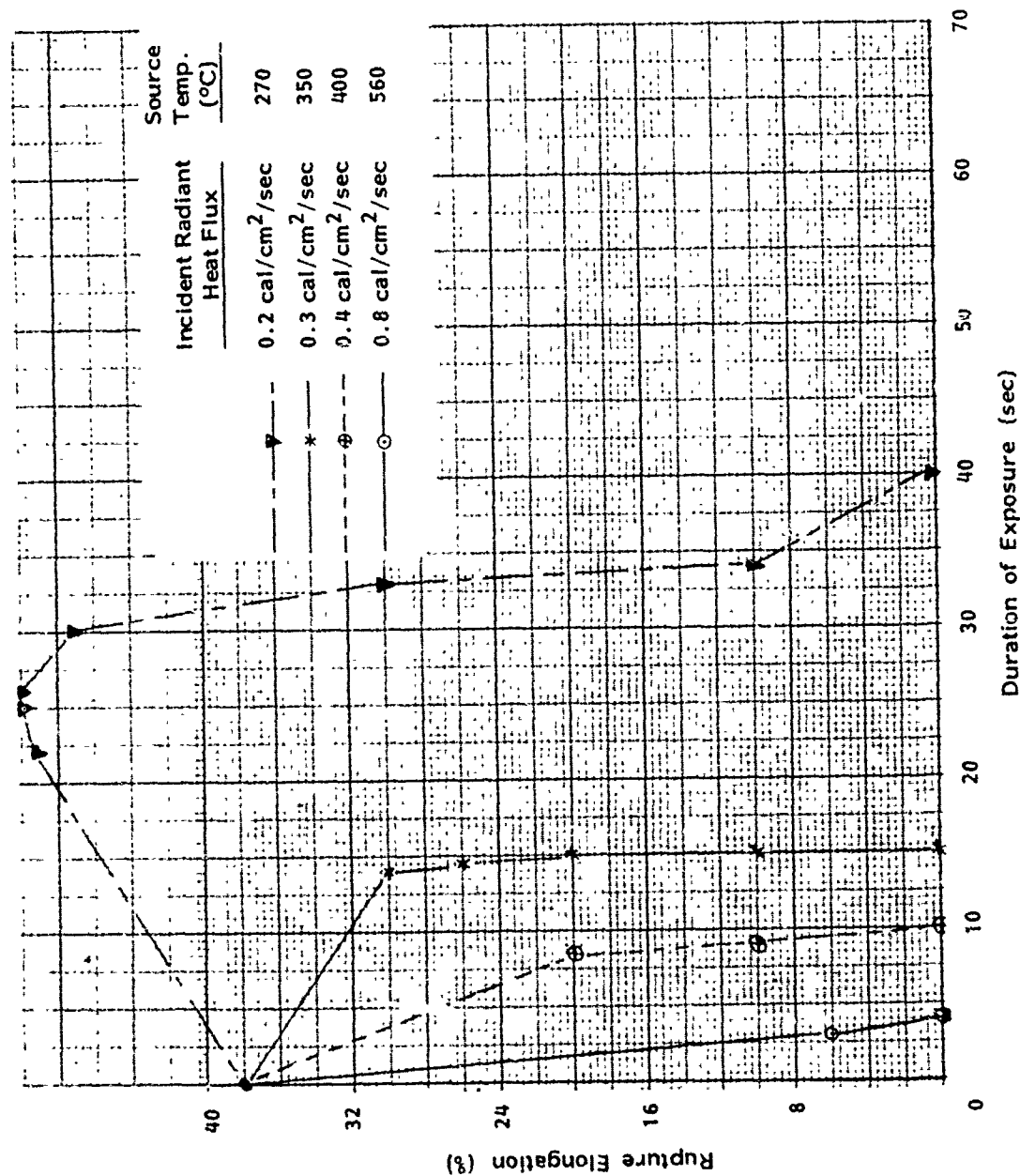


Figure 19. Rupture Elongation of Nylon Fabric in the Warp Direction at Various Bilateral Radiant Heat Flux Levels

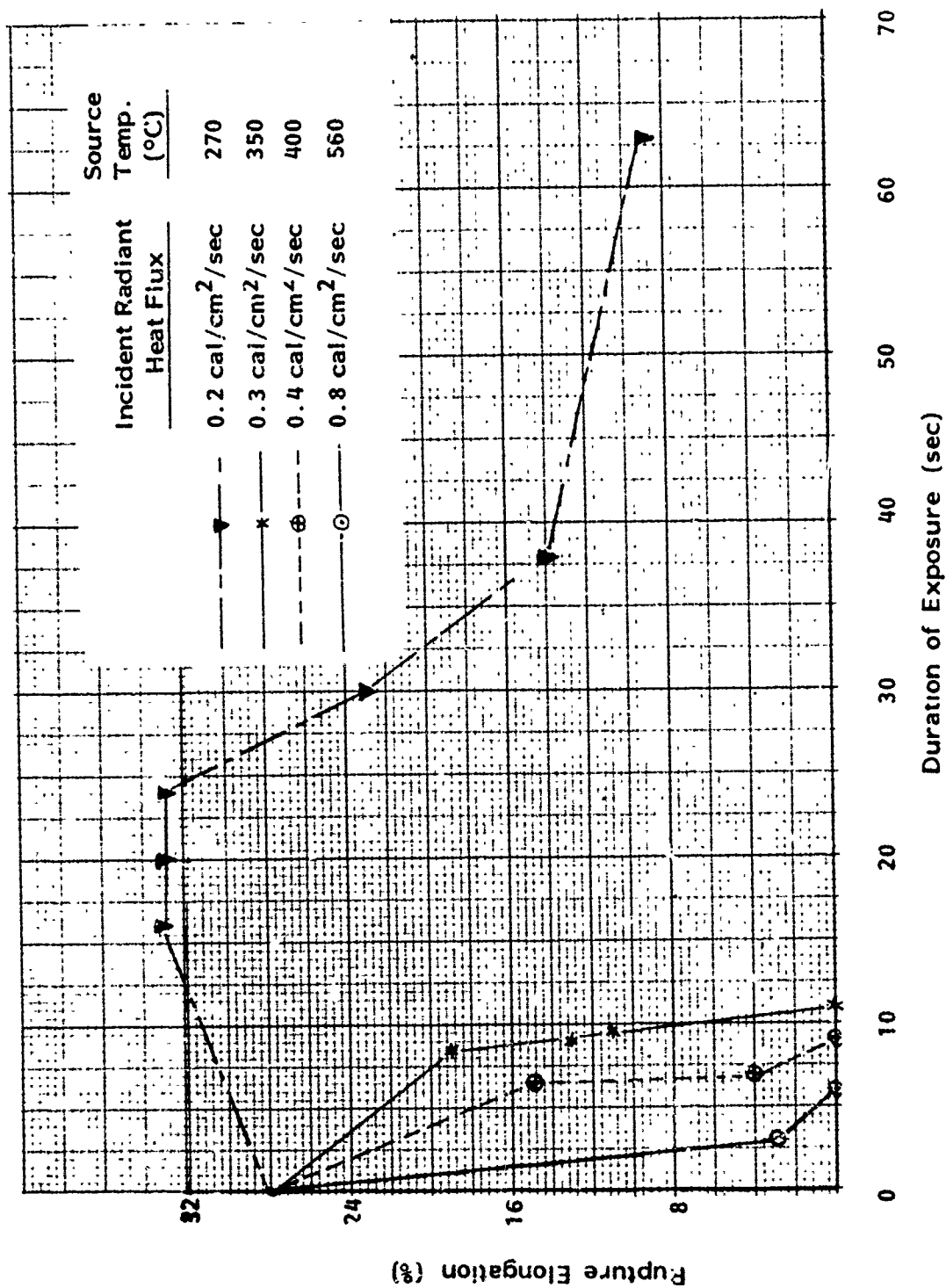


Figure 20. Rupture Elongation of Polyester Fabric in the Warp Direction at Various Bilateral Radiant Heat Flux Levels

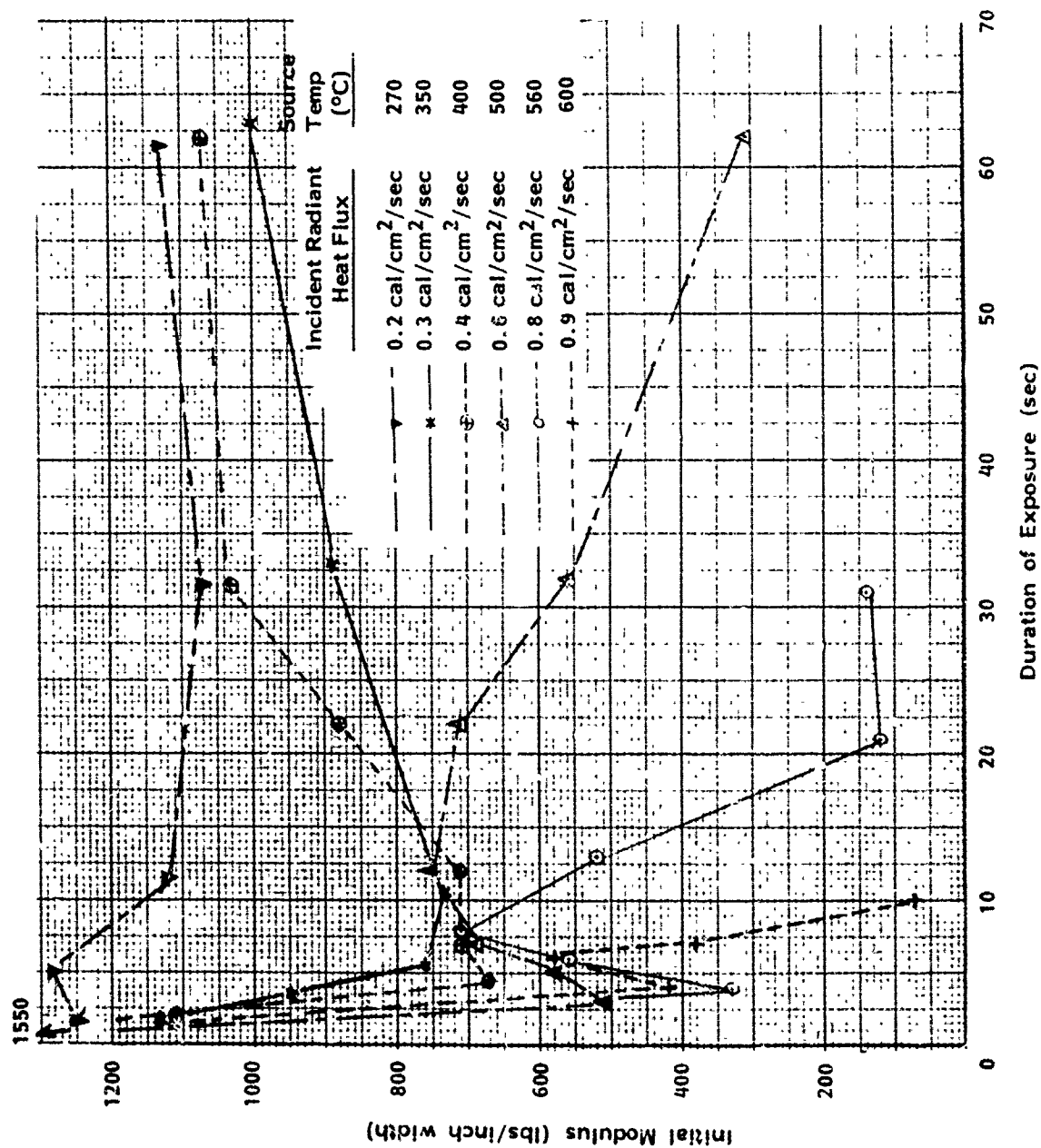


Figure 21. Initial Modulus of HT-4 Fabric in the Filling Direction at Various Bilateral Radiant Heat Flux Levels

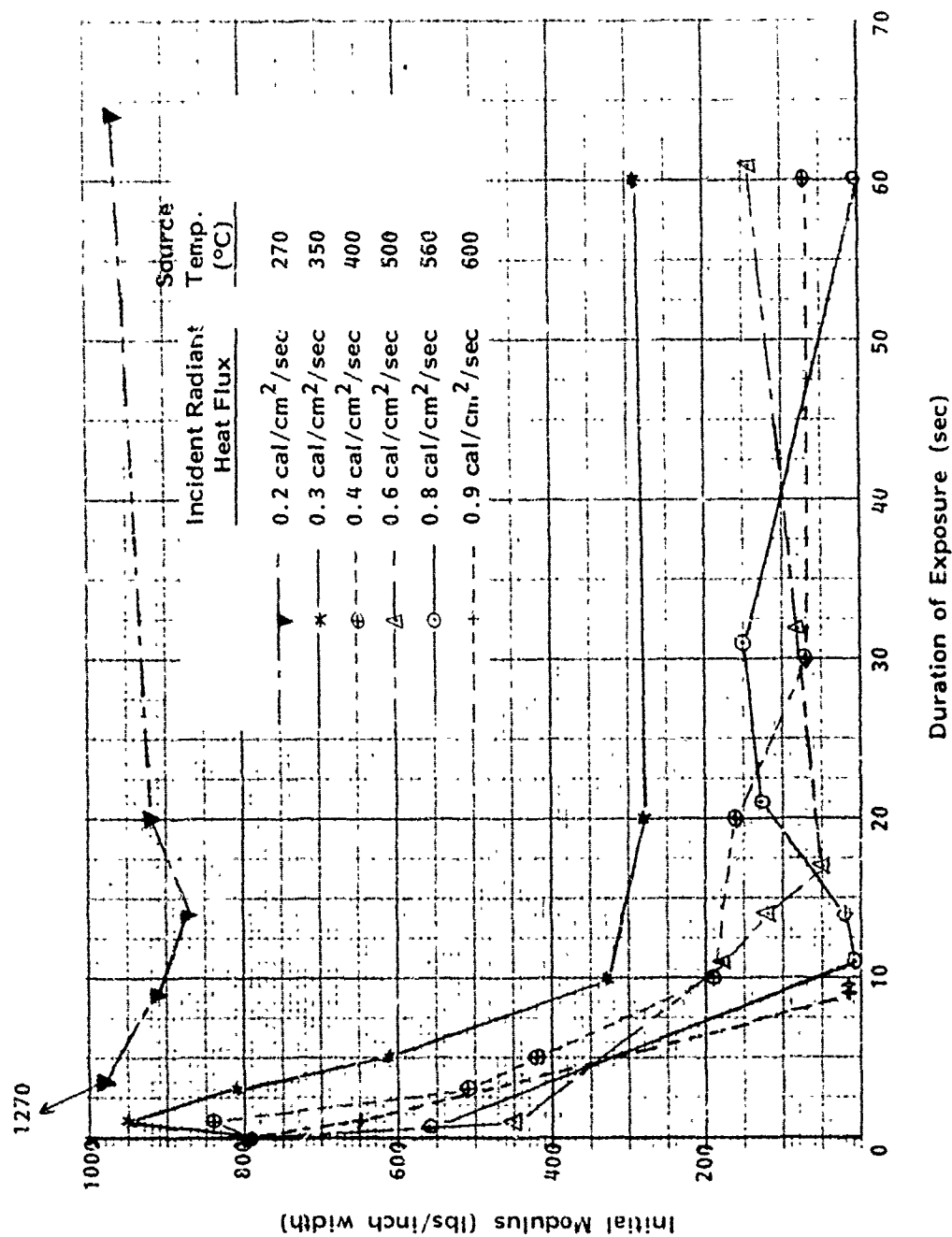


Figure 22. Initial Modulus of Durette Fabric in the Warp Direction at Various Bilateral Radiant Heat Flux Levels

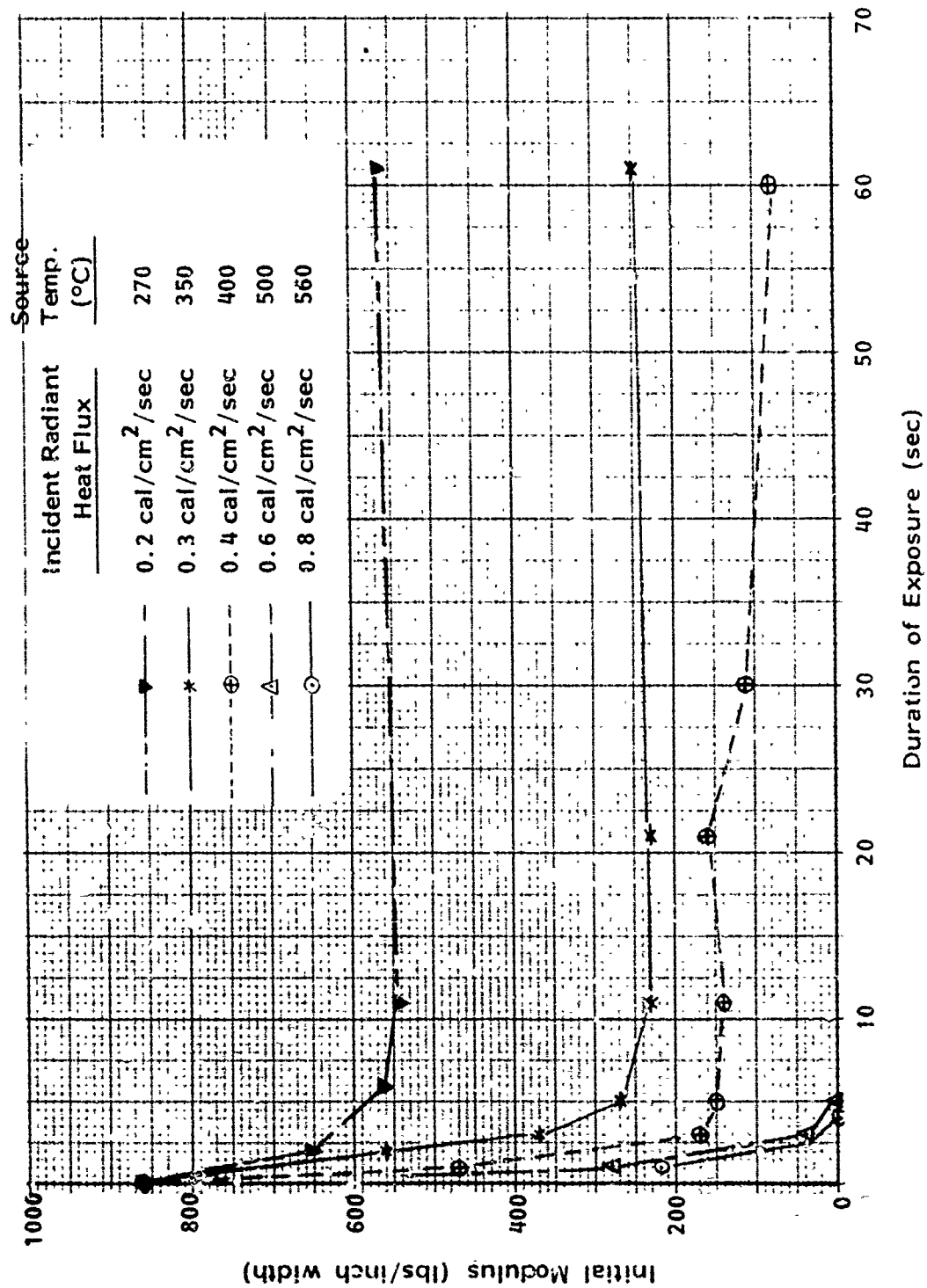


Figure 23. Initial Modulus of Nomex I Fabric in the Warp Direction at Various Bilateral Radiant Heat Flux Levels

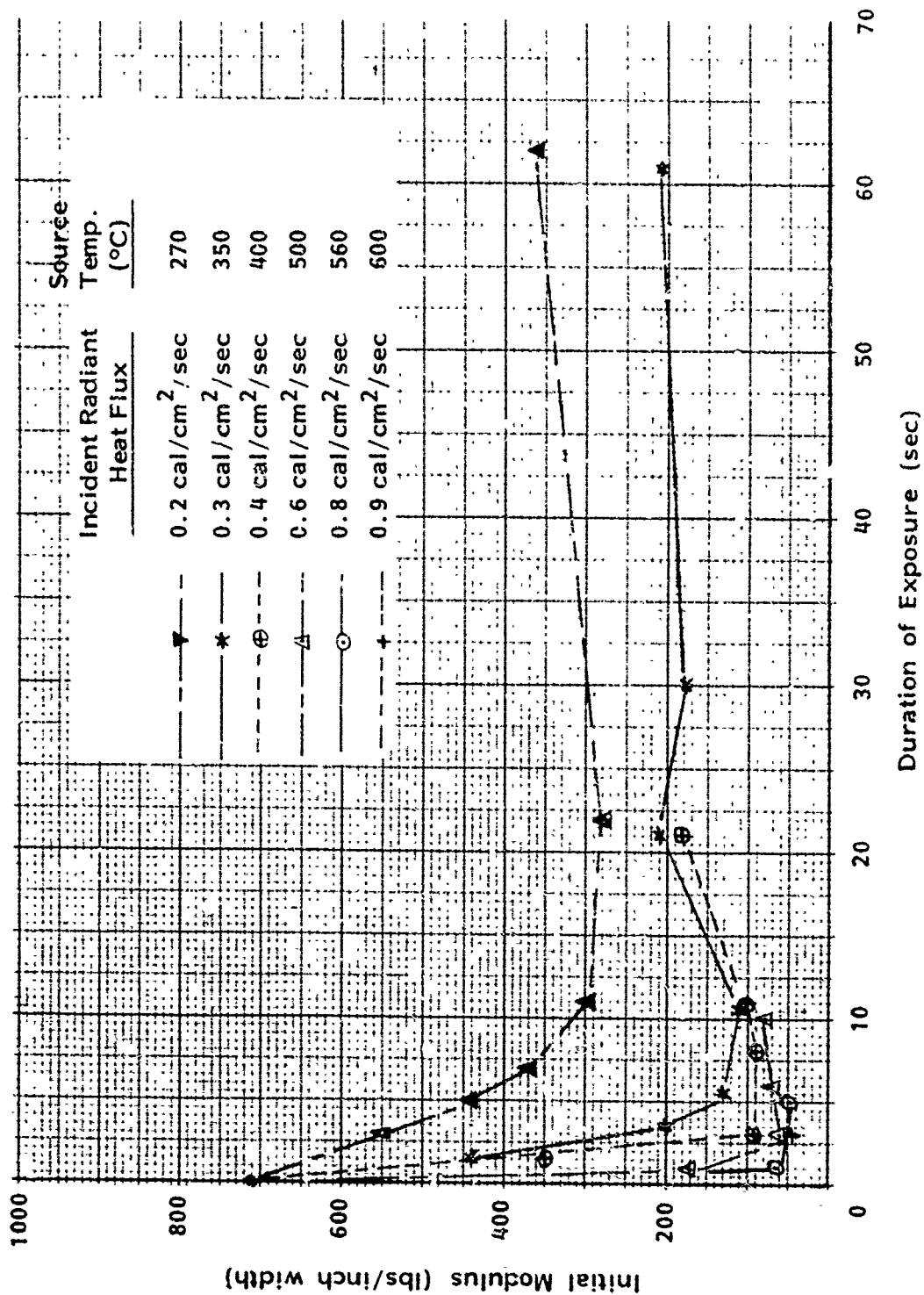


Figure 24. Initial Modulus of Kynol Fabric in the Warp Direction at Various Bilateral Radiant Heat Flux Levels

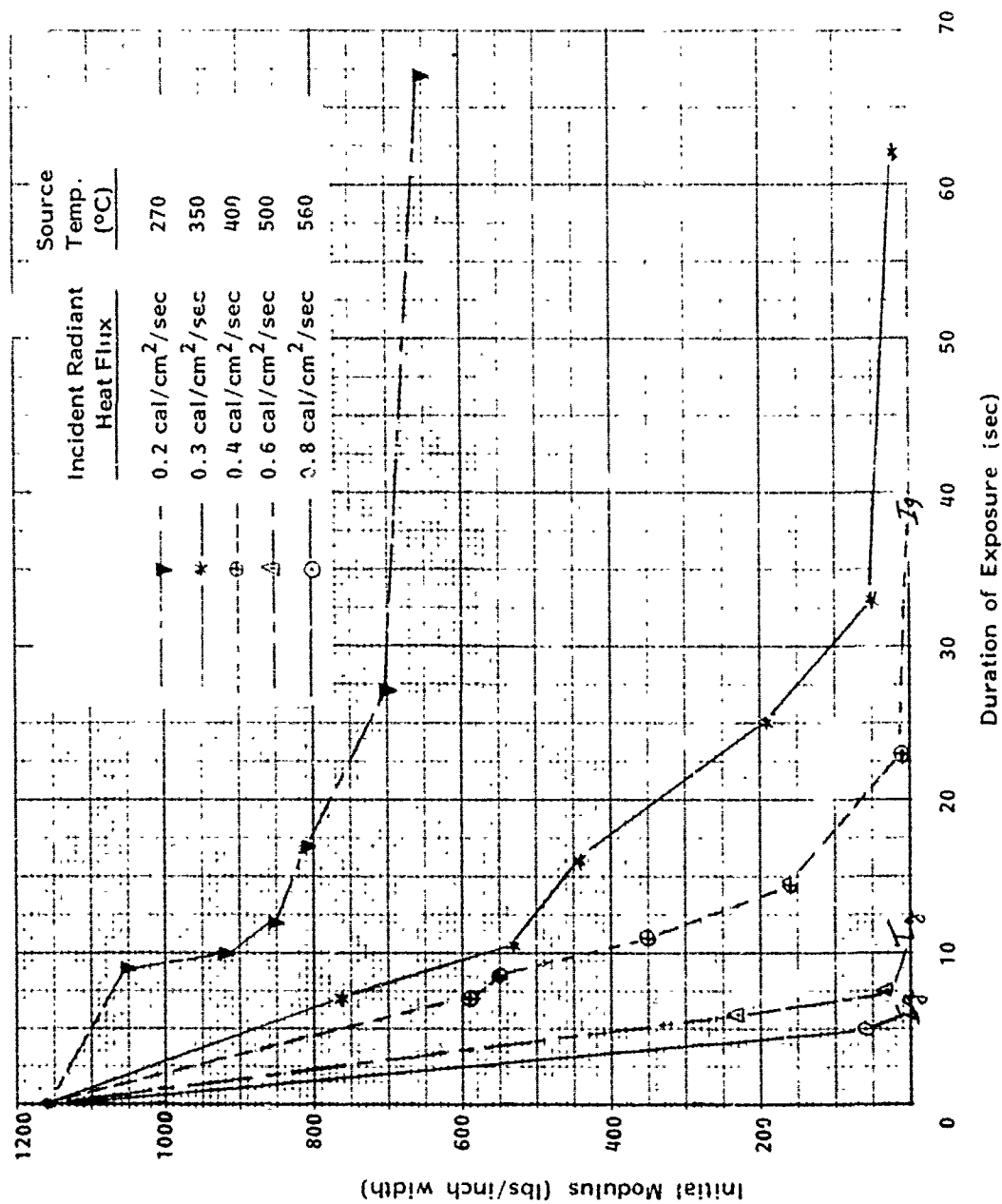


Figure 25. Initial Modulus of Cotton Fabric in the Filling Direction at Various Bilateral Radiant Heat Flux Levels

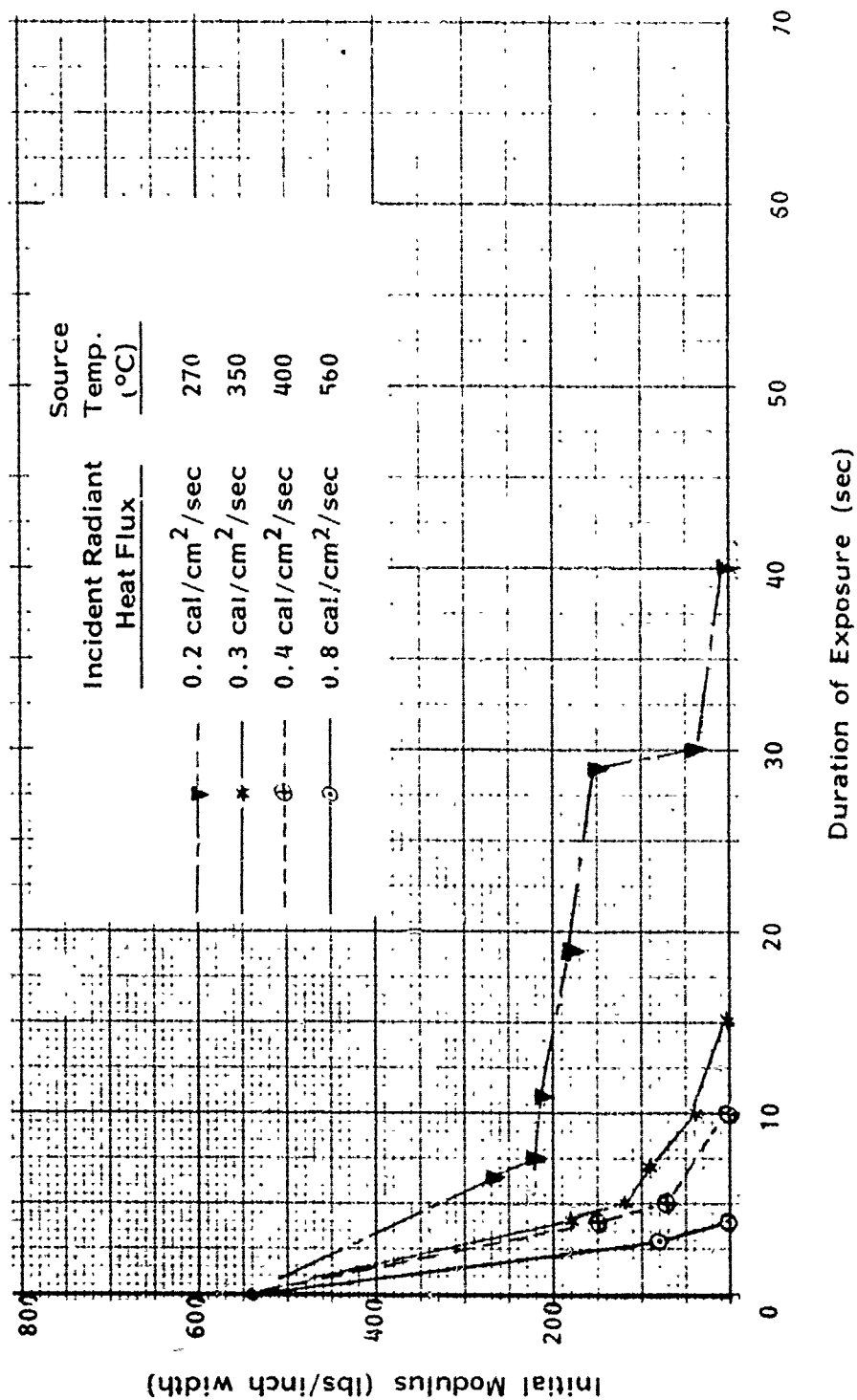


Figure 26. Initial Modulus of Nylon Fabric in the Warp Direction at Various Bilateral Radiant Heat Flux Levels

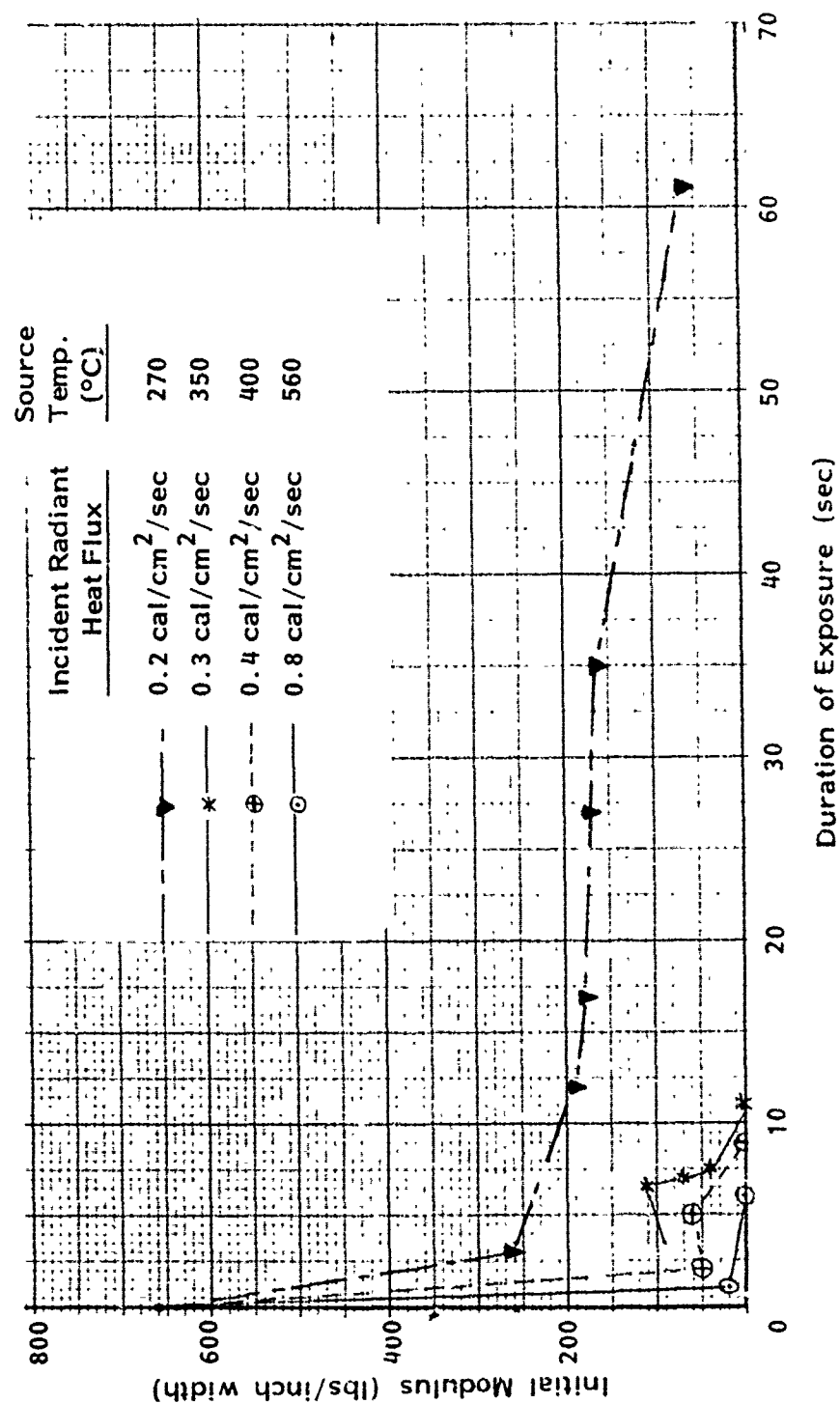


Figure 27. Initial Modulus of Polyester Fabric in the Warp Direction at Various Bilateral Radiant Heat Flux Levels

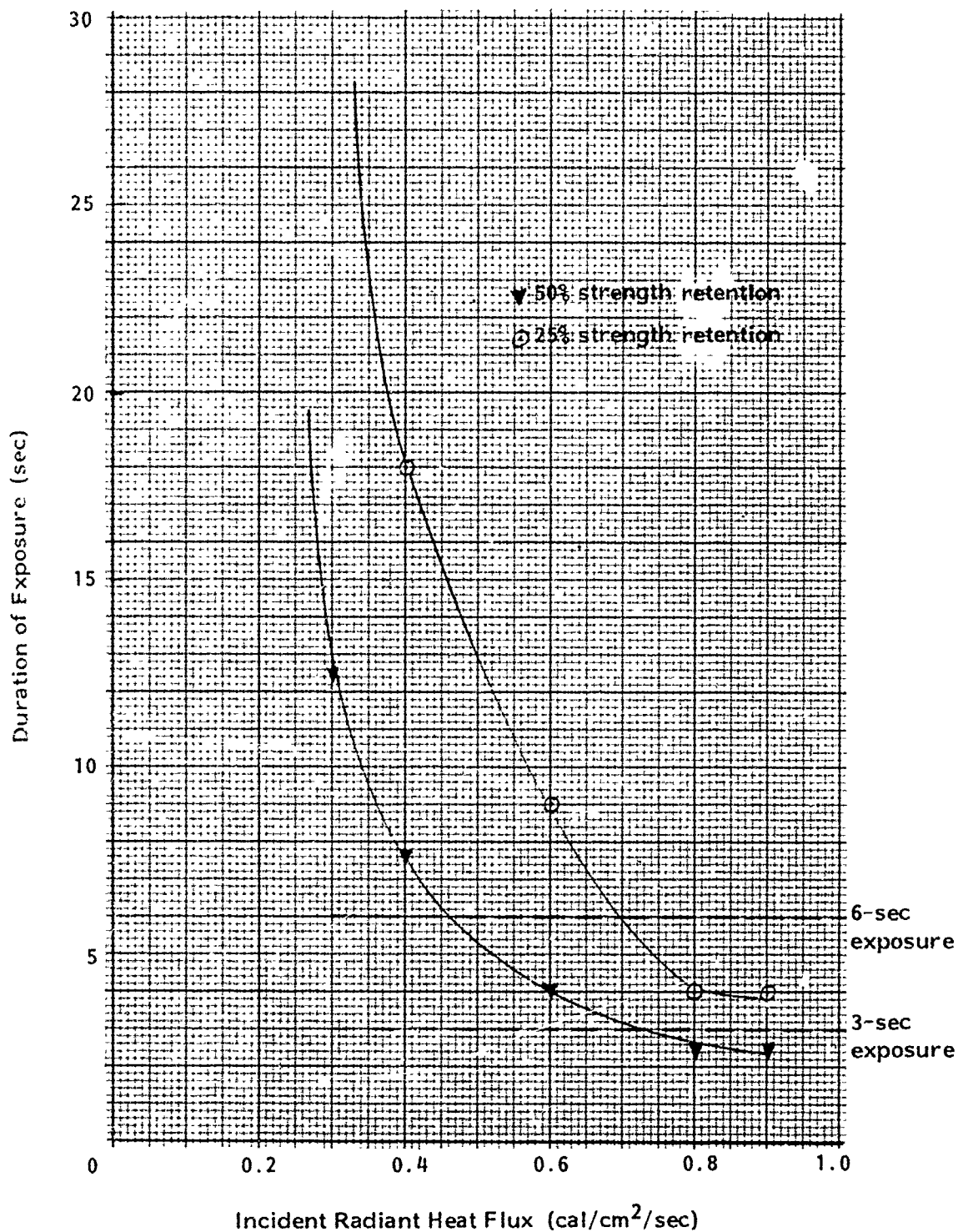


Figure 28. Duration of Exposure at Various Heat Flux Levels for which HT-4 Fabric Retains 25% and 50% of Its Original Strength

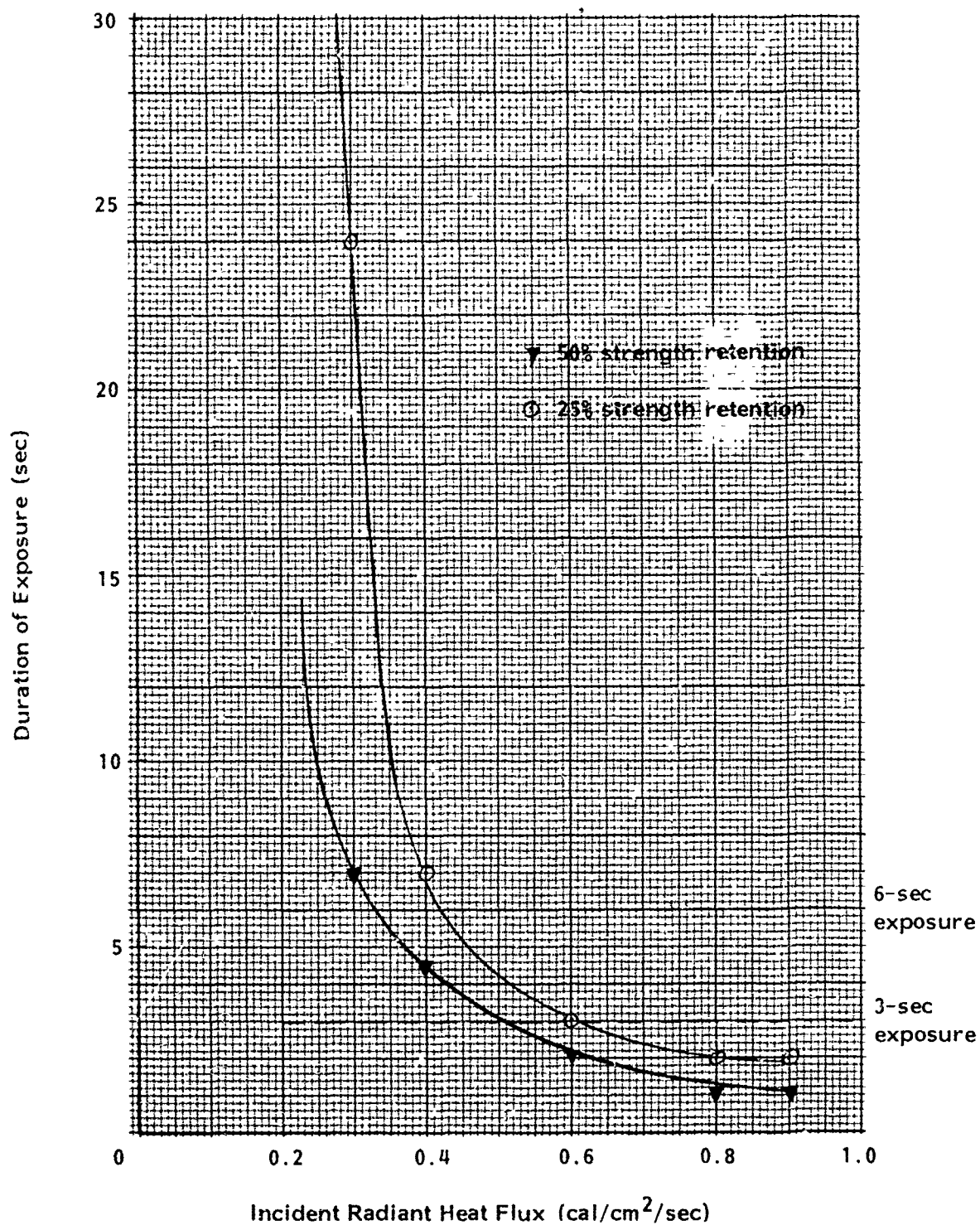


Figure 29. Duration of Exposure at Various Heat Flux Levels for which Durette Fabric Retains 25% and 50% of Its Original Strength

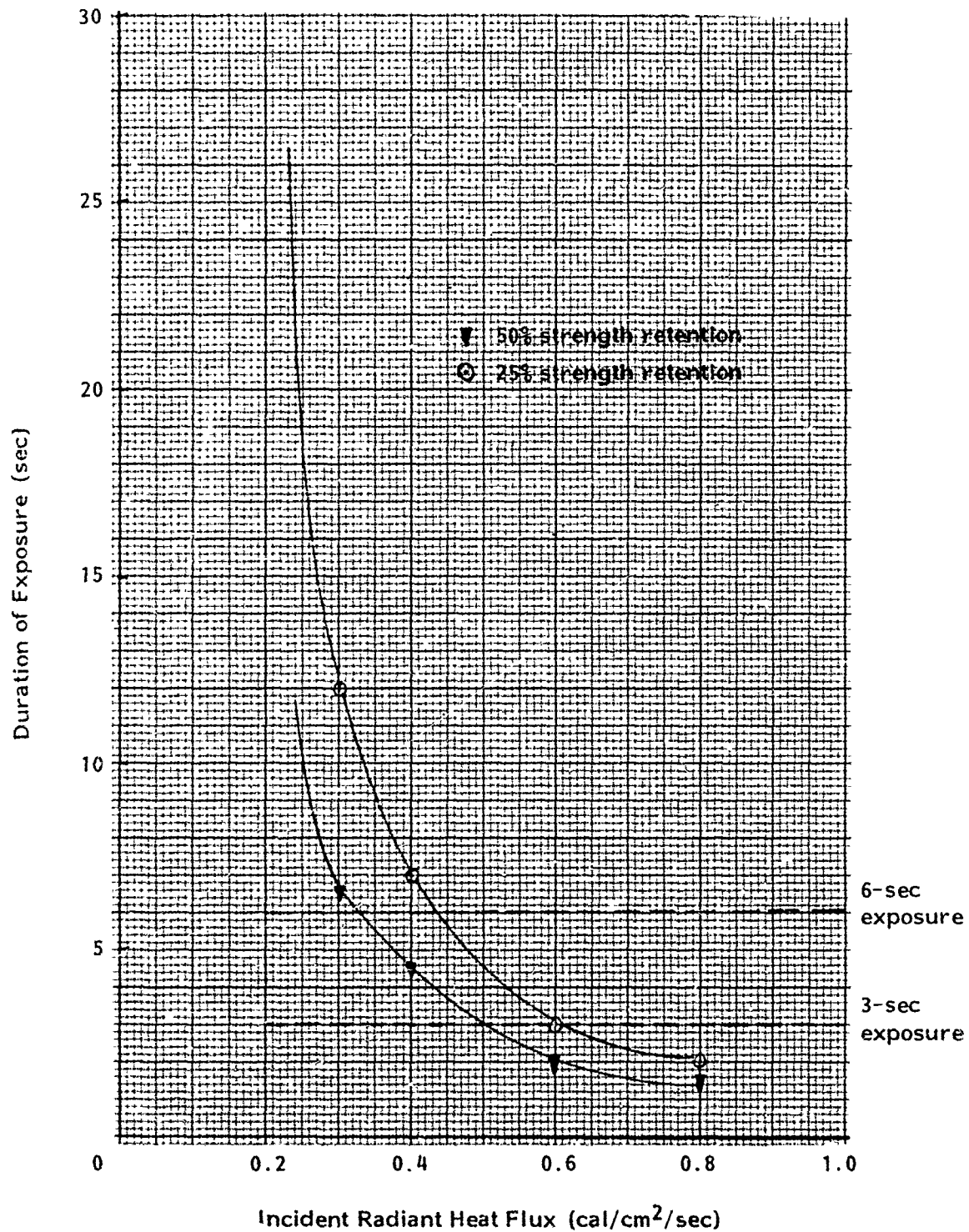


Figure 30. Duration of Exposure at Various Heat Flux Levels for which Nomex I Fabric Retains 25% and 50% of Its Original Strength

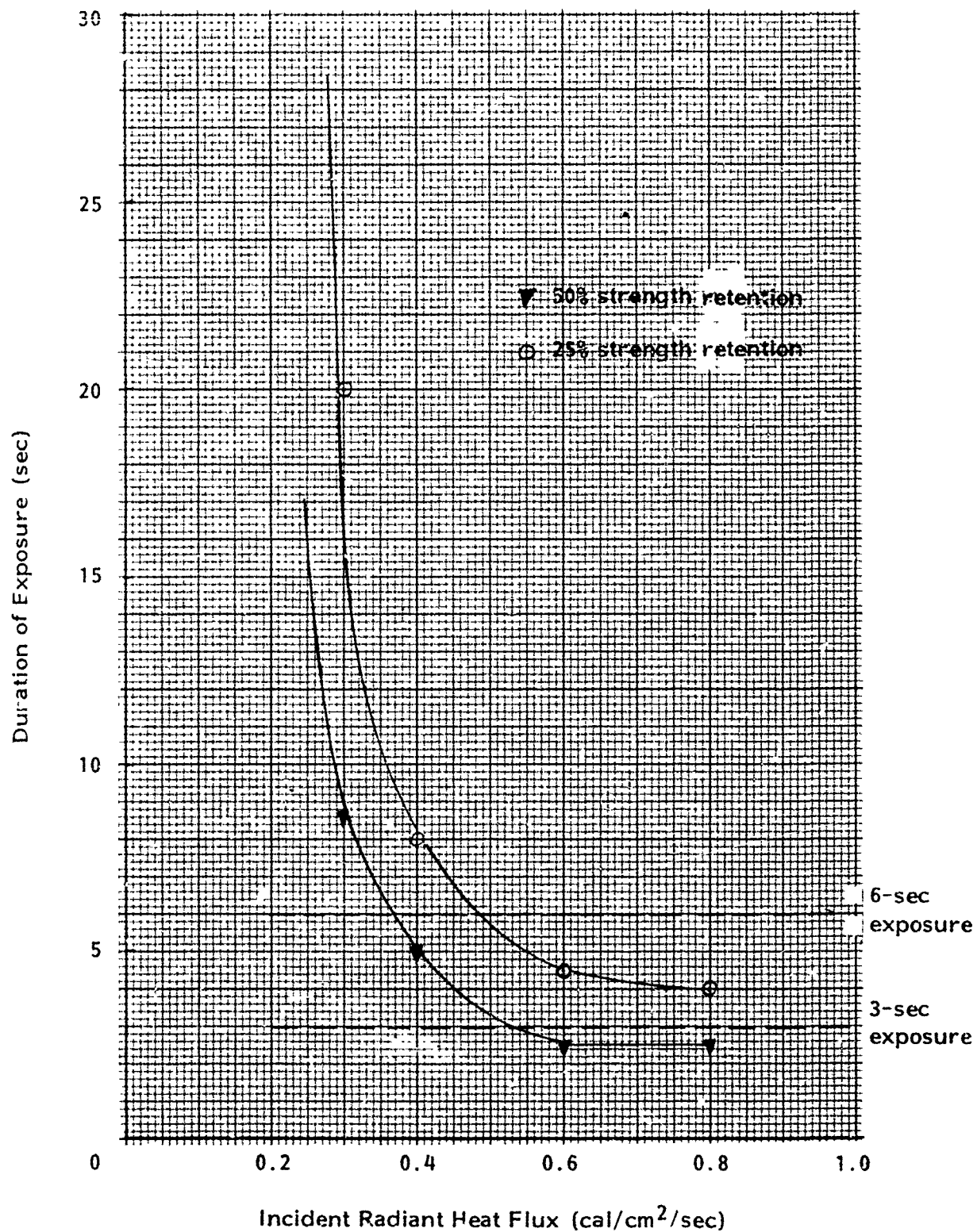


Figure 31. Duration of Exposure at Various Heat Flux Levels for which Kynol Fabric Retains 25% and 50% of Its Original Strength

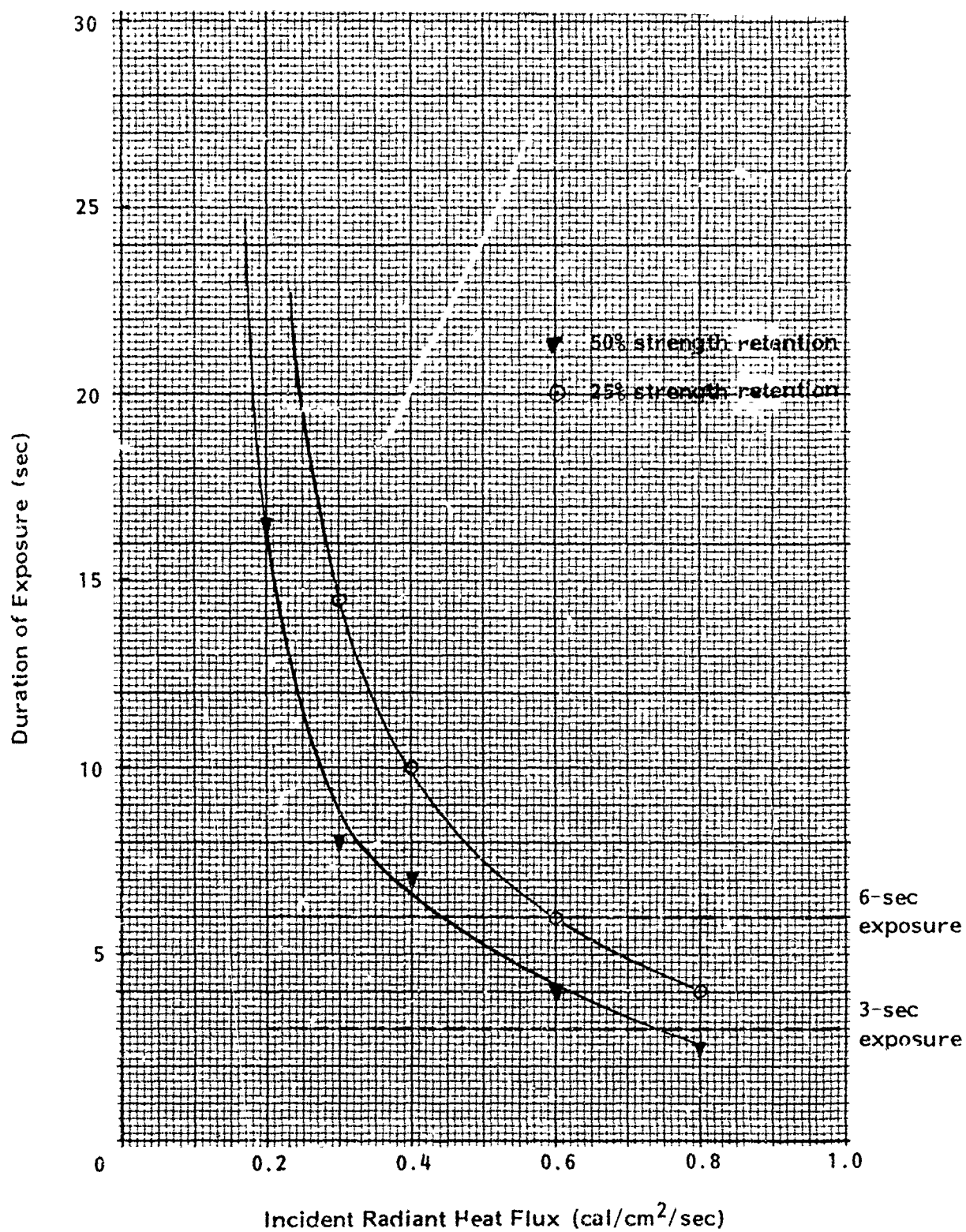


Figure 32. Duration of Exposure at Various Heat Flux Levels for which Cotton Fabric Retains 25% and 50% of Its Original Strength

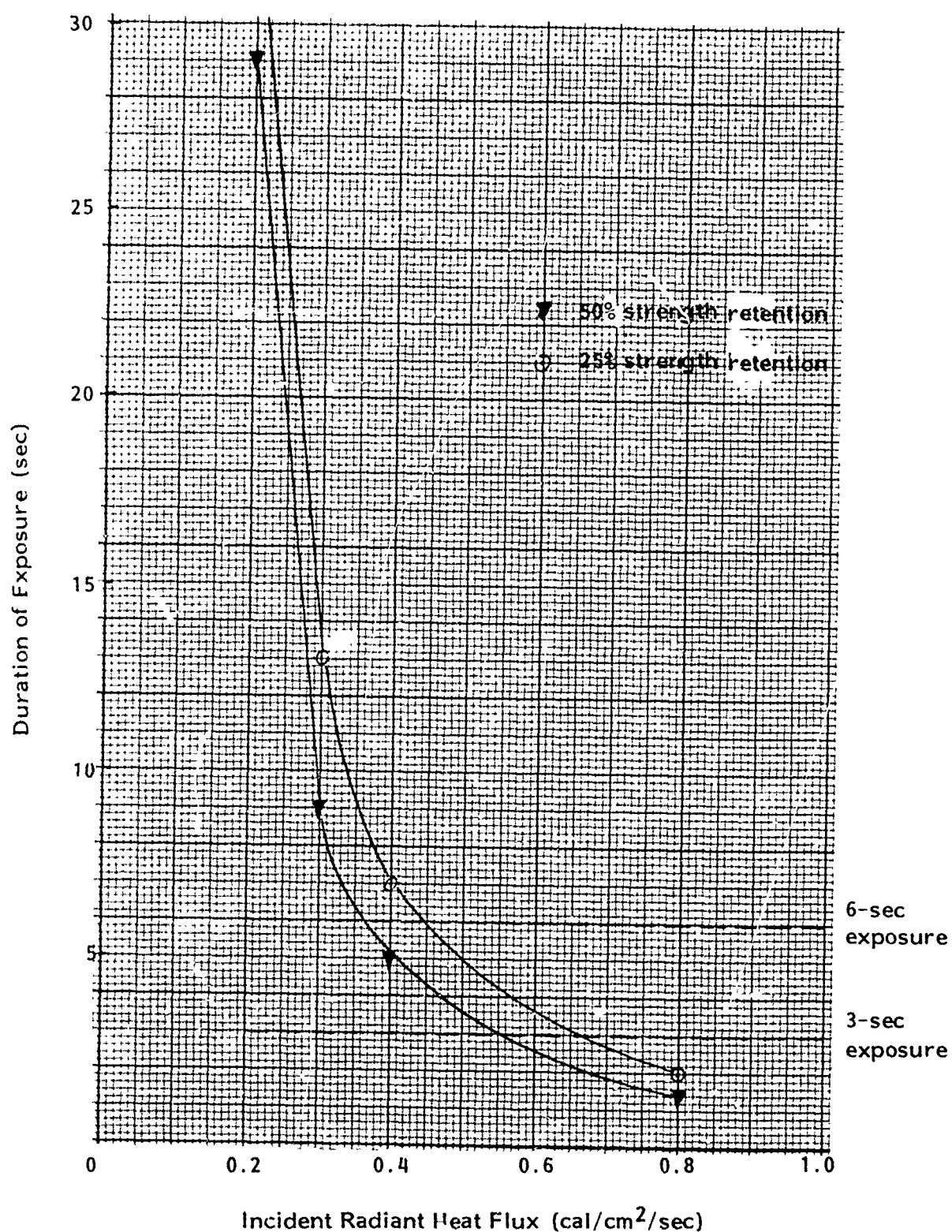


Figure 33. Duration of Exposure at Various Heat Flux Levels for which Nylon Fabric Retains 25% and 50% of Its Original Strength

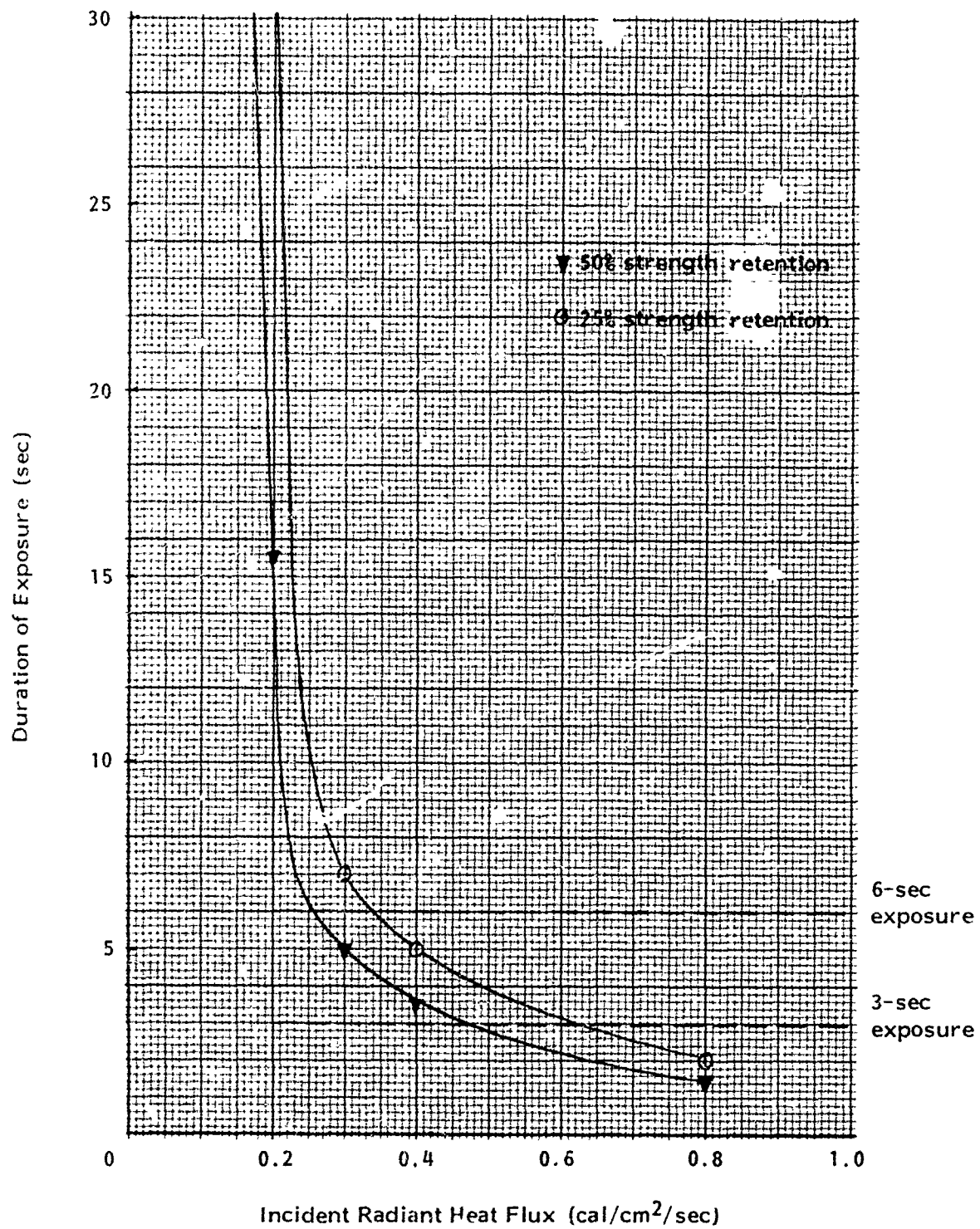


Figure 34. Duration of Exposure at Various Heat Flux Levels for which Polyester Fabric Retains 25% and 50% of Its Original Strength

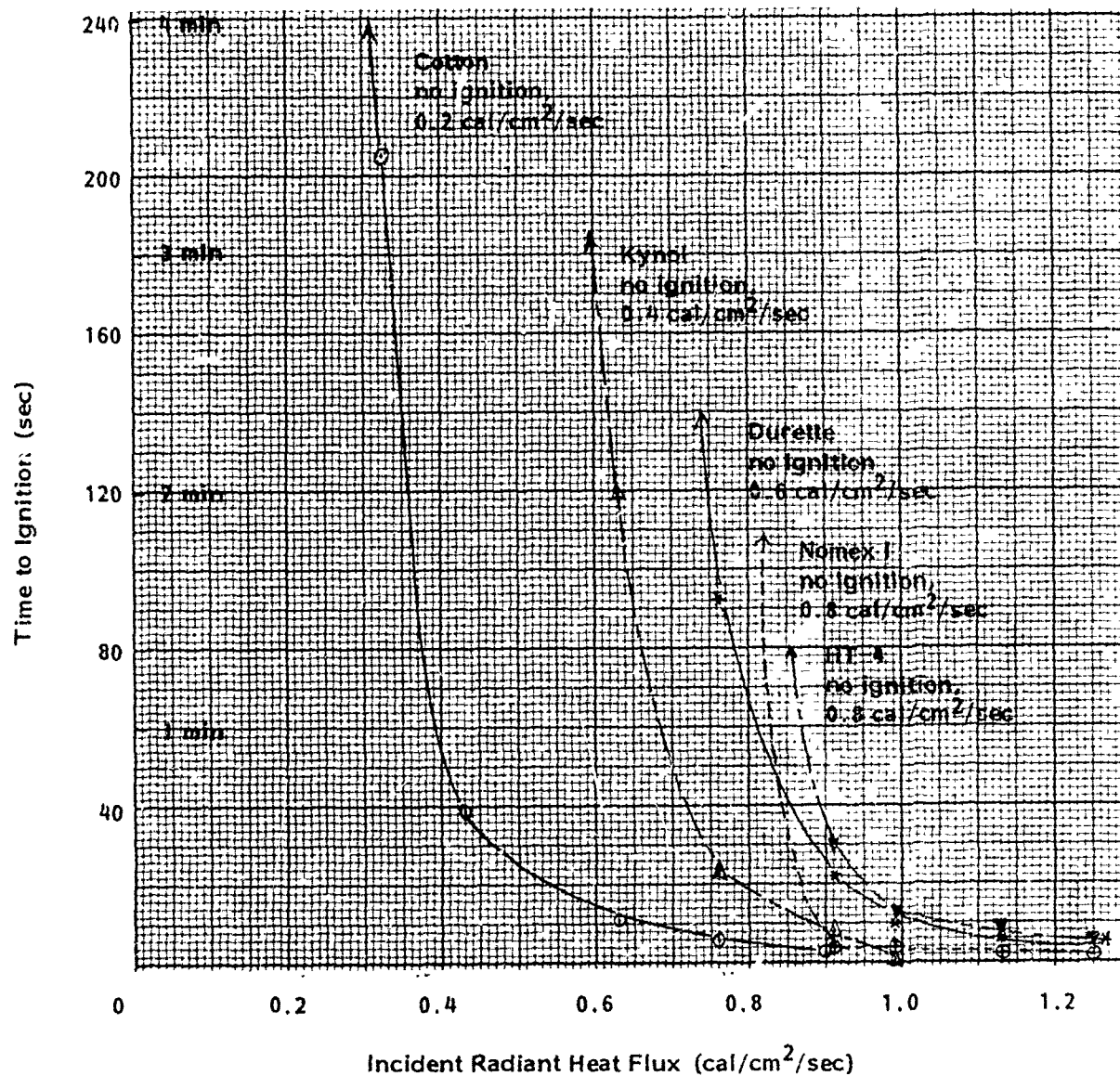


Figure 35. Fabric Ignition Times at Various Bilateral Radiant Heat Flux Levels

Curve	Test Configuration	Specimen Temp. (°C)	Source Temp. (°C)	Incident Heat Flux (cal/cm ² /sec)
1	unilateral	210-300	375-500	0.2-0.3
2	bilateral	~270	270	0.2
3	bilateral	~350	350	0.3
4	unilateral	280-450	520-685	0.3-0.5
5	bilateral	~400	400	0.4

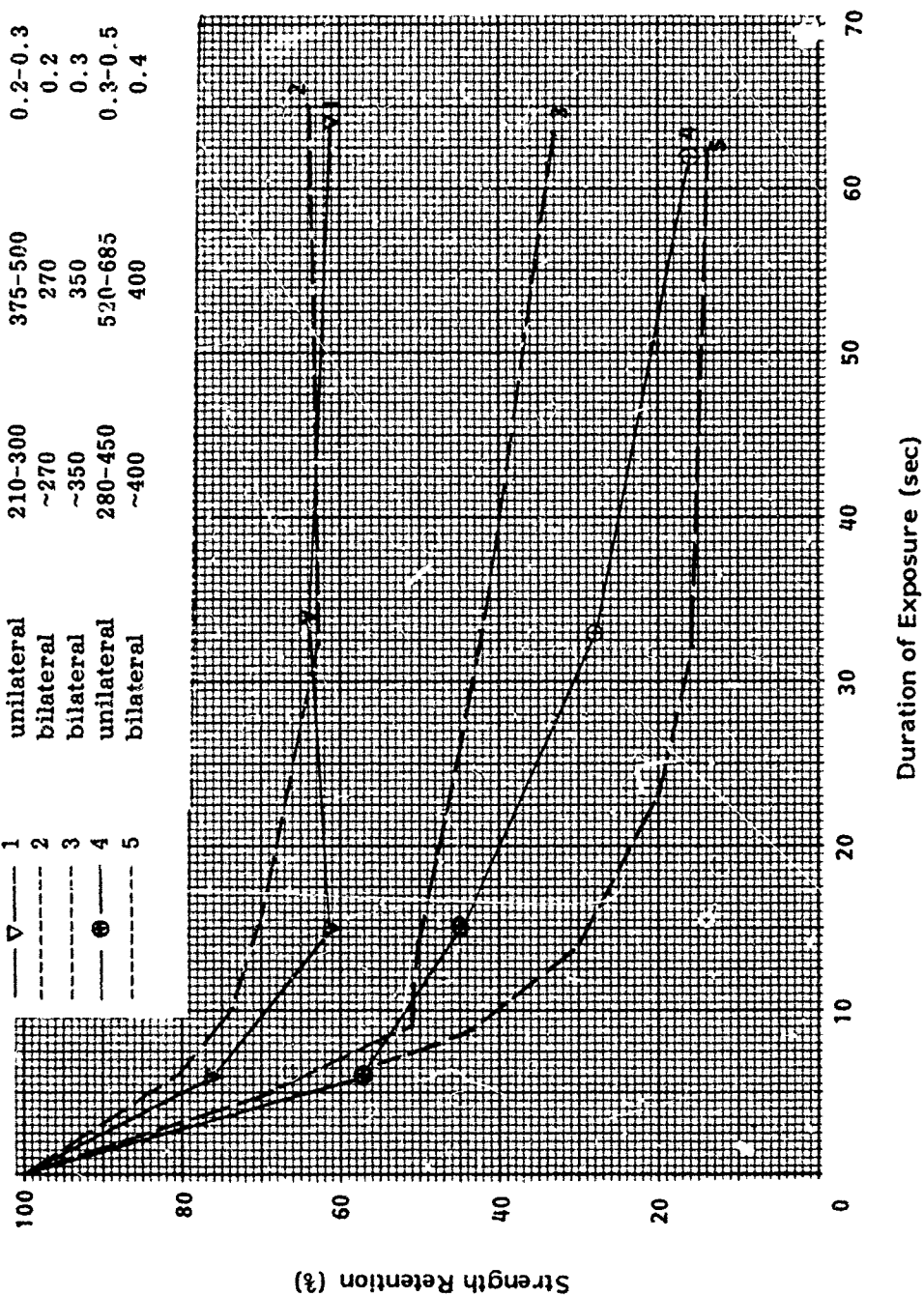


Figure 36. Comparison of the Strength Retention of HT-4 Fabric in the Filling Direction at Similar Unilateral and Bilateral Radiant Heat Flux Levels

Curve	Test Configuration	Specimen Temp. (°C)	Source Temp. (°C)	Incident Heat Flux (cal/cm ² /sec)
—▽— 1	unilateral	210-300	375-500	0.2-0.3
- - - 2	bilateral	~270	270	0.2
- - - 3	bilateral	~350	350	0.3
- - - 4	unilateral	280-450	520-685	0.3-0.5
- - - 5	bilateral	~400	400	0.4

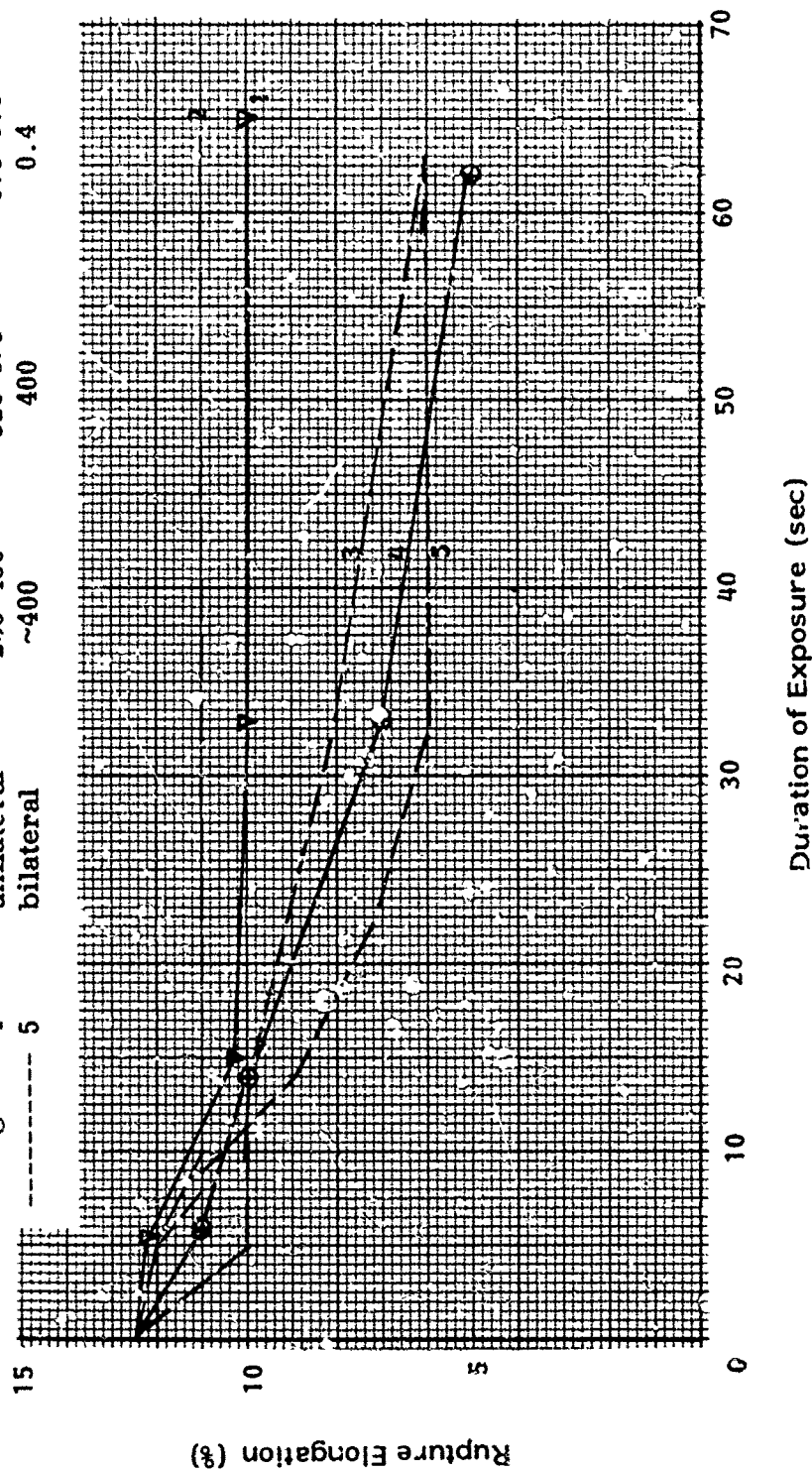


Figure 37. Comparison of the Rupture Elongation of HT-4 Fabric in the Filling Direction at Similar Unilateral and Bilateral Radiant Heat Flux Levels

Curve	Test Configuration	Specimen Temp. (°C)	Source Temp. (°C)	Incident Heat Flux (cal/cm ² /sec)
1	unilateral	210-300	375-500	0.2-0.3
2	bilateral	~270	270	0.2
3	bilateral	~350	350	0.3
4	unilateral	280-450	520-685	0.3-0.5
5	bilateral	~400	400	0.4

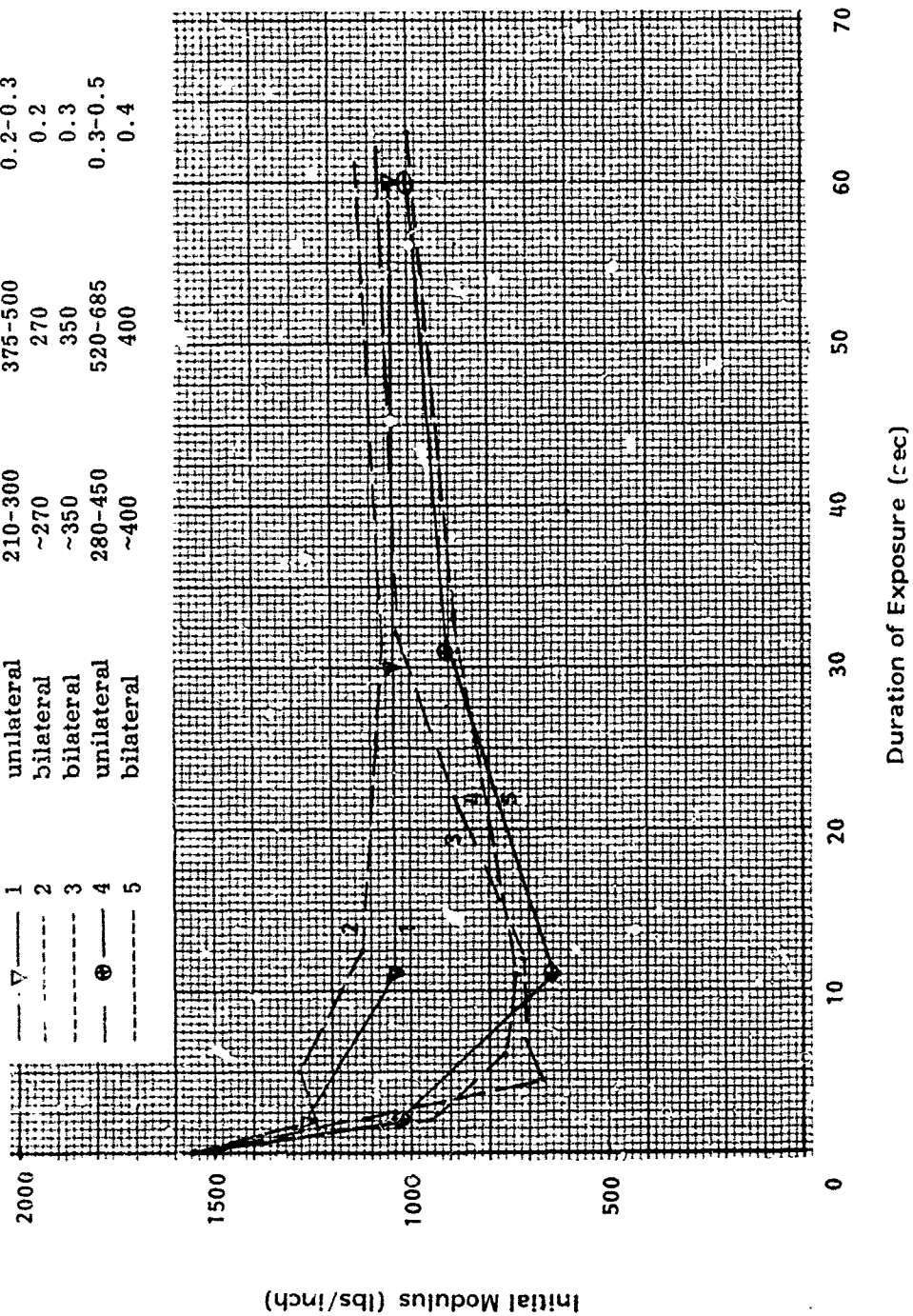


Figure 38. Comparison of the Initial Modulus of HT-4 Fabric in the Filling Direction at Similar Unilateral and Bilateral Radiant Heat Flux Levels

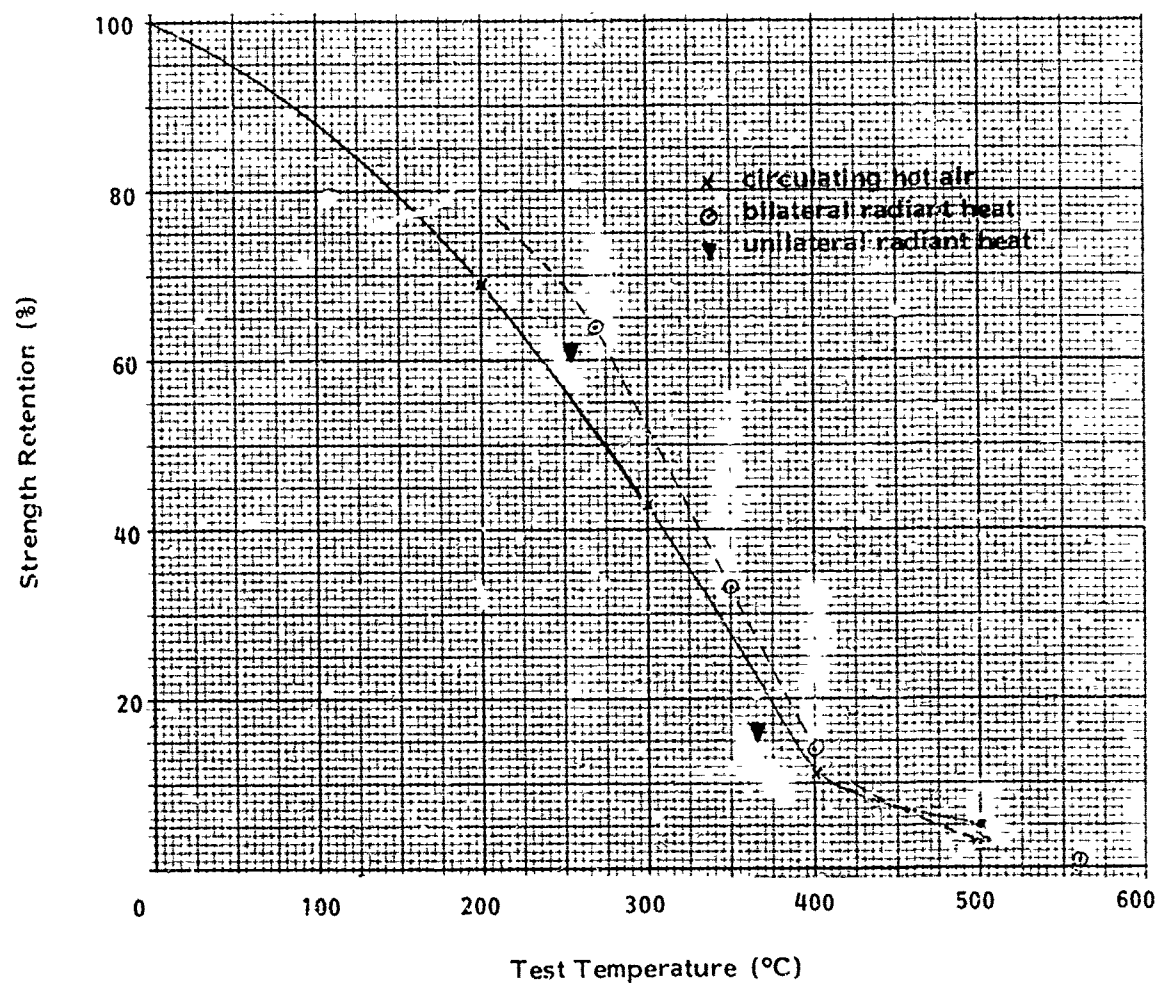


Figure 36. Strength Retention of HT-4 Fabric in the Filling Direction at Various Temperatures

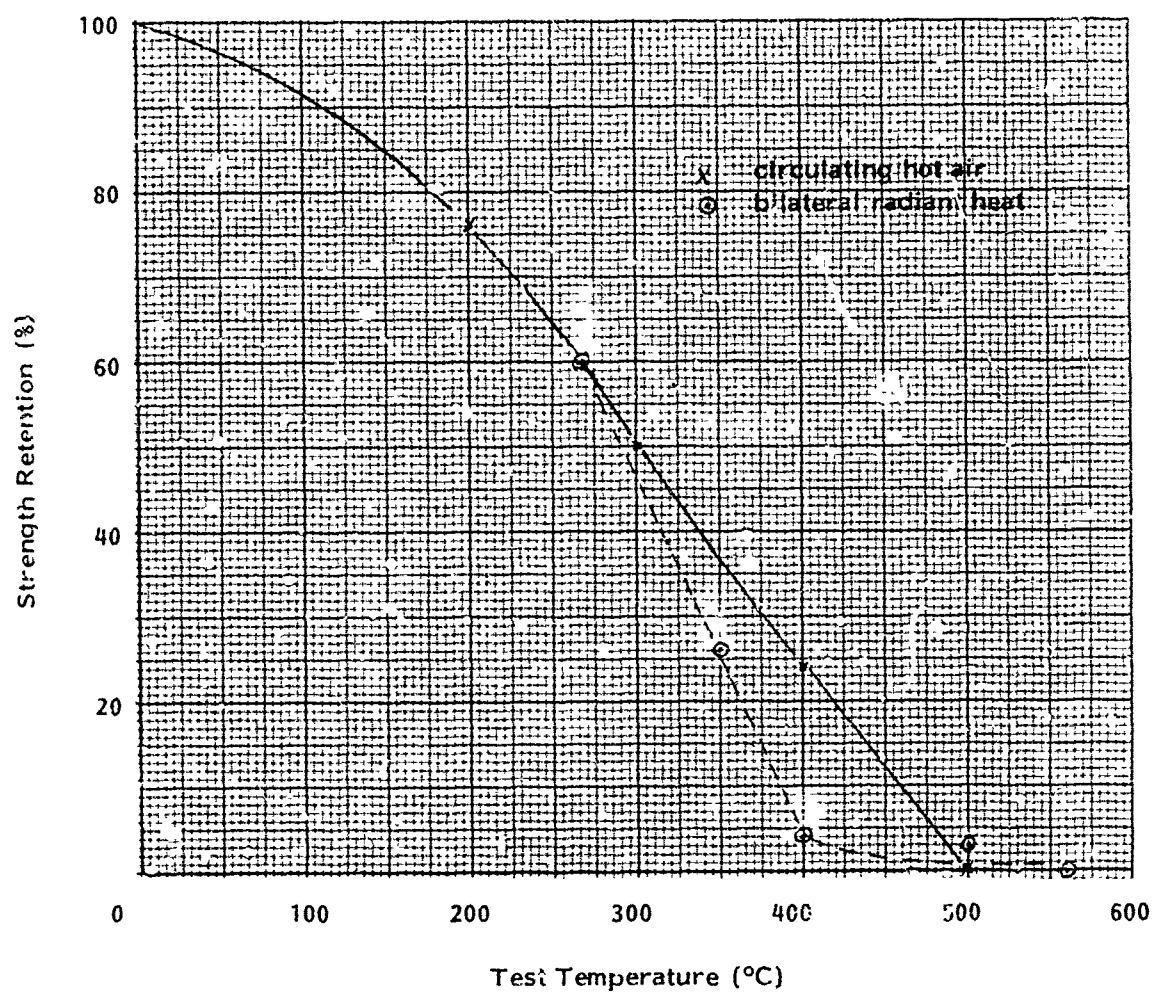


Figure 40. Strength Retention of Durette Fabric in the Warp Direction at Various Temperatures

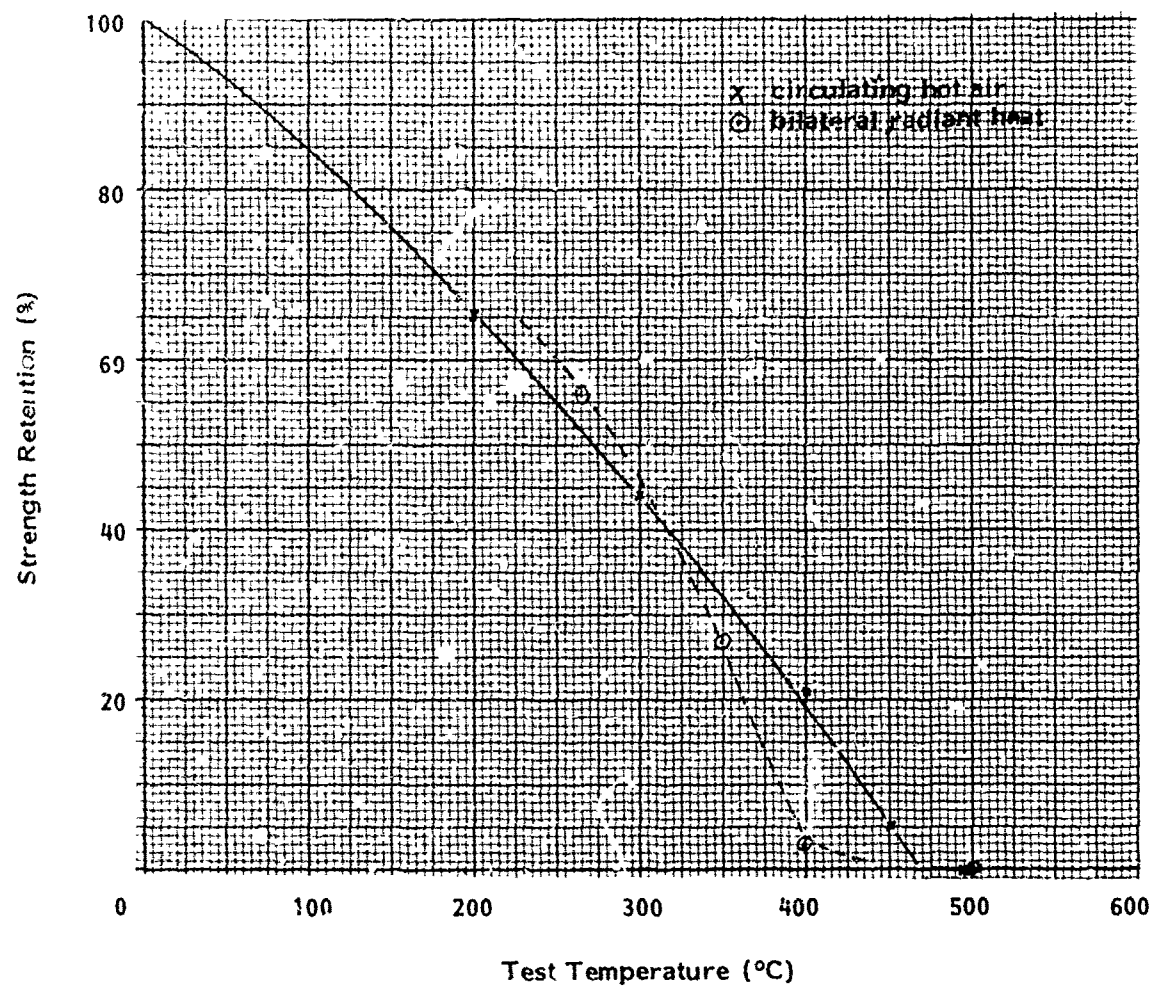


Figure 41. Strength Retention of Nomex I Fabric in the Warp Direction at Various Temperatures

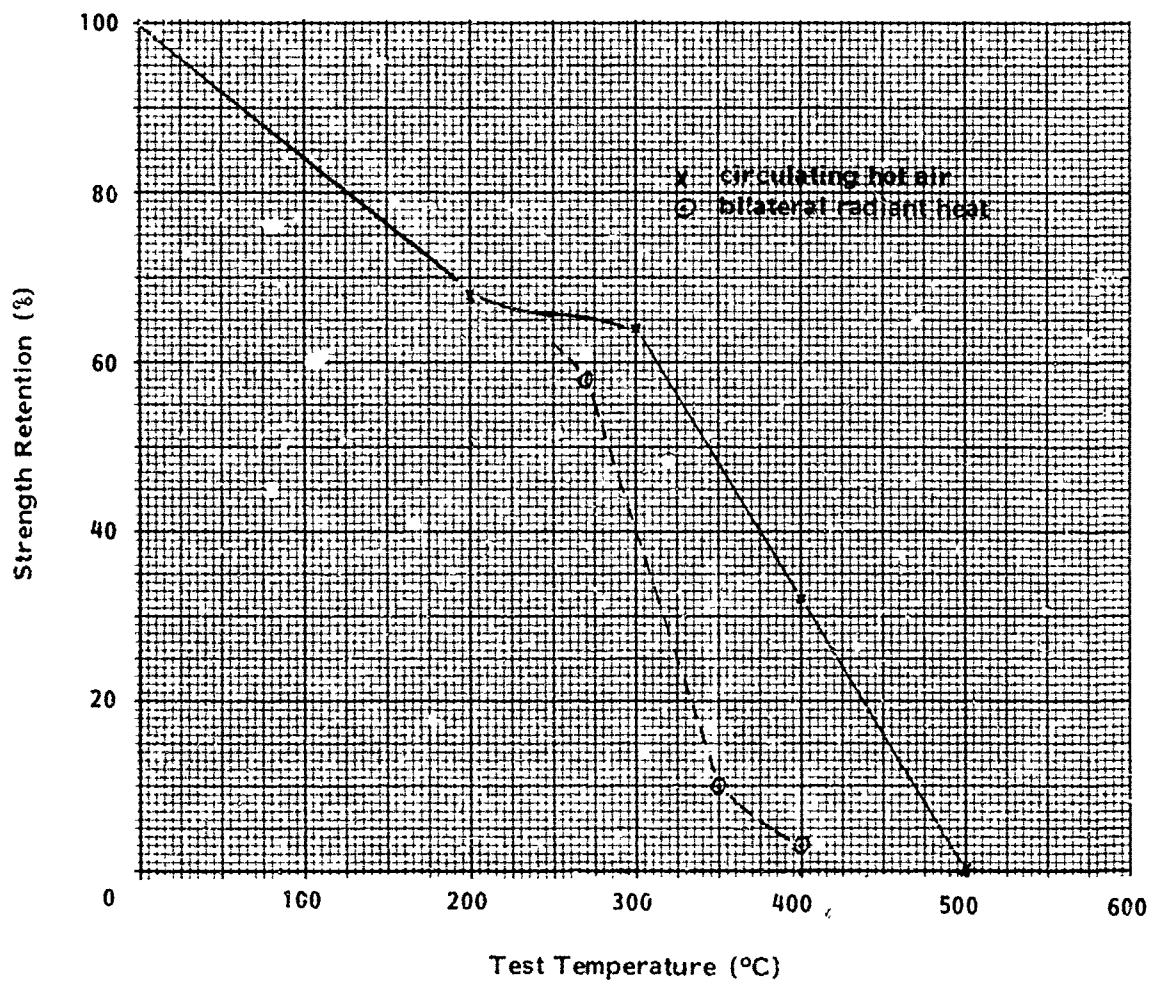


Figure 42. Strength Retention of Kynol Fabric in the Warp Direction at Various Temperatures

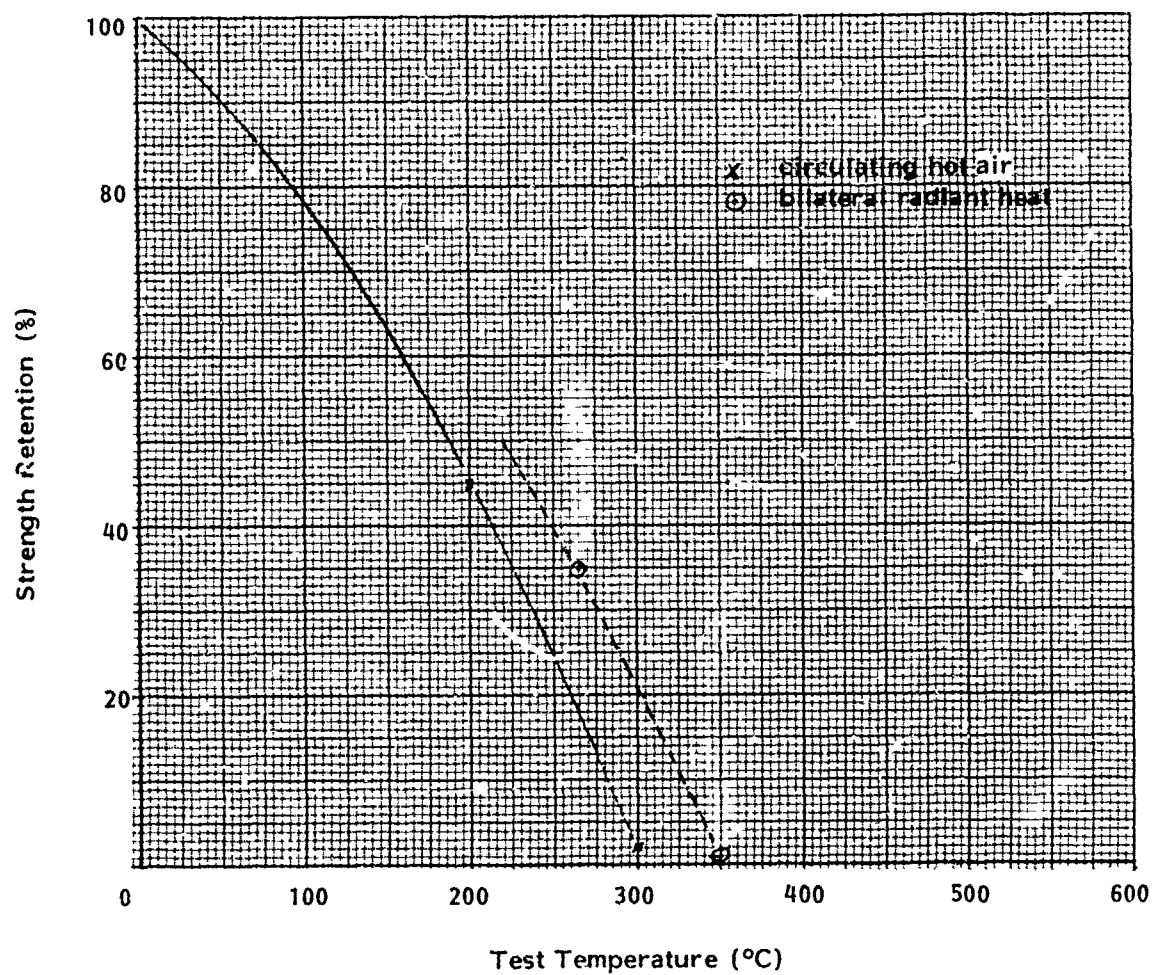


Figure 43. Strength Retention of Cotton Fabric in the Filling Direction at Various Temperatures

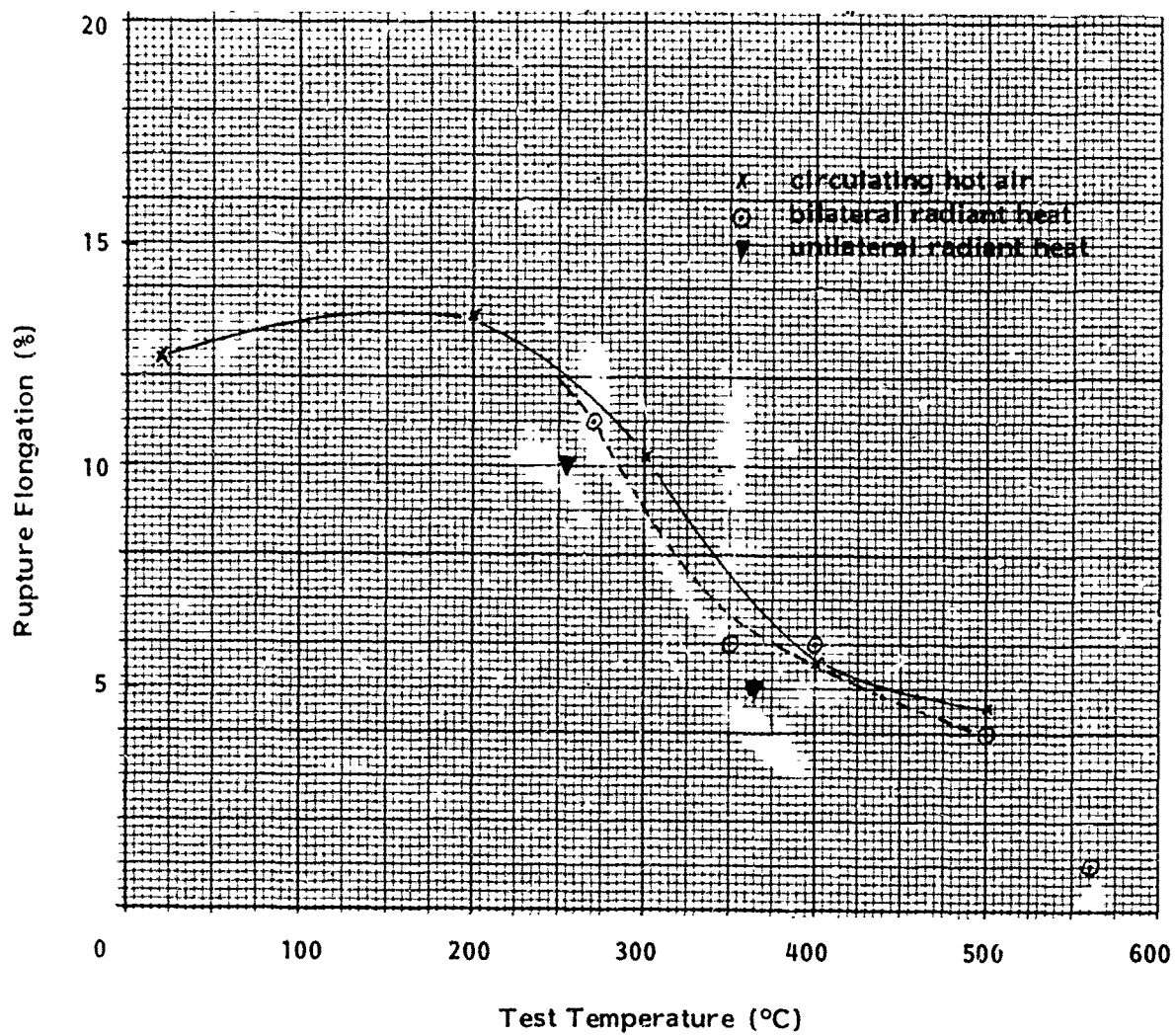


Figure 44. Rupture Elongation of HT-4 Fabric in the Filling Direction at Various Temperatures

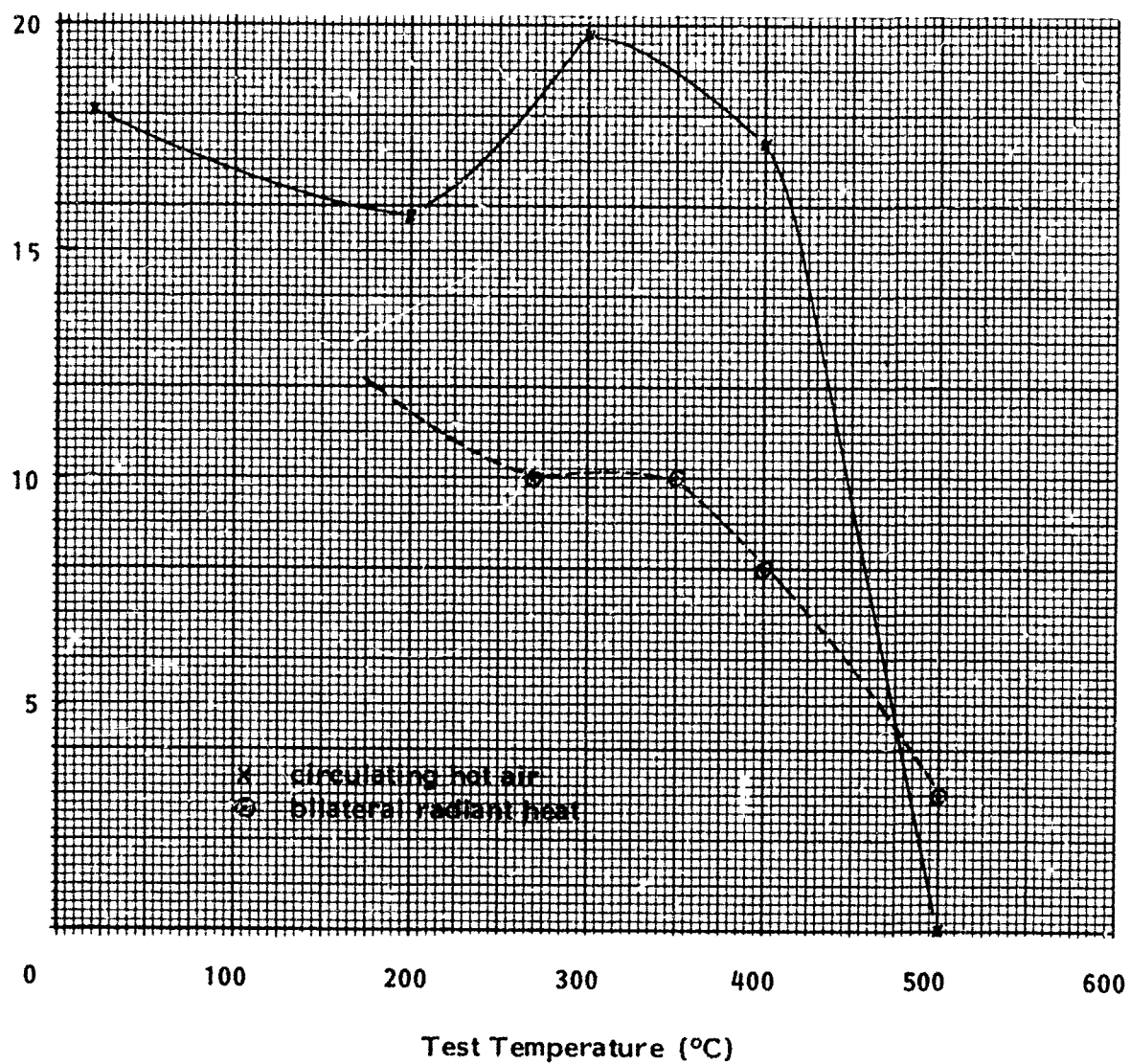


Figure 45. Rupture Elongation of Durette Fabric in the Warp Direction at Various Temperatures

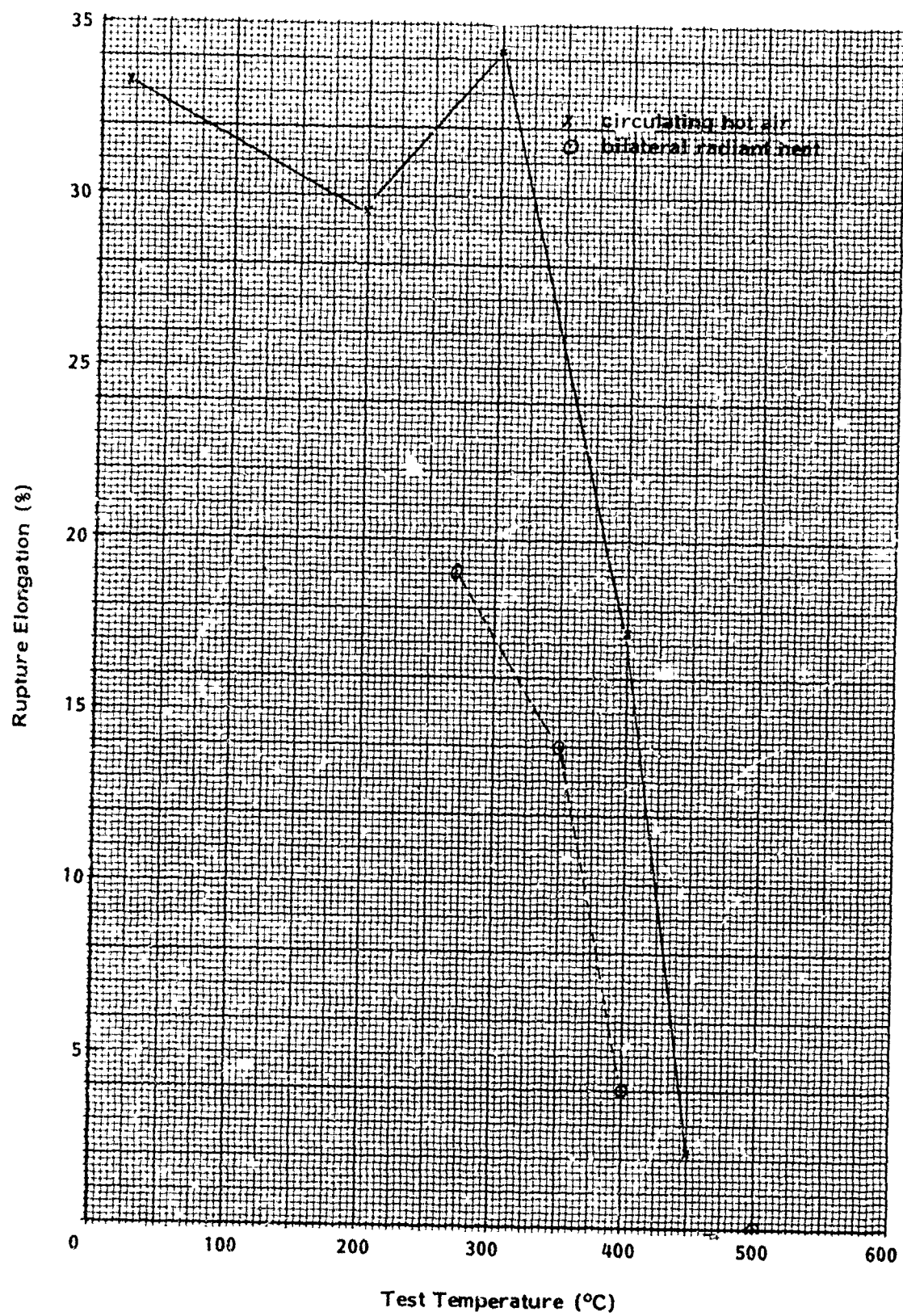


Figure 46. Rupture Elongation of Nomex I Fabric in the Warp Direction at Various Temperatures

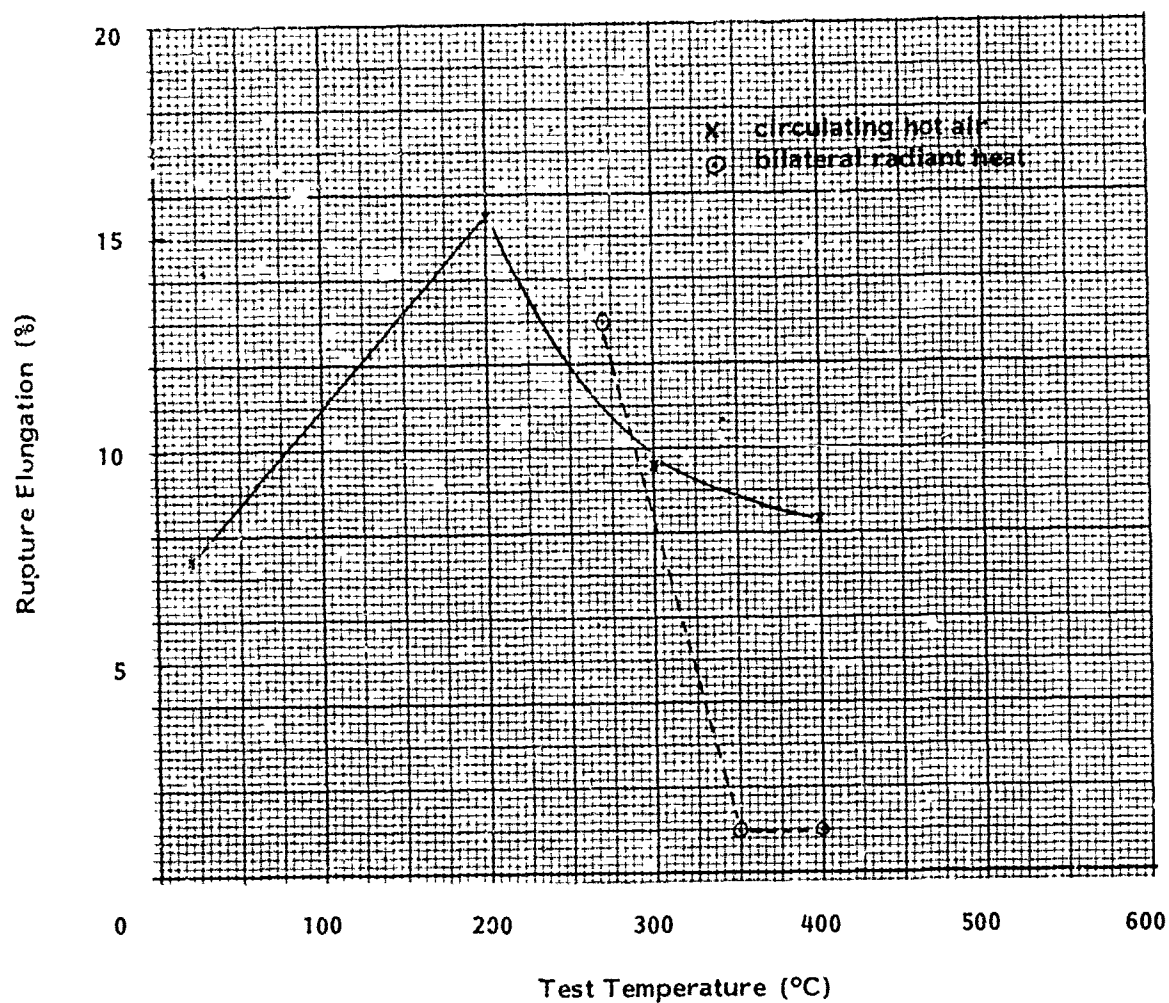


Figure 47. Rupture Elongation of Kynol Fabric in the Warp Direction at Various Temperatures

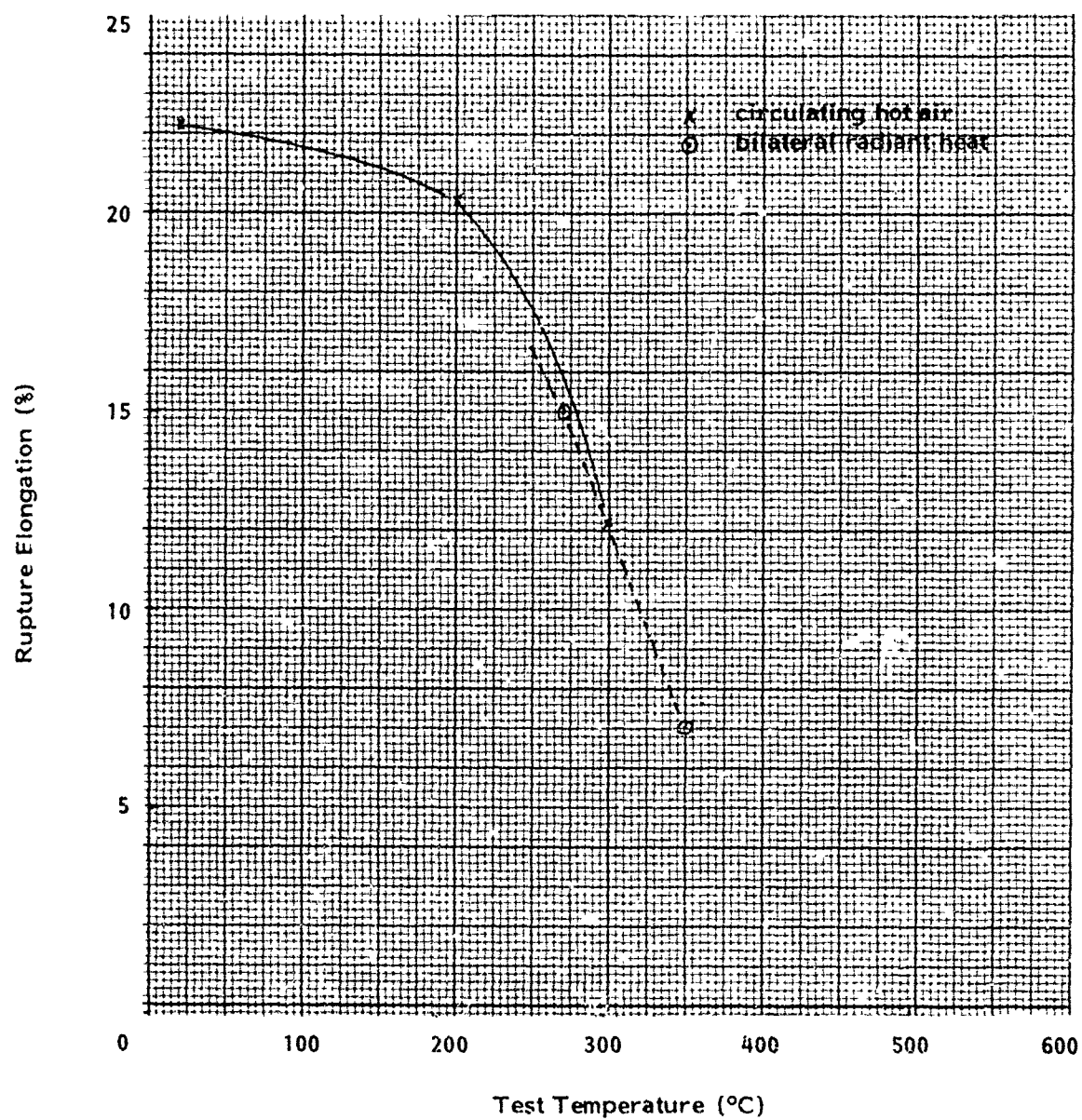


Figure 48. Rupture Elongation of Cotton Fabric in the Filling Direction at Various Temperatures

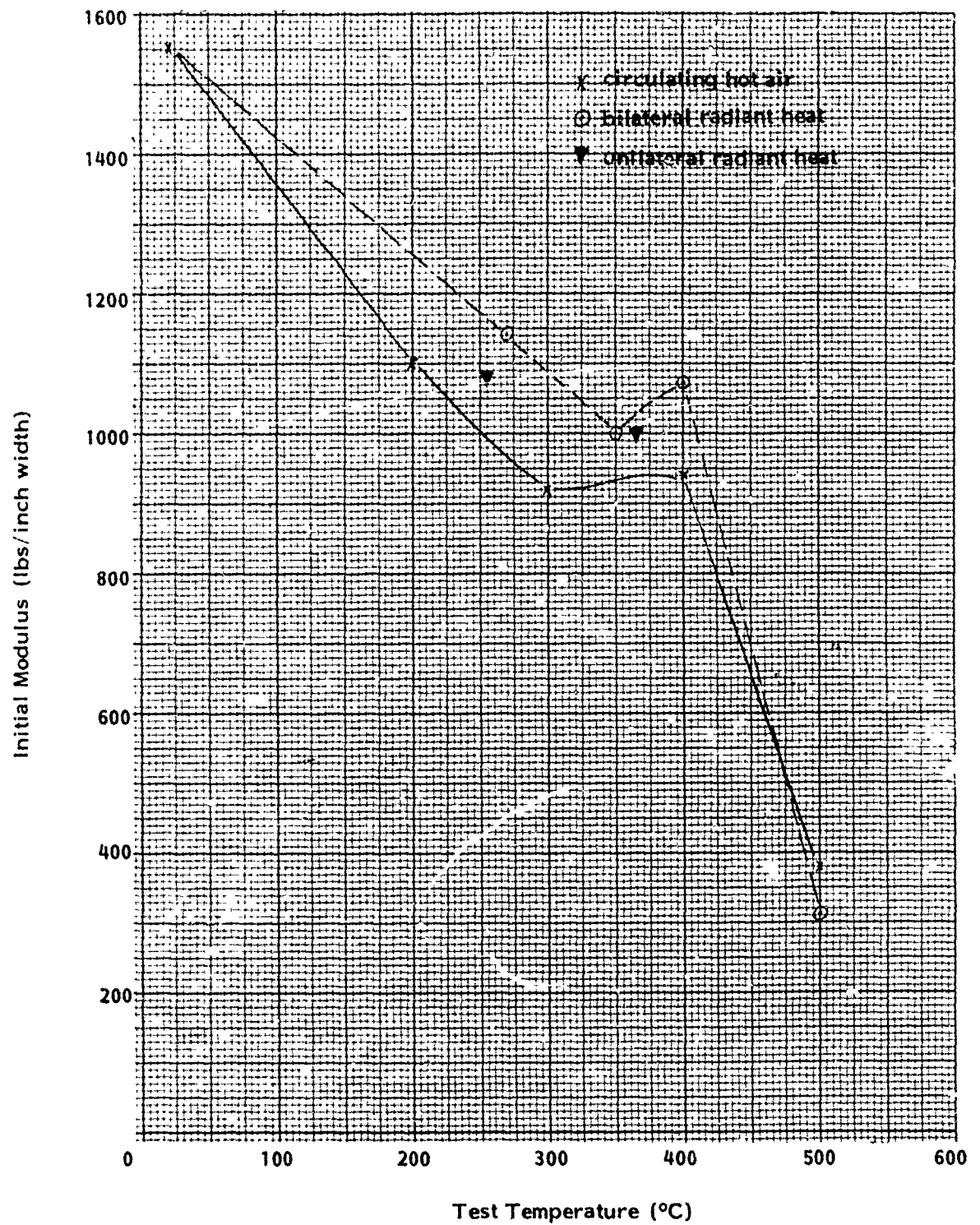


Figure 49. Initial Modulus of HT-4 Fabric in the Filling Direction at Various Temperatures

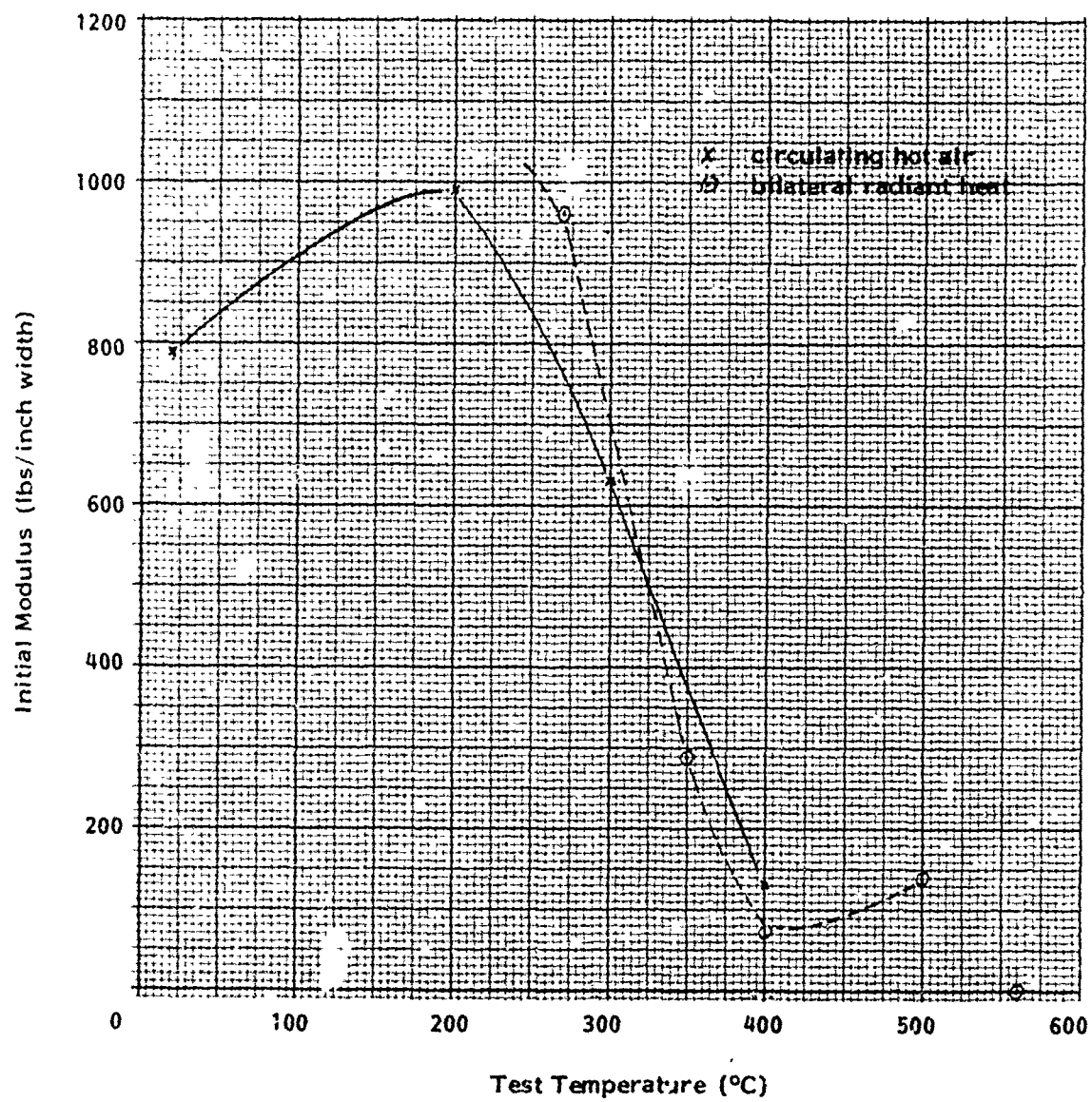


Figure 50. Initial Modulus of Durette Fabric in the Warp Direction at Various Temperatures

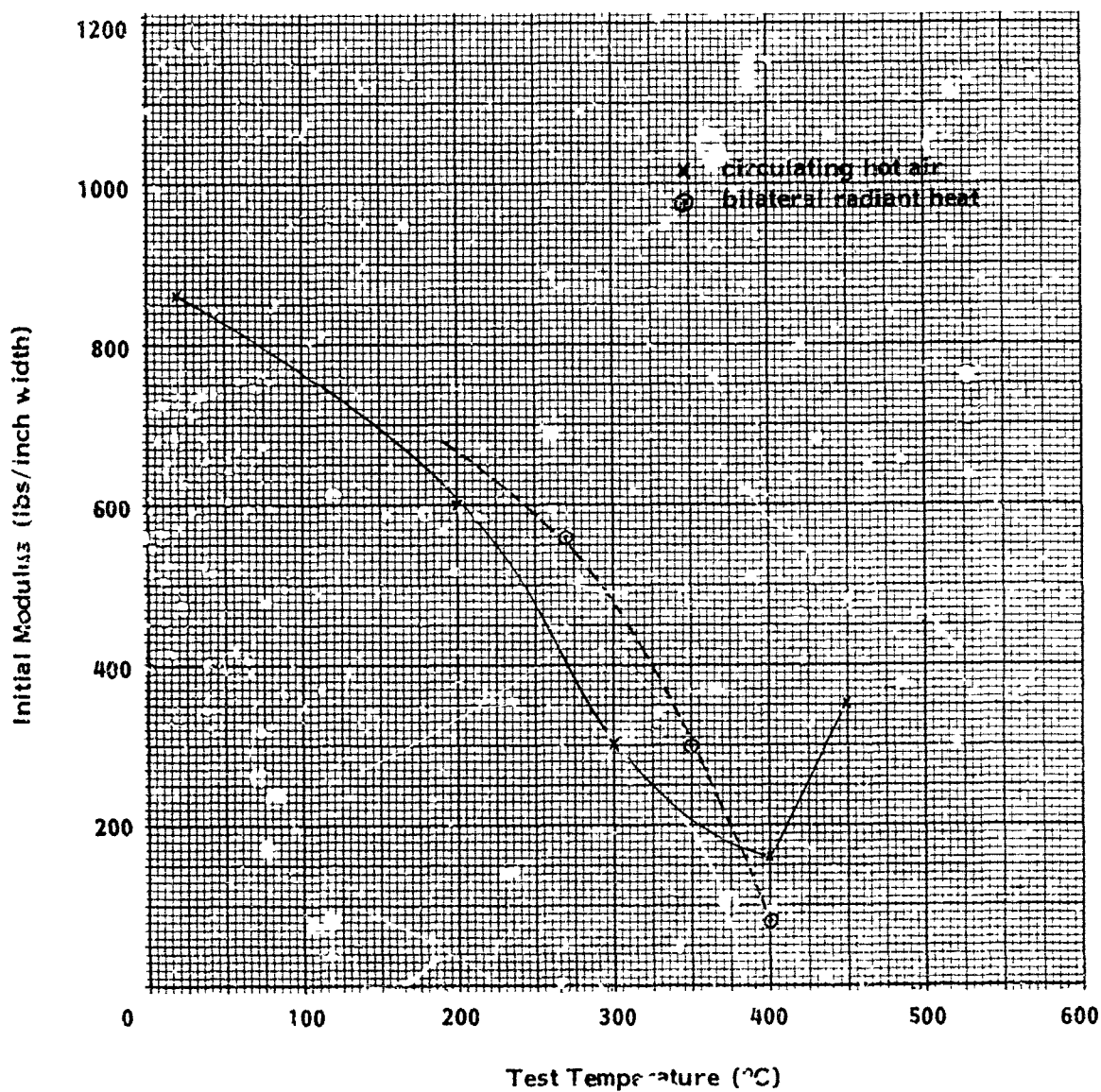


Figure 51. Initial Modulus of Nomex I Fabric in the Warp Direction at Various Temperatures

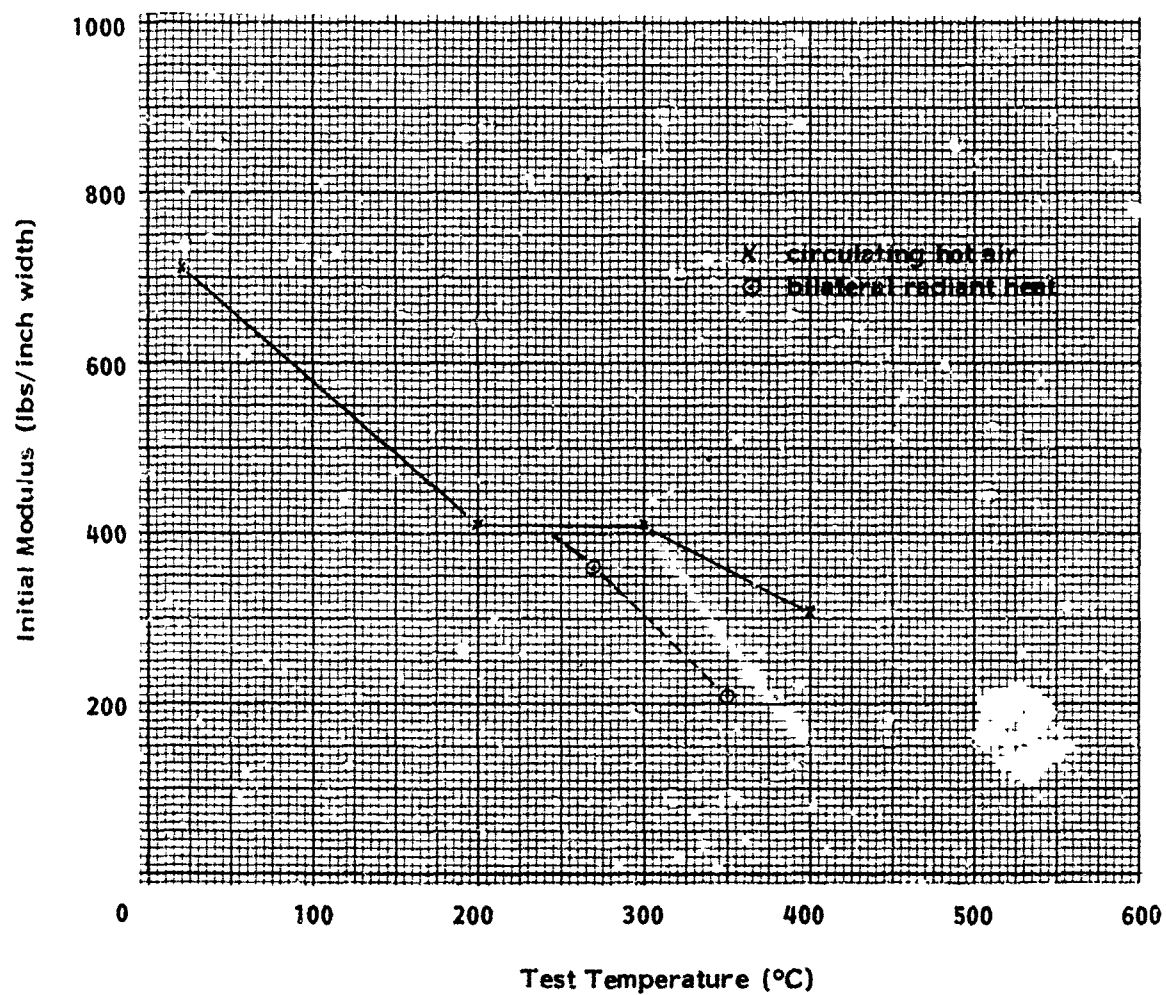


Figure 52. Initial Modulus of Kynol Fabric in the Warp Direction at Various Temperatures

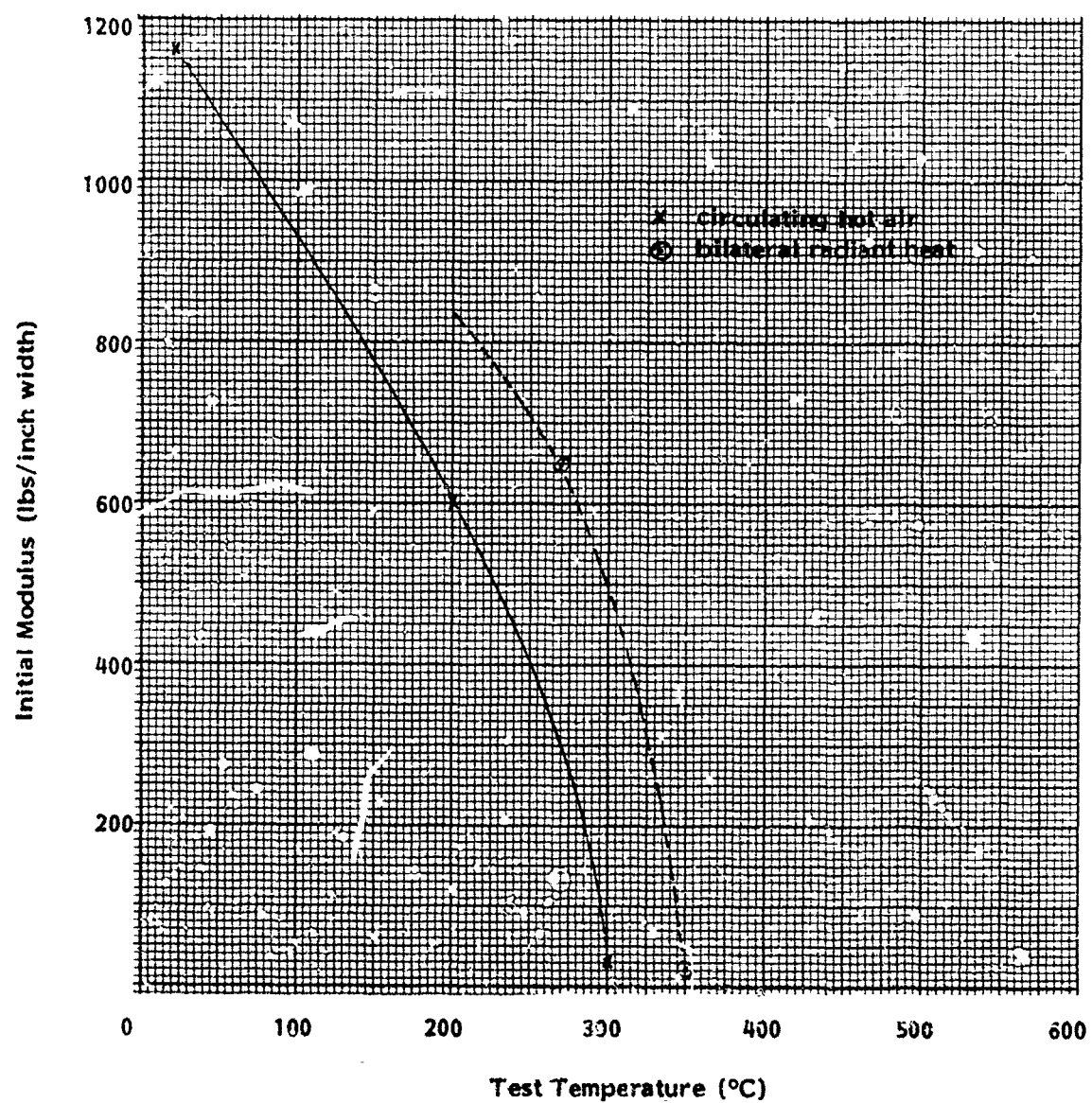


Figure 53. Initial Modulus of Cotton Fabric in the Filling Direction at Various Temperatures



Figure 54. Appearance of Abraded Kevlar Webbing:
Face in Contact with Hexagonal Bar



Figure 55. Appearance of Abraded Kevlar
Webbing: Unabraded Surface



Figure 56. Original Appearance of Kevlar Webbing

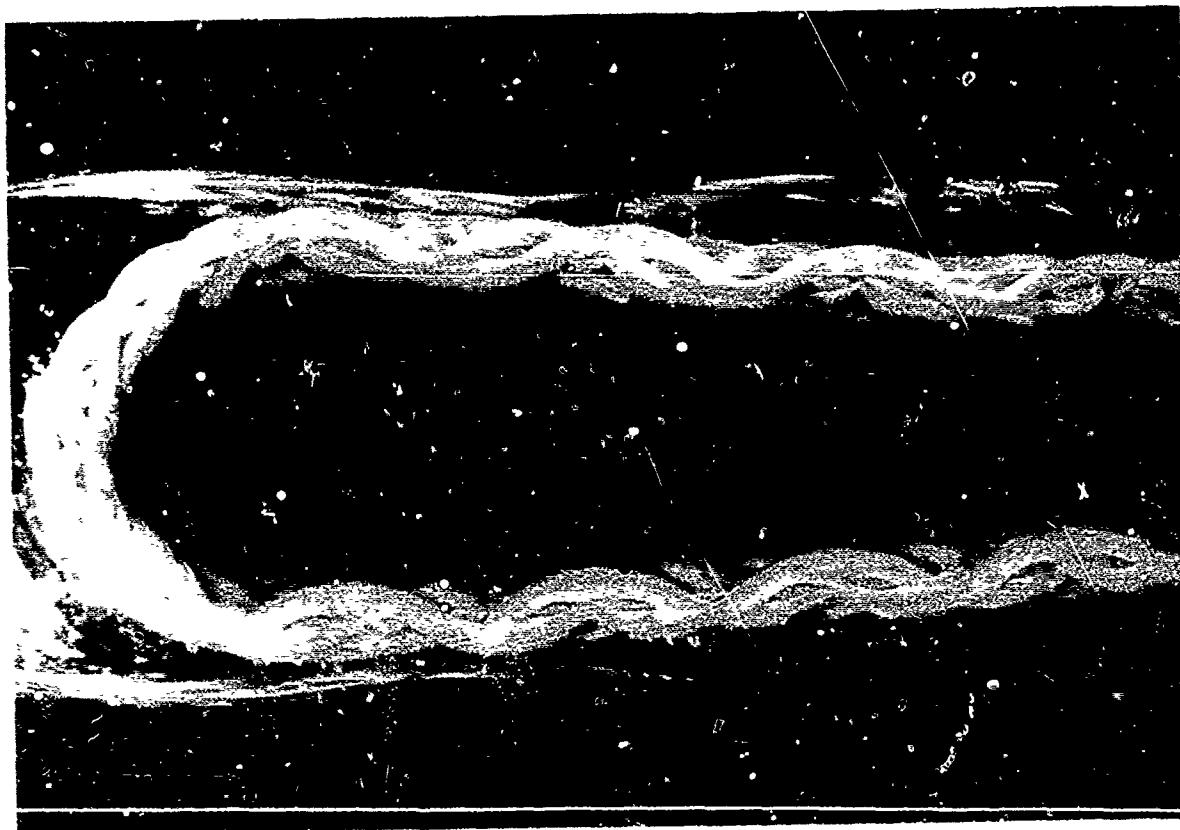


Figure 57. Section Parallel to the Warp Yarns of Kevlar Webbing in Bending Test Configuration Before Cycling

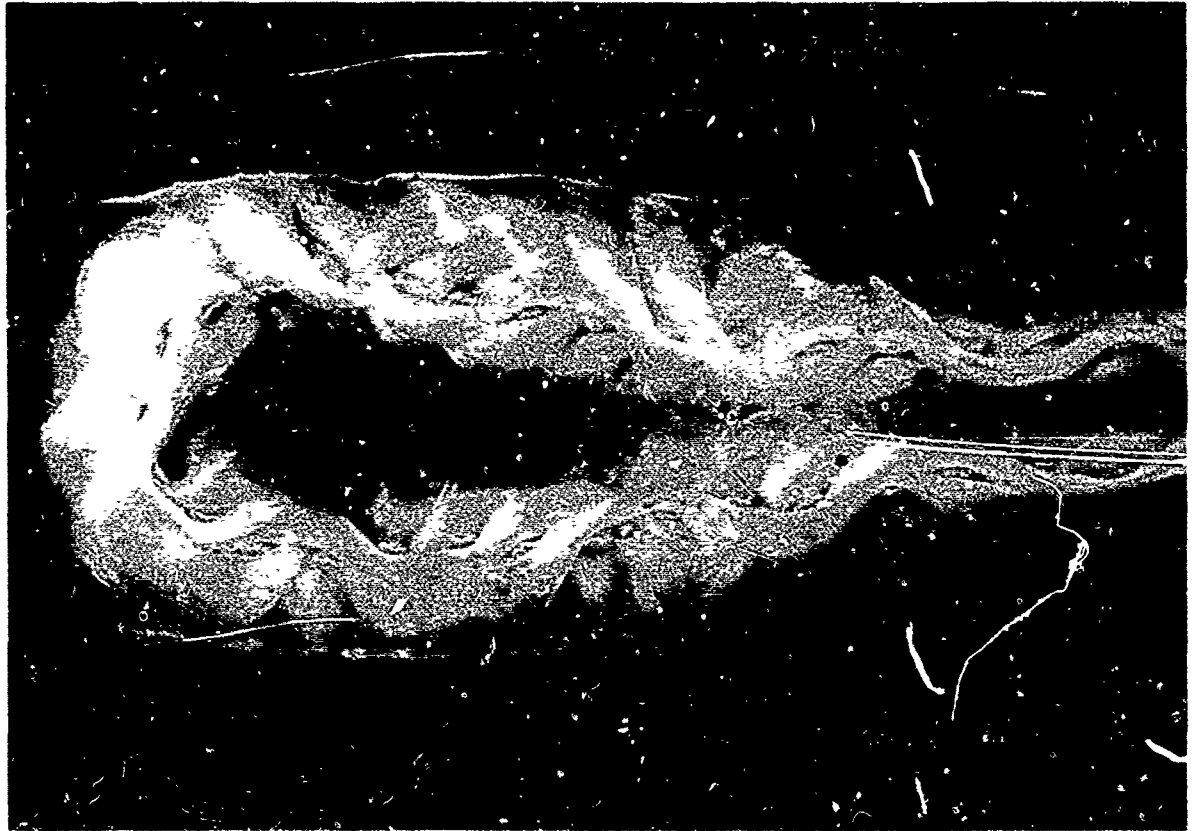


Figure 58. Section Parallel to the Warp Yarns of Kevlar Webbing in Bending Test Configuration After 3200 Cycles

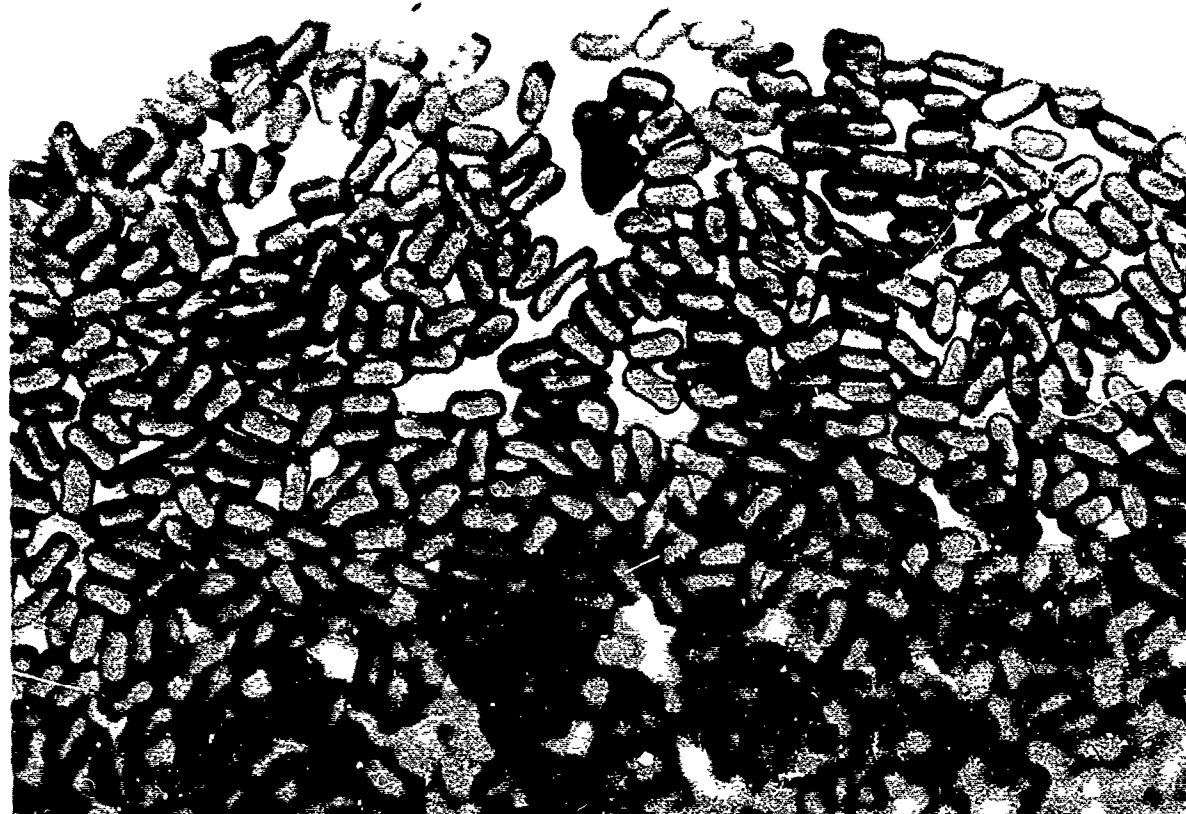


Figure 59. Cross-Section of Nomex Fibers

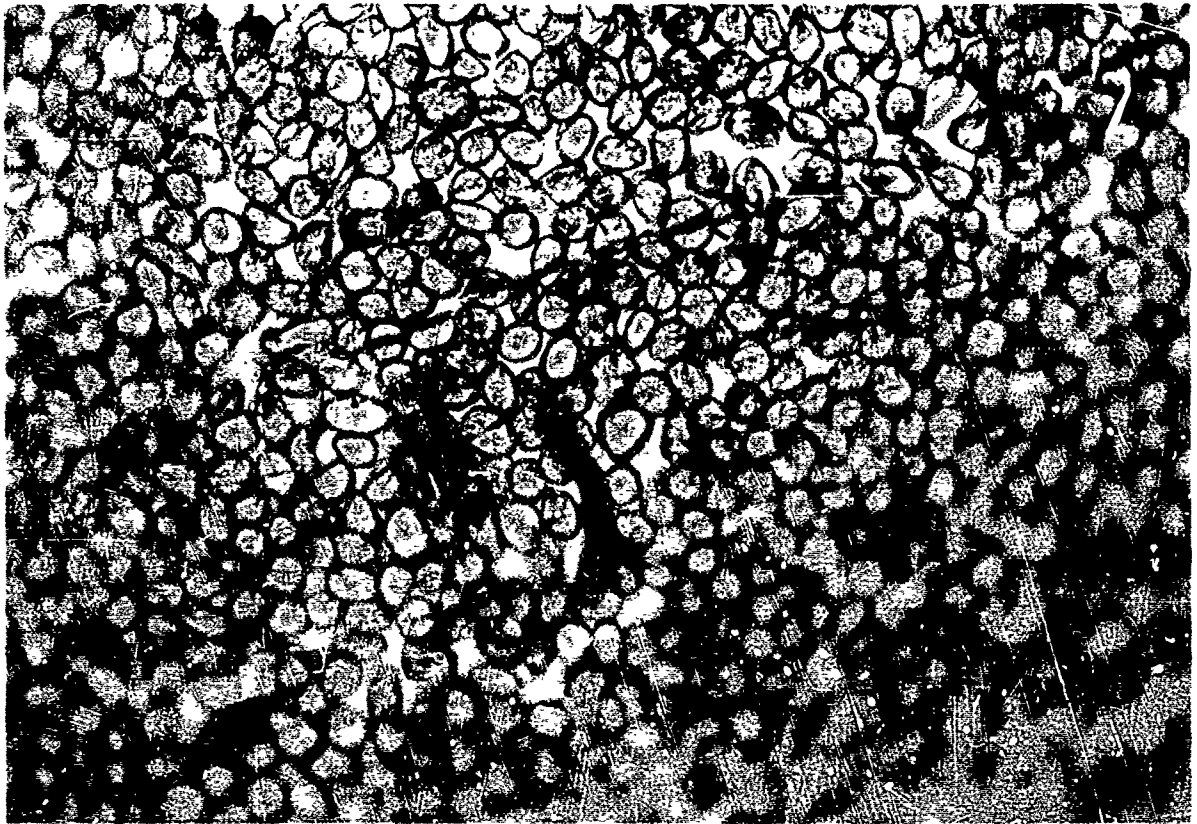


Figure 60. Cross-Section of HT-4 Fibers

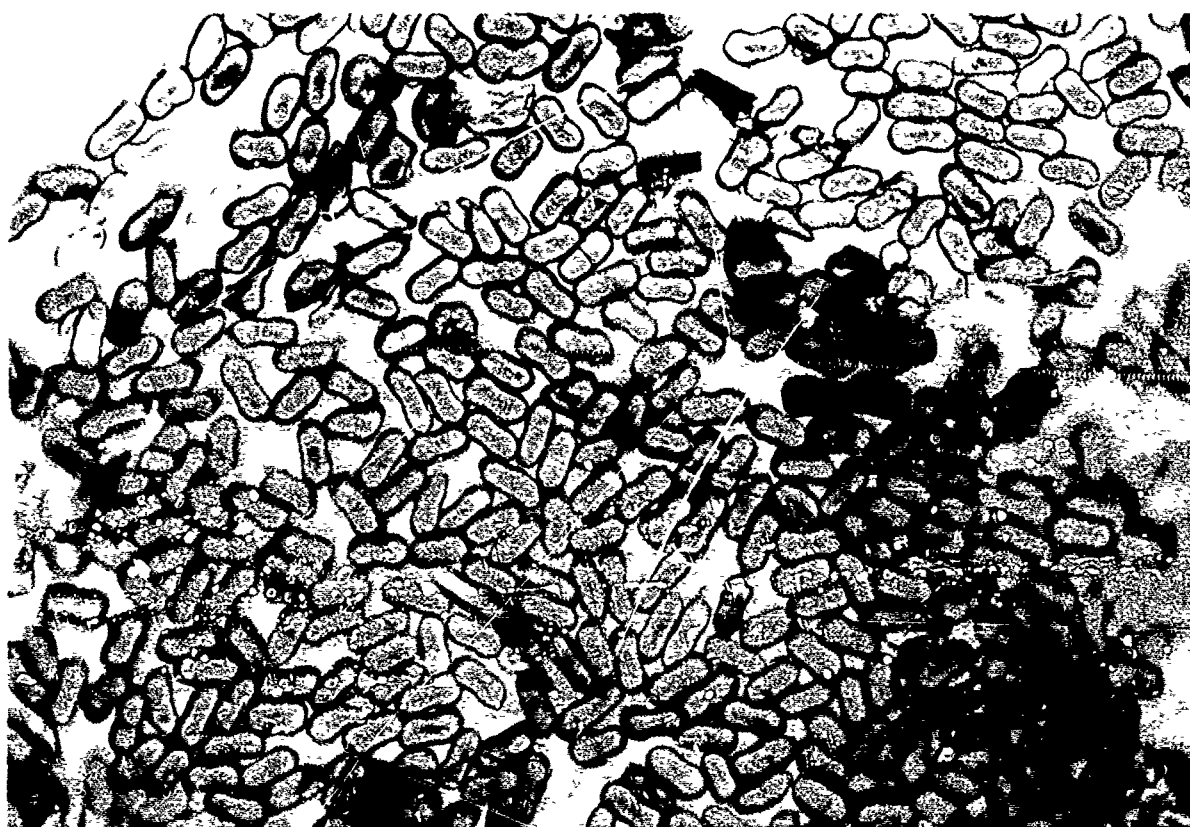


Figure 61. Cross-Section of E-11 Blend

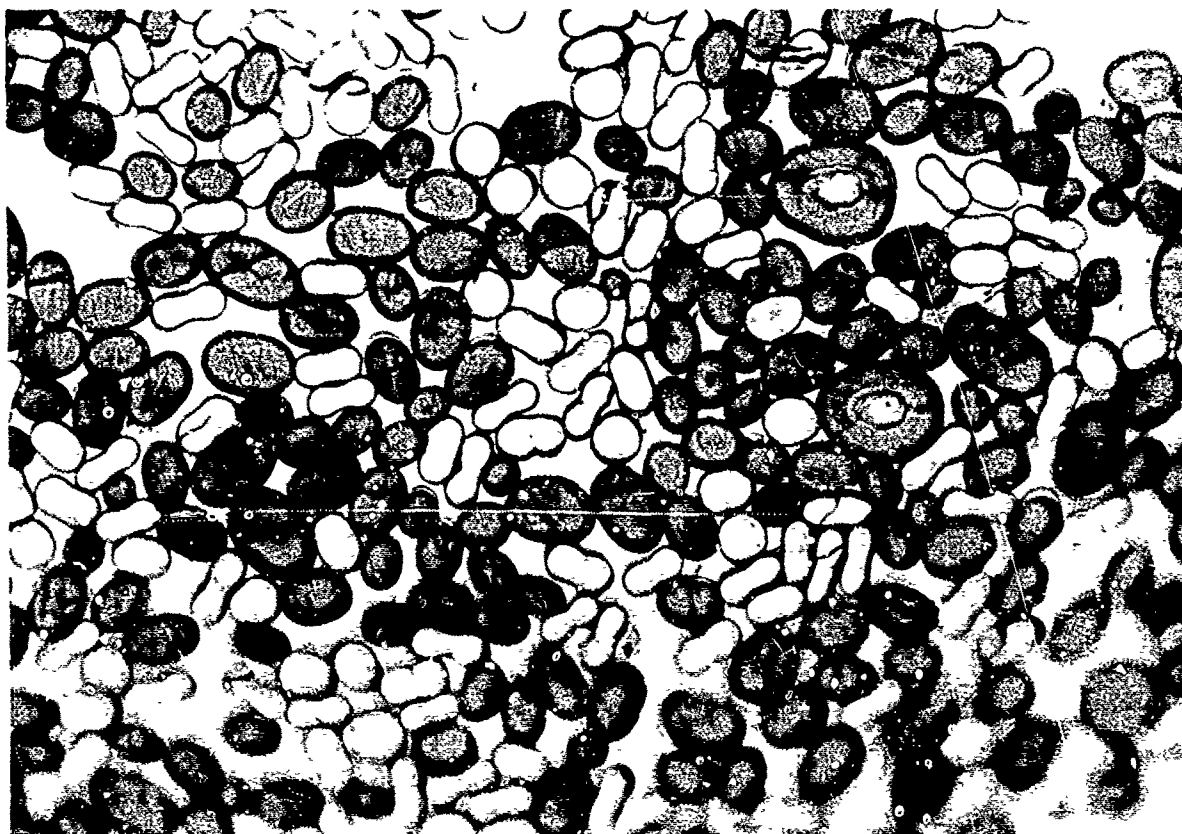


Figure 62. Cross-Section of Dyed Kynol/Nomex Blend



Figure 63a. Failed Drone Retrieval Parachute Webbing:
Back Side



Figure 63b. Failed Drone Retrieval Parachute Webbing:
Back Side



Figure 63c. Failed Drone Retrieval Parachute Webbing:
Back Side

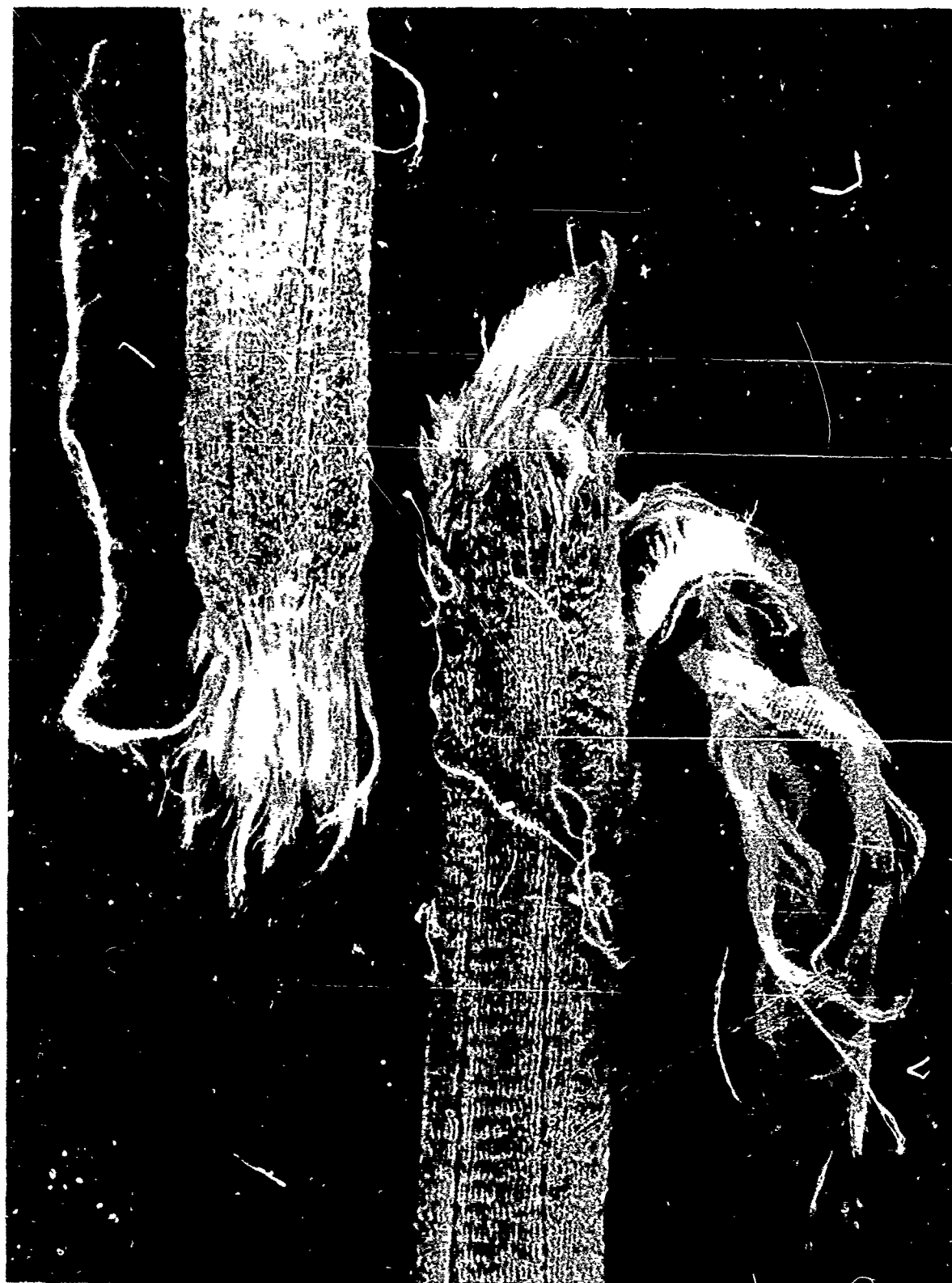


Figure 64a. Failed Drone Retrieval Parachute Webbing:
Face Side



Figure 64b. Failed Drone Retrieval Parachute Webbing:
Face Side



Figure 64c. Failed Drone Retrieval Parachute Webbing;
Face Side

APPENDIX

TABLE 7

TENSILE PROPERTIES OF HT-4 FABRIC IN THE FILLING DIRECTION
AT VARIOUS BILATERAL RADIANT HEAT FLUX LEVELS

Incident Radiant Heat Flux (cal/cm ² /sec)	Exposure Time (seconds)		Initial Modulus (lbs/inch)	Rupture Elongation (%)	Rupture Load (lbs/inch)	Strength Retention (%)
	At Start	At Rupture				
0.2	1	6	1230	12	96	
			1270	12	96	
			1240	11	90	
			Avg 1250	12	94	80
	5	10	1280	11	86	
			1300	11	88	
			1250	11	85	
			Avg 1280	11	86	73
	10	15	1130	12	81	
			1110	11	80	
			1110	11	87	
			Avg 1120	11	83	70
	30	32	1030	11	74	
			1110	11	76	
			1080	11	73	
			Avg 1070	11	74	63
	50	64	1100	11	77	
			1190	11	81	
			1100	11	71	
			Avg 1130	11	76	64

TABLE 7 (Cont.)

TENSILE PROPERTIES OF HT-4 FABRIC IN THE FILLING DIRECTION
AT VARIOUS BILATERAL RADIANT HEAT FLUX LEVELS

Incident Radiant Heat Flux (cal/cm ² /sec)	Exposure Time (seconds)		Initial Modulus (lbs/inch)	Rupture Elongation (%)	Rupture Load (lbs/inch)	Strength Retention (%)
	At Start	At Rupture				
0.3	1	5	1160	10	84	
			1120	11	82	
			1110	10	76	
			Avg 1130	10	81	69
	3	7	1000	10	70	
			960	11	66	
			900	10	60	
			Avg 950	10	65	55
	5	9	720	10	58	
			770	10	60	
			790	10	63	
			Avg 760	10	60	51
	10	14	720	10	61	
			750	10	59	
			720	10	56	
			Avg 730	10	59	50
	30	33	880	8	52	
			890	8	49	
			900	8	48	
			Avg 890	8	50	42
	60	63	970	7	40	
			980	6	39	
			1050	6	39	
			Avg 1000	6	39	33

TABLE 7 (Cont.)

TENSILE PROPERTIES OF HT-4 FABRIC IN THE FILLING DIRECTION
AT VARIOUS BILATERAL RADIANT HEAT FLUX LEVELS

Incident Radiant Heat Flux (cal/cm ² /sec)	Exposure Time (seconds)		Initial Modulus (lbs/inch)	Rupture Elongation (%)	Rupture Load (lbs/inch)	Strength Retention (%)
	At Start	At Rupture				
0.4	1	6	1090	12	69	
			1120	12	70	
			1110	12	71	
			Avg 1110	12	70	59
	3	8	660	11	56	
			670	12	58	
			690	11	57	
			Avg 670	11	57	48
	5	9	720	11	49	
			690	11	52	
			720	11	53	
			Avg 710	11	51	43
	10	14	720	9	36	
			700	9	35	
			710	9	37	
			Avg 710	9	36	30
	20	23	960	7	24	
			840	6	22	
			840	8	26	
			Avg 820	7	24	20
	30	32	1010	6	19	
			1040	6	15	
			1040	6	22	
			Avg 1030	6	19	16

TABLE 7 (Cont.)

TENSILE PROPERTIES OF HT-4 FABRIC IN THE FILLING DIRECTION
AT VARIOUS BILATERAL RADIANT HEAT FLUX LEVELS

Incident Radiant Heat Flux (cal/cm ² /sec)	Exposure Time (seconds)		Initial Modulus (lbs/inch)	Rupture Elongation (%)	Rupture Load (lbs/inch)	Strength Retention (%)
	At Start	At Rupture				
0.4 (cont.)	60	62	1160	5	18	
			1000	6	15	
			1040	6	14	14
			Avg 1070	6	16	
0.6	1	6	590	11	46	
			450	10	41	
			480	10	42	39
			Avg 510	10	43	
	3	6	590	5	19	
			580	5	19	
			570	5	17	16
			Avg 580	5	18	
	5	8	660	5	9	
			690	5	12	
			730	-	12	9
			Avg 690	5	11	
	10	13	---	5	10	
			720	5	9	
			830	4	11	
			Avg 750	4	9	8
				5	10	

TABLE 7 (Cont.)
TENSILE PROPERTIES OF HT-4 FABRIC IN THE FILLING DIRECTION
AT VARIOUS BILATERAL RADIANT HEAT FLUX LEVELS

Incident Radiant Heat Flux (cal/cm ² /sec)	Exposure Time (seconds)		Initial Modulus (lbs/inch)	Rupture Elongation (%)	Rupture Load (lbs/inch)	Strength Retention (%)	
	At Start	At Rupture					
0.6 (cont)	20	22	---	5	8		
			---	5	9		
			630	4	8		
			760	4	10		
			730	4	9		
	Avg		710	4	9	7	
	30	32	570	5	7		
			550	5	7		
			570	5	6		
			560	5	7		
	Avg					6	
60	63	290	3	4			
		---	4	4			
		340	4	5			
		310	4	4			
		Avg				3	
0.8	1	4	360	8	19		
			310	8	23		
			310	8	21		
			330	8	21		
			Avg				18
	3	6	620	5	11		
			560	6	11		
			560	5	11		
			520	6	10		
			Avg	560	6	11	
							9

TABLE 7 (Cont.)

TENSILE PROPERTIES OF HT-4 FABRIC IN THE FILLING DIRECTION
AT VARIOUS BILATERAL RADIANT HEAT FLUX LEVELS

Incident Radiant Heat Flux (cal/cm ² /sec)	Exposure Time (seconds)		Initial Modulus (lbs/inch)	Rupture Elongation (%)	Rupture Load (lbs/inch)	Strength Retention (%)
	At Start	At Rupture				
0.8 (cont)	5	8	600	6	10	
			770	6	10	
			770	5	12	
			Avg 710	6	11	9
	10	13	470	5	6	
			610	5	8	
			490	4	7	
			Avg 520	5	7	6
	20	21	120	1	1	
			110	1	1	
			130	1	1	
			Avg 120	1	1	1
0.9	30	31	140	1	1	
			140	1	1	
			140	1	1	
			Avg 140	1	1	1
	1	5	450	7	12	
			380	8	13	
			440	7	14	
			Avg 420	7	13	11
	3	6	530	5	"	
			550	5	8	
			650	4	7	
			Avg 580	5	7	6

TABLE 8

TENSILE PROPERTIES OF DURETTE FABRIC IN THE WARP DIRECTION
AT VARIOUS BILATERAL RADIANT HEAT FLUX LEVELS

Incident Radiant Heat Flux (cal/cm ² /sec)	Exposure Time (seconds)		Initial Modulus (lbs/inch)	Rupture Elongation (%)	Rupture Load (lbs/inch)	Strength Retention (%)
	At Start	At Rupture				
0.2	1	7	1140	13	57	
			1270	14	61	
			1390	14	62	
			Avg 1270	14	60	88
	3	7	1000	11	51	
			1020	11	53	
			930	11	51	
			Avg 980	11	52	76
	5	9	950	11	49	
			940	8	42	
			850	10	46	
			Avg 910	10	46	68
	10	14	910	9	43	
			860	10	45	
			850	10	43	
			Avg 870	10	44	65
	20	24	840	8	36	
			950	10	40	
			980	10	43	
			Avg 920	9	40	59
	60	64	910	12	41	
			960	10	42	
			1020	9	40	
			Avg 960	10	41	60

TABLE 8 (Cont.)
TENSILE PROPERTIES OF DURETTE FABRIC IN THE WARP DIRECTION
AT VARIOUS BILATERAL RADIANT HEAT FLUX LEVELS

Incident Radiant Heat Flux (cal/cm ² /sec)	Exposure Time (seconds)		Initial Modulus (lbs/inch)	Rupture Elongation (%)	Rupture Load (lbs/inch)	Strength Retention (%)
	At Start	At Rupture				
0.3	1	5	980	10	45	
			940	9	42	
			930	12	45	65
			Avg 950	10	44	
	3	7	870	9	34	
			750	10	32	
			820	9	35	50
			Avg 810	9	34	
	5	9	620	11	22	
			560	8	22	
			640	8	24	34
			Avg 610	9	23	
	10	14	380	10	21	
			310	11	19	
			300	9	19	29
			Avg 330	10	20	
	20	24	300	9	19	
			240	10	17	
			270	10	18	26
			Avg 270	10	18	
	60	64	300	10	20	
			300	10	18	
			280	9	17	26
			Avg 290	10	18	

TABLE 8 (Cont.)
TENSILE PROPERTIES OF DURETTE FABRIC IN THE WARP DIRECTION
AT VARIOUS BILATERAL RADIANT HEAT FLUX LEVELS

Incident Radiant Heat Flux (cal/cm ² /sec)	Exposure Time (seconds)		Initial Modulus (lbs/inch)	Rupture Elongation (%)	Rupture Load (lbs/inch)	Strength Retention (%)
	At Start	At Rupture				
0.4	1	5	780	9	30	
			940	3	33	
			810	9	30	
			Avg 840	9	31	46
	3	7	510	9	13	
			480	11	15	
			550	10	13	
			Avg 510	10	14	20
	5	9	380	11	8	
			410	11	9	
			480	10	9	
			Avg 420	11	9	13
	10	14	240	10	5	
			130	10	4	
			190	10	5	
			Avg 190	10	5	7
	20	24	160	9	5	
			160	9	3	
			150	10	4	
			Avg 160	9	4	6
	30	34	90	8	3	
			70	9	3	
			60	9	3	
			Avg 70	9	3	4

TABLE 8 (Cont.)
TENSILE PROPERTIES OF DURETTE FABRIC IN THE WARP DIRECTION
AT VARIOUS BILATERAL RADIANT HEAT FLUX LEVELS

Incident Radiant Heat Flux (cal/cm ² /sec)	Exposure Time (seconds)		Initial Modulus (lbs/inch)	Rupture Elongation (%)	Rupture Load (lbs/inch)	Strength Retention (%)
	At Start	At Rupture				
0.4 (cont)	60	63	80	7	3	
			70	8	3	
			70	8	3	
			Avg 70	8	3	4
0.6	1	3	440	4	13	
			450	5	15	
			450	5	17	
			Avg 450	5	15	22
	1	11	200	18	2	
			140	20	2	
			190	19	2	
			Avg 180	19	2	3
	5	14	80	24	2	
			170	20	2	
			110	22	2	
			Avg 120	22	2	3
	10	17	50	17	2	
			50	17	2	
			60	17	2	
			Avg 50	17	2	3
	30	32	70	6	2	
			80	6	2	
			80	7	2	
			Avg 80	6	2	3

TABLE 8 (Cont.)

TENSILE PROPERTIES OF DURETTE FABRIC IN THE WARP DIRECTION
AT VARIOUS BILATERAL RADIANT HEAT FLUX LEVELS

Incident Radiant Heat Flux (cal/cm ² /sec)	Exposure Time (seconds)		Initial Modulus (lbs/inch)	Rupture Elongation (%)	Rupture Load (lbs/inch)	Strength Retention (%)
	At Start	At Rupture				
0.6 (cont)	60	61	130	3	2	
			160	3	2	
			130	3	2	3
			Avg 140	3	2	
0.8	1	2	610		12	
			500		10	
			570		12	16
			Avg 560	--	11	
	1	10		25	1	
				23	1	
				23	1	2
			Avg ---	24	1	
	5	11	10	15	2	
			10	11	1	
			10	14	1	2
			Avg 10	13	1	
	10	14	20	6	1	
			20	6	1	
			20	7	2	2
			Avg 20	6	1	
	20	21	130	3	1	
			130	2	2	
			---	3	2	3
			Avg 130	3	2	

TABLE 8 (Cont.)

TENSILE PROPERTIES OF DURETTE FABRIC IN THE WARP DIRECTION
AT VARIOUS BILATERAL RADIANT HEAT FLUX LEVELS

Incident Radiant Heat Flux ^a (cal/cm ² /sec)	Exposure Time (seconds)		Initial Modulus (lbs/inch)	Rupture Elongation (%)	Rupture Load (lbs/inch)	Strength Retention (%)
	At Start	At Rupture				
0.8 (cont)	30	31	160	2	2	
			140	2	2	
			150	2	2	3
			Avg			
0.9	60	69	~0	~0	~0	
	1	2	720	3	10	
			680	4	6	
			540	2	7	
			650	3	8	12
			Avg			
	3	9	16	11	1	
			13	11	1	
			14	11	1	1
			Avg			
	5	9	21	7	1	
			14	8	1	
			18	7	1	1

TABLE 8 (Cont.)

TENSILE PROPERTIES OF HT-4 FABRIC IN THE FILLING DIRECTION
AT VARIOUS BILATERAL RADIANT HEAT FLUX LEVELS

Incident Radiant Heat Flux (cal/cm ² /sec)	Exposure Time (seconds)		Initial Modulus (lbs/inch)	Rupture Elongation (%)	Rupture Load (lbs/inch)	Strength Retention (%)
	At Start	At Rupture				
0.9 (cont)	5	7	350	3	4	3
			400	4	4	
			390	4	4	
			Avg 380	4	4	
	10	11	70	2	2	1
			70	2	1	
			80	2	1	
			Avg 70	2	1	

TABLE 9

TENSILE PROPERTIES OF NOMEX I FABRIC IN THE WARP DIRECTION
AT VARIOUS BILATERAL RADIANT HEAT FLUX LEVELS

Incident Radiant Heat Flux (cal/cm ² /sec)	Exposure Time (seconds)		Initial Modulus (lbs/inch)	Rupture Elongation (%)	Rupture Load (lbs/inch)	Strength Retention (%)
	At Start	At Rupture				
0.2	1	10	650	21	78	
			640	22	80	
			650	21	81	
			Avg 650	21	80	69
	5	13	560	21	67	
			590	20	69	
			540	20	65	
			Avg 560	20	67	58
0.3	10	18	540	20	66	
			540	19	65	
			530	20	63	
			Avg 540	20	65	56
	60	68	570	19	66	
			560	20	66	
			550	19	63	
			Avg 560	19	65	56
	1	8	540	16	48	
			600	18	47	
			560	17	47	
			550	16	46	
			Avg 560	17	47	41

TABLE 9 (Cont.)
TENSILE PROPERTIES OF NOMEX I FABRIC IN THE WARP DIRECTION
AT VARIOUS BILATERAL RADIANT HEAT FLUX LEVELS

Incident Radiant Heat Flux (cal/cm ² /sec)	Exposure Time (seconds)		Initial Modulus (lbs/inch)	Rupture Elongation (%)	Rupture Load (lbs/inch)	Strength Retention (%)
	At Start	At Rupture				
0.3 (cont)	3	10	390	16	32	
			359	16	32	
			380	17	32	
			Avg 370	16	32	28
	5	12	280	17	32	
			290	16	31	
			240	16	29	
			Avg 270	16	31	27
	10	19	220	17	31	
			250	17	32	
			230	17	32	
			Avg 230	17	32	28
0.4	20	27	240	16	32	
			230	15	32	
			230	17	32	
			Avg 230	16	32	28
	60	65	270	14	33	
			240	13	30	
			250	14	31	
			Avg 250	14	31	27
	1	7	500	16	31	
			440	16	25	
			480	17	32	
			Avg 470	16	29	25

TABLE 9 (Cont.)

TENSILE PROPERTIES OF NOMEX I FABRIC IN THE WARP DIRECTION
AT VARIOUS BILATERAL RADIANT HEAT FLUX LEVELS

Incident Radiant Heat Flux (cal/cm ² /sec)	Exposure Time (seconds)		Initial Modulus (lbs/inch)	Rupture Elongation (%)	Rupture Load (lbs/inch)	Strength Retention (%)
	At Start	At Rupture				
0.4 (cont)	3	8	170	14	18	
			150	12	15	
			200	14	18	
			Avg	13	17	15
	5	10	160	13	16	
			150	13	16	
			130	11	14	
			Avg	12	15	13
	10	14	100	7	9	
			170	12	19	
			140	7	10	
		Avg	9	13	11	
	20	23	120	7	9	
			180	8	14	
			160	7	12	
			Avg	8	15	10
	30	33	120	7	8	
			120	8	9	
			100	7	7	
			Avg	7	8	7

TABLE 9 (Cont.)
TENSILE PROPERTIES OF NOMEX I FABRIC IN THE WARP DIRECTION
AT VARIOUS BILATERAL RADIANT HEAT FLUX LEVELS

Incident Radiant Heat Flux (cal/cm ² /sec)	Exposure Time (seconds)		Initial Modulus (lbs/inch)	Rupture Elongation (%)	Rupture Load (lbs/inch)	Strength Retention (%)
	At Start	At Rupture				
0.4 (cont)	60	32	100	5	4	
			80	4	2	
			50	4	2	
			Avg 80	4	3	3
0.6	1	4	300	8	8	
			280	8	9	
			250	8	9	
			Avg 280	8	9	8
	3	4	30	3	3	
			40	2	3	
			50	2	3	
			Avg 40	2	3	3
0.8	5	5		shrinkage	1	
				load	1	
					1	1
	1	3	220	6	6	
			210	6	6	
			230	7	6	
			Avg 220	6	6	5
	3	4		1	2	
				1	2	
				2	2	
			~0	1	2	2

TABLE 10

TENSILE PROPERTIES OF KYNOL FABRIC IN THE WARP DIRECTION
AT VARIOUS BILATERAL RADIANT HEAT FLUX LEVELS

Incident Radiant Heat Flux (cal/cm ² /sec)	Exposure Time (seconds)		Initial Modulus (lbs/inch)	Rupture Elongation (%)	Rupture Load (lbs/inch)	Strength Retention (%)
	At Start	At Rupture				
0.2	1	6	530	10	24	
			560	10	25	
			560	11	26	
			Avg 550	10	25	81
	3	9	450	13	23	
			440	13	22	
			420	12	21	
			Avg 440	13	22	71
	5	12	360	17	18	
			370	15	20	
			380	16	20	
			Avg 370	16	19	61
	10	18	300	17	18	
			290	18	19	
			300	17	18	
			Avg 300	17	18	58
	20	28	270	20	20	
			290	19	18	
			270	19	19	
			Avg 280	19	19	61
	60	67	370	14	19	
			360	12	18	
			340	14	18	
			Avg 360	13	18	58

TABLE 10 (Cont.)
TENSILE PROPERTIES OF KYNOL FABRIC IN THE WARP DIRECTION
AT VARIOUS BILATERAL RADIANT HEAT FLUX LEVELS

Incident Radiant Heat Flux (cal/cm ² /sec)	Exposure Time (seconds)		Initial Modulus (lbs/inch)	Rupture Elongation (%)	Rupture Load (lbs/inch)	Strength Retention (%)
	At Start	At Rupture				
0.3	1	8	420	19	18	
			480	18	19	
			420	17	18	
			Avg 440	18	18	58
	3	10	190	17	10	
			200	16	10	
			210	18	10	
			Avg 200	17	10	32
	5	12	90	15	10	
			140	18	12	
			160	19	12	
			Avg 130	17	11	35
	10	16	110	15	14	
			100	12	11	
			110	15	13	
			Avg 110	14	13	42
	20	21	210	3	6	
			220	3	6	
			210	2	5	
			Avg 210	3	6	19
	30	31	180	1	2	
			180	1	2	
			180	1	2	
			Avg 180	1	2	6

TABLE 10 (Cont.)

TENSILE PROPERTIES OF KYNOL FABRIC IN THE WARP DIRECTION
AT VARIOUS BILATERAL RADIANT HEAT FLUX LEVELS

Incident Radiant Heat Flux (cal/cm ² /sec)	Exposure Time (seconds)		Initial Modulus (lbs/inch)	Rupture Elongation (%)	Rupture Load (lbs/inch)	Strength Retention (%)
	At Start	At Rupture				
0.3 (cont)	60	61	220	1	2	
			190	2	3	
			---	1	3	
			Avg 210	1	3	10
0.4	1	3	350		12	
			340		12	
			360		13	
			Avg 350		12	40
	1	5			8	
				16	7	
				15	8	
				14	8	26
	3	8			9	
			100	15	8	
			80	14	8	
			80	13	8	26
	5	8			7	
			90	8	7	
			100	8	7	
			80	9	7	22
	10	11			4	
			100	3	3	
			100	3	3	
			110	3	3	10
			Avg 100			

TABLE 10 (Cont.)

TENSILE PROPERTIES OF KYNOL FABRIC IN THE WARP DIRECTION
AT VARIOUS BILATERAL RADIANT HEAT FLUX LEVELS

Incident Radiant Heat Flux (cal/cm ² /sec)	Exposure Time (seconds)		Initial Modulus (lbs/inch)	Rupture Elongation (%)	Rupture Load (lbs/inch)	Strength Retention (%)
	At Start	At Rupture				
0.4 (cont)	20	21	150	1	1	
			170	1	1	
			190	1	1	
			Avg 170	1	1	3
	30	30		1	1	
			---	1	1	3
				1	1	
	1	5	200	11	4	
			170	11	5	
			140	11	6	
0.6			Avg 170	11	5	16
	3	5	60	5	4	
			50	4	3	
			70	6	4	
			Avg 60	5	4	13
	5	6	80	2	2	
			70	2	1	
			70	2	2	
			Avg 70	2	2	7
	10	10	80	1	1	
			50	1	1	
			110	1	1	
			Avg 80	1	1	3
	16	16			0	0

TABLE 10 (Cont.)

TENSILE PROPERTIES OF KYNOL FABRIC IN THE WARP DIRECTION
AT VARIOUS BILATERAL RADIANT HEAT FLUX LEVELS

Incident Radiant Heat Flux (cal/cm ² /sec) ..	Exposure Time (seconds)		Initial Modulus (lbs/inch)	Rupture Elongation (%)	Rupture Load (lbs/inch)	Strength Retention (%)
	At Start	At Rupture				
0.8	1	5	40	10	3	
			40	11	3	
			90	11	4	
			Avg 60	11	3	10
	5	6	50	3	1	
			50	2	1	
			50	2	1	
			Avg 50	2	1	3
	10	10			~0	0
	1	5	50	7	3	
0.9			50	8	3	
			40	8	2	
			Avg 50	8	3	9

TABLE 11

TENSILE PROPERTIES OF COTTON FABRIC IN THE FILLING DIRECTION
AT VARIOUS BILATERAL RADIANT HEAT FLUX LEVELS

Incident Radiant Heat Flux (cal/cm ² /sec)	Exposure Time (seconds)		Initial Modulus (lbs/inch)	Rupture Elongation (%)	Rupture Load (lbs/inch)	Strength Retention (%)
	At Start	At Rupture				
0.2	1	10	1150	17	63	
			910	18	57	
			1080	18	63	67
			Avg 1050	18	61	
	3	11	910	17	54	
			910	16	53	
			930	16	57	
			Avg 920	16	55	60
	5	13	950	16	48	
			700	16	50	
			900	17	50	54
			Avg 850	16	49	
	10	18	760	16	43	
			780	16	40	
			880	16	48	
			Avg 810	16	44	48
	20	28	700	15	37	
			700	16	39	
			690	13	37	42
			Avg 700	15	38	
	60	67	650	15	31	
			630	14	30	
			670	15	35	35
			Avg 650	15	32	

TABLE 11 (Cont.)

TENSILE PROPERTIES OF COTTON FABRIC IN THE FILLING DIRECTION
AT VARIOUS BILATERAL RADIANT HEAT FLUX LEVELS

Incident Radiant Heat Flux (cal/cm ² /sec)	Exposure Time (seconds)		Initial Modulus (lbs/inch)	Rupture Elongation (%)	Rupture Load (lbs/inch)	Strength Retention (%)
	At Start	At Rupture				
0.3	1	8	700	17	45	
			820	17	41	
			Avg 760	17	43	47
	5	12	510	15	25	
			550	17	28	
			Avg 530	16	26	29
	10	17	500	16	22	
			380	16	16	
			Avg 440	16	19	21
	20	25	190	14	7	
0.4			200	12	7	
			Avg 190	13	7	8
	30	34	40	9	2	
			50	9	2	
			Avg 50	9	2	2
	60	62	20	6	1	
			20	7	1	
			Avg 20	7	1	1
	1	9	610	18	33	
			540	18	29	
			Avg 600	21	33	
			Avg 590	19	32	35

TABLE 11 (Cont.)

TENSILE PROPERTIES OF COTTON FABRIC IN THE FILLING DIRECTION
AT VARIOUS BILATERAL RADIANT HEAT FLUX LEVELS

Incident Radiant Heat Flux (cal/cm ² /sec)	Exposure Time (seconds)		Initial Modulus (lbs/inch)	Rupture Elongation (%)	Rupture Load (lbs/inch)	Strength Retention (%)
	At Start	At Rupture				
0.4 (cont)	3	9	570	15	29	
			520	15	28	
			Avg 550	15	28	31
	5	12	360	16	16	
			350	16	17	
			Avg 350	16	16	18
0.6	10	15	160	12	6	
			160	13	6	
			Avg 160	13	6	6
	20	24	8	13	1	
			9	16	1	
			Avg 9	14	1	1
0.8	1	7	230	16	14	15
	3	7	30	10	1	
			30	10	2	
			Avg 30	10	2	2
0.8	1	5	60	12	3	
			50	12	3	
			Avg 60	12	3	4

TABLE 12

TENSILE PROPERTIES OF NYLON FABRIC IN THE WARP DIRECTION
AT VARIOUS BILATERAL RADIANT HEAT FLUX LEVELS

Incident Radiant Heat Flux (cal/cm ² /sec)	Exposure Time (seconds)		Initial Modulus (lbs/inch)	Rupture Elongation (%)	Rupture Load (lbs/inch)	Strength Retention (%)
	At Start	At Rupture				
0.2	1	22	280	46	97	
			260	50	93	
			270	51	88	
			Avg	49	93	70
	3	25	220	--	80	
			230	49	82	
			210	51	77	
			Avg	50	80	61
	5	26	220	51	76	
			210	50	79	
			210	48	77	
			Avg	50	77	58
	10	30	180	47	60	
			180	42	54	
			180	51	75	
			Avg	46	60	47
	20	33	160	30	37	
			160	30	39	
			140	29	32	
			Avg	30	36	27
	30	34	40	10	4	
			40	10	4	
			40	10	4	
			Avg			3

TABLE 12 (Cont.)

TENSILE PROPERTIES OF NYLON FABRIC IN THE WARP DIRECTION
AT VARIOUS BILATERAL RADIANT HEAT FLUX LEVELS

Incident Radiant Heat Flux (cal/cm ² /sec)	Exposure Time (seconds)		Initial Modulus (lbs/inch)	Rupture Elongation (%)	Rupture Load (lbs/inch)	Strength Retention (%)
	At Start	At Rupture				
0.2 (cont)	40	40	~0			0
0.3	1	14	190	29	32	
			190	31	33	
			170	30	31	
			Avg 180	30	32	24
	3	14	120	27	24	
			120	24	21	
			120	26	23	
			Avg 120	26	23	17
	15	15	100	20	16	
			90	19	13	
			80	20	11	
			Avg 90	20	13	10
	10	15	40	10	4	
			50	10	4	
			40	10	4	
			Avg 40	10	4	3
15					0	0

TABLE 12 (Cont.)

TENSILE PROPERTIES OF NYLON FABRIC IN THE WARP DIRECTION
AT VARIOUS BILATERAL RADIANT HEAT FLUX LEVELS

Incident Radiant Heat Flux (cal/cm ² /sec)	Exposure Time (seconds)		Initial Modulus (lbs/inch)	Rupture Elongation (%)	Rupture Load (lbs/inch)	Strength Retention (%)
	At Start	At Rupture				
0.4	1	9	150	21	17	
			160	19	17	
			Avg 150	20	17	13
	5	9	70	10	6	
0.8			70	10	6	
			Avg 70	10	6	5
		10	melted			0
	1	3	90	6	4	
			70	6	3	
			80	6	3	
			Avg 80	6	3	2
		4	melted			0

TABLE 13
TENSILE PROPERTIES OF POLYESTER FABRIC IN THE WARP DIRECTION
AT VARIOUS BILATERAL RADIANT HEAT FLUX LEVELS

Incident Radiant Heat Flux (cal/cm ² /sec)	Exposure Time (seconds)		Initial Modulus (lbs/inch)	Rupture Elongation (%)	Rupture Load (lbs/inch)	Strength Retention (%)
	At Start	At Rupture				
0.2	1	16	230	34	45	
			270	34	45	
			270	32	46	
			Avg 260	33	45	48
	5	20	180	32	41	
			190	33	43	
			190	33	43	
			Avg 190	33	42	45
	10	24	170	32	40	
			180	34	41	
			190	33	42	
			Avg 180	33	41	44
	20	30	170	18	20	
			170	27	32	
			170	25	33	
			180	22	27	
			Avg 170	23	28	30
	30	38	270	18	20	
			160	18	21	
			120	12	10	
			100	9	6	
			Avg 160	14	14	15

TABLE 13 (Cont.)

TENSILE PROPERTIES OF POLYESTER FABRIC IN THE WARP DIRECTION
AT VARIOUS BILATERAL RADIANT HEAT FLUX LEVELS

Incident Radiant Heat Flux (cal/cm ² /sec)	Exposure Time (seconds)		Initial Modulus (lbs/inch)	Rupture Elongation (%)	Rupture Load (lbs/inch)	Strength Retention (%)
	At Start	At Rupture				
0.2 (cont)	60	63	40	10	4	
			121	11	8	
			30	6	1	
			Avg 60	9	4	4
0.3	1	9	100	19	15	
			110	19	14	
			110	18	14	
			Avg 110	19	14	15
	3	9	80	13	7	
			80	13	8	
			60	13	6	
			Avg 70	13	7	7
	5	9	40	10	4	
			40	11	4	
			50	11	4	
			Avg 40	11	4	4
0.4	11				0	0
	1	7	40	14	6	
			59	15	8	
			Avg 50	15	7	7

TABLE 13 (Cont.)

TENSILE PROPERTIES OF POLYESTER FABRIC IN THE WARP DIRECTION
AT VARIOUS BILATERAL RADIANT HEAT FLUX LEVELS

Incident Radiant Heat Flux (cal/cm ² /sec)	Exposure Time (seconds)		Initial Modulus (lbs/inch)	Rupture Elongation (%)	Rupture Load (lbs/inch)	Strength Retention (%)
	At Start	At Rupture				
0.4 (cont)	5	7	50	4	1	
			70	4	1	
			Avg 60	4	1	1
0.8		9	melted			0
	1	3	20	3	1	
			20	3	1	
			Avg 20	3	1	1
		6	melted			0

TABLE 14

TENSILE PROPERTIES OF HT-4 FABRIC IN THE FILLING DIRECTION
AT VARIOUS UNILATERAL RADIANT HEAT FLUX LEVELS

Incident Radiant Heat Flux (cal/cm ² /sec)	Exposure Time (seconds)		Initial Modulus (lbs/inch)	Rupture Elongation (%)	Rupture Load (lbs/inch)	Strength Retention (%)
	At Start	At Rupture				
0.2-0.3	1	6	1290	11	90	
			1300	12	91	
			1170	12	88	
			Avg 1250	12	90	76
	10	15	1030	10	71	
			1050	10	75	
			1000	10	70	
			Avg 1030	10	72	61
	30	34	1070 1040	11 10	83 68	
			1090 1030	10 10	72 70	
			960 1060	10 11	79 75	
			Avg 1040	10	75	64
0.4-0.5	60	64	1130	10	77	
			950	10	65	
			980	10	69	
			1110	10	78	
			Avg 1040	10	72	61

TABLE 14 (Cont.)

TENSILE PROPERTIES OF HT-4 FABRIC IN THE FILLING DIRECTION
AT VARIOUS UNILATERAL RADIANT HEAT FLUX LEVELS

Incident Radiant Heat Flux (cal/cm ² /sec)	Exposure Time (seconds)		Initial Modulus (lbs/inch)	Rupture Elongation (%)	Rupture Load (lbs/inch)	Strength Retention (%)
	At Start	At Rupture				
0.3-0.5	1	6	1100	11	68	
			990	11	69	
			1010	11	67	
		Avg	1030	11	68	58
	10	15	630	9	47	
			620	10	55	
			680	11	57	
		Avg	640	10	53	45
	30	33	710	9	44	
			1040	6	34	
			890	6	35	
			990	5	20	
		Avg	900	7	33	28
	60	62	1080	5	28	
			1060	4	17	
			1180	4	14	
			900	5	20	
			930	5	16	
		Avg	1030	5	19	16

TABLE 15

TENSILE PROPERTIES OF HT-4 FABRIC IN THE FILLING
DIRECTION AT VARIOUS TEMPERATURES IN CIRCULATING HOT AIR

(10 Minute Exposure)

<u>Test Temperature (°C)</u>	<u>Initial Modulus (lbs/inch)</u>	<u>Rupture Elongation (%)</u>	<u>Rupture Load (lbs/inch)</u>	<u>Strength Retention (%)</u>
70	1550	12	118	--
200	1040	13	76	
	1100	13	82	
	1180	14	86	
	Avg 1090	13	81	69
300	960	10	52	
	880	10	50	
	940	10	50	
	Avg 930	10	51	43
400	940	5	14	
	---	6	12	
	---	6	12	
	Avg 940	6	13	11
500	410	4	6	
	350	4	5	
	380	5	6	
	Avg 380	4	6	5

TABLE 16

TENSILE PROPERTIES OF DURETTE FABRIC IN THE WARP
DIRECTION AT VARIOUS TEMPERATURES IN CIRCULATING HOT AIR

(10 Minute Exposure)

<u>Test Temperature (°C)</u>	<u>Initial Modulus (lbs/inch)</u>	<u>Rupture Elongation (%)</u>	<u>Rupture Load (lbs/inch)</u>	<u>Strength Retention (%)</u>
70	790	18	68	--
200	1020	17	54	
	980	16	52	
	970	15	50	
	Avg 990	16	52	76
300	840	20	33	
	620	20	36	
	640	19	34	
	Avg 630	20	34	50
400	120	22	17	
	140	14	16	
	130	16	16	
	Avg 130	17	16	24
500	---	--	0.2	~0

TABLE 17

TENSILE PROPERTIES OF NOMEX I FABRIC IN THE WARP DIRECTION
AT VARIOUS TEMPERATURES IN CIRCULATING HOT AIR

(10 Minute Exposure)

<u>Test Temperature (°C)</u>	<u>Initial Modulus (lbs/inch)</u>	<u>Rupture Elongation (%)</u>	<u>Rupture Load (lbs/inch)</u>	<u>Strength Retention (%)</u>
70	860	33	116	--
200	610	30	77	
	590	28	74	
	600	30	75	
	Avg 600	29	75	65
300	320	35	52	
	300	33	50	
	290	34	50	
	Avg 300	34	51	44
400	160	17	23	
	150	18	24	
	170	17	25	
	Avg 160	17	24	21
450	370	2	6	
	350	2	6	
	340	3	7	
	Avg 350	2	6	5

TABLE 18

**TENSILE PROPERTIES OF KYNOL FABRIC IN THE WARP
DIRECTION AT VARIOUS TEMPERATURES IN CIRCULATING HOT AIR**

(10 Minute Exposure)

<u>Test Temperature (°C)</u>	<u>Initial Modulus (lbs/inch)</u>	<u>Rupture Elongation (%)</u>	<u>Rupture Load (lbs/inch)</u>	<u>Strength Retention (%)</u>
70	710	7	31	--
200	410	16	21	
	420	16	21	
	410	15	22	
	Avg 410	16	21	68
300	450	11	24	
	330	8	12	
	420	10	23	
	420	9	20	
	430	10	21	
	Avg 410	10	20	17
400	300	7	9	
	330	9	10	
	320	9	10	
	Avg 320	8	10	32
500	---	-	~0	~0

TABLE 19

TENSILE PROPERTIES OF COTTON FABRIC IN THE FILLING
DIRECTION AT VARIOUS TEMPERATURES IN CIRCULATING HOT AIR

(10 Minute Exposure)

<u>Test Temperature (°C)</u>	<u>Initial Modulus (lbs/inch)</u>	<u>Rupture Elongation (%)</u>	<u>Rupture Load (lbs/inch)</u>	<u>Strength Retention (%)</u>
70	1160	22	91	--
200	610	20	40	
	<u>610</u>	<u>20</u>	<u>42</u>	
	Avg 610	20	41	45
300	29	13	2	
	30	13	2	
	<u>30</u>	<u>11</u>	<u>2</u>	
	Avg 30	12	2	2
400	ignition after approximate, 5 minutes of exposure			

References

1. Abbott, N.J. et al, Some Properties of Kevlar and Other Heat-Resistant, Nonflammable Fibers, Yarns and Fabrics, pp. 45-98, AFML-TR-74-65, Part III, March 1975.
2. Sparrow, E.M. and Cess, R.D., Radiation Heat Transfer, pp. 39, 41, 48, 52, Brooks/Cole Publishing Co., 1966.
3. Singham, J.R., Tables of Emissivity of Surfaces, Intern. J. Heat Mass Transfer, Vol. 5, pp. 67-76, 1962.
4. Gubareff, G.G., Jansen, J.E., and Torborg, R.H., Thermal Radiation Properties Survey, pp. 203, 236, Honeywell Research Center, 1960.
5. Howell, J.R., and Siegel, R., Thermal Radiation Heat Transfer, Vol. II, pp. 73, 74, NASA SP-164, 1969.
6. Morse, H.L. et al, Analysis of the Thermal Response of Protective Fabrics, pp. 87, AFML-TR-73-17, January 1973.
7. Freeston, W.D. Jr., et al, Flammability and Heat Transfer Characteristics of PBI Fabric, pp. 49, AFML-TR-70-267, January 1971.
8. Abbott, N.J., Donovan, J.G. and Schoppee, M.M., The Effect of Temperature and Strain Rate on the Tensile Properties of Kevlar and PBI Yarns, pp. 10, AFML-TR-74-65, Part II, May 1974.